Final Report

to the

NATIONAL SCIENCE FOUNDATION

for

Grant GK-30853

A RATIONAL ANALYSIS AND DESIGN PROCEDURE FOR WOOD JOIST FLOOR SYSTEMS

Principal Investigators

Department of Civil Engineering

Dr. M. D. Vanderbilt, Associate Professor

Dr. J. R. Goodman, Professor

Dr. M. E. Criswell, Assistant Professor

Department of Forest and Wood Science

Dr. J. Bodig, Professor

Colorado State University
Fort Collins, Colorado
November 1974

ACKNOWLEDGMENTS

The authors wish to acknowledge the assistance of the many individuals, agencies and industries who aided in the development and performance of the research project. Acknowledgment is given to the National Science Foundation for the financial support of the project through Grant No. GK-30853. The counsel of Dr. Edward G. King, Jr., Director of Technical Programs of the National Forest Products Association is greatly appreciated. Other individuals contributing ideas to the project should also be singled out. Mr. David C. Countryman, Assistant Director of the American Plywood Association and Mr. Neal I. Pinson, Director of Technical Services of the Western Wood Products Association contributed significantly to the project.

The assistance of the following companies in donating test material to the project is greatly appreciated

Colorado Forest Products

Cook Lumber Company

Kaibab Lumber Company

San Juan Lumber Company

Weyerhaeuser Company

Special thanks are due Dr. Erik G. Thompson, Colorado State University, for his help in formulation of finite element procedures. Finally, but not last, the efforts of the graduate research assistants who carried out the detailed work is greatly appreciated.

ABSTRACT

Wood joist structural systems in housing and other construction account for a large percentage of the total use of wood, one of man's most important renewable resources. The current method of design of wood systems is based on grossly simplifying assumptions which can lead to inefficient use and unpredictable performance.

In the fall of 1971, an interdisciplinary team of researchers was organized at Colorado State University under the sponsorship of the National Science Foundation to develop a rational analysis procedure for wood joist structural systems. The goal of this research was to develop a mathematical model describing the behavior of joist systems and to verify its validity by a series of carefully controlled tests on full-scale structures. This model, now developed and verified, provides the correct engineering basis for developing new, radically improved design procedures for wood joist structural systems. Design methods leading to more efficient use of materials, cost-benefit relationships, and the benefits of upgrading material property assessments can now be studied and quantified. Thus, this investigation has made considerable progress toward the goal of better utilization of a critical natural resource and at the same time, the quantification of a rational analysis method which will lead to design methods which will assure the nation's consumers of reliable, safe, and economical wood joist structural systems.

Table of Contents

1. INTRODUCTION

1.1 Need for Study

The challenge of providing the quantity of economical housing having the quality expected by today's home buyer is becoming an increasing concern of our society. Achieving this task in ways consistent with the increasing pressures for efficient use of our natural resources and the preservation of environmental quality is properly becoming more important. The suitability of wood housing in providing the major portion of the needed construction is attested to by its wide use. Approximately three-fourths of all residential housing in this country is currently constructed with wood.

In spite of the wide use and economic importance of wood construction, the current methods used for its design and analysis lag far behind the modern design methods available for other building materials such as steel and reinforced concrete. The structural analysis procedure for wood housing has changed little in the past century and is, for the most part, still based on extremely conservative assumptions. Interaction among the individual pieces of a wood structural system is generally ignored. In addition, due to the wide natural variation in material properties of wood, allowable stresses for design generally have not been based on average material strengths, but on minimum strengths exceeded by all but five percent of all individual pieces. Although this piece-by-piece design method has produced few structural failures, it is generally recognized to be inefficient and uneconomical. It also results in structures displaying a wide range of deflection and vibration response to service load.

The limitations of the design procedures used in wood house construction have long been recognized. The following remarks made by Whittemore in 1948 (50)* still apply to methods currently used in design:

> "Houses have never been designed like engineering structures. Since prehistoric times, safe house constructions have been found by the tedious and wasteful method of trial and error. If the modern research that

---

*Numbers in parentheses refer to entries in the list of references.

> has proved so successful in the solution of other problems had been applied to houses, not only would homes be more satisfactory as dwellings, but, much more important, the cost would be much less. This would be an outstanding contribution to the problem of providing acceptable houses for the low-income groups in this country. . .
>
> There appears to be a great need for the application of sound engineering principles to the development of new construction having just the necessary strength with which to use material efficiently."

The structural joist floor system is a major component of the wood house. Besides its obvious structural purpose, the performance of the floor is more noticeable to the occupant than most of the other components of the house. The floor contains a sizable portion of the materials used in the house, especially larger dimension lumber and thicker sheathing.

The imperative need at this time for a definitive study to place the analysis of wood joist floors on a fully rational basis arises from the highly increased demand for, and cost of housing in recent years. When it is considered that millions of families will purchase homes containing billions of square feet of wood joists floors in the next decade alone, it is evident that even a slight reduction in material requirements, resulting from improved design procedures, will lead to material and monetary savings which will be large in the aggregate.

1.2 Problem Definition

The current design method generally employed for wood joist floor design is based on the simplifying and usually grossly conservative assumption that each component of the structural system behaves independently. The sheathing is assumed to act as a wide beam carrying loads to the adjacent joists and these joists then act alone to carry the loads to the supports. Physically, however, the floor is an extremely complicated system with complex beneficial interactions occurring among its components, interactions which are not recognized in the piece-by-piece design procedure.

In the fall of 1971, an interdisciplinary team of researchers was organized at Colorado State University under the sponsorship of the National Science Foundation (Grant GK-30853) to develop a rational analysis procedure for wood joist floor systems.

The objective of the current study was to develop and verify a mathematical model of wood joist floor systems which recognizes the floor as a multilayer orthotropic planar structural system with interlayer slip, varying interlayer connection properties, discontinuities due to gaps in the sheathing layer, and with variable joist and sheathing material properties.

The major problems to be solved at the inception of the project were the determination of the nature of composite and two-way behavior of joists and sheathing and the response of the floor system to all types of static loads. The basic method of attack was to develop a mathematical model of the system which could then be verified by a full-scale testing program. Finally, using the verified model, a series of parameter studies was planned to establish the nature of the influence of key variables such as the degree of composite and two-way actions on the performance of the system. The scope of the research developed during the course of this study is indicated by the flow diagram shown in Fig. 1.1.

A description of the research completed in each phase of the proposed project as shown in Fig. 1.1 is given in the following chapters of this report. Further descriptions and details are found in the many publications by the principal investigators and research assistants who worked on the project. A list of these documents is given in Section 1.4 of this report.

To aid in understanding the report, several items and concepts which are used throughout are defined here for the reader's convenience.

Interlayer slip, or relative motion between adjoining layers (normally a joist layer and one or two sheathing layers) of a system, results when the connection between layers is not perfectly rigid. Such is the case for nails and elastomeric glues. The ratio between the shear force transferred between layers and the accompanying interlayer slip is given by the slip modulus, k. The slip modulus is a function of both the connector properties and the properties of the materials (stiffness, direction of grain, thickness, etc.) joined in the vicinity of the connector. This modulus is usually nonlinear. Because of interlayer slip, and the presence of shear lag and possible gaps

SCOPE OF RESEARCH PROJECT - NSF GRANT NO. GK-30853

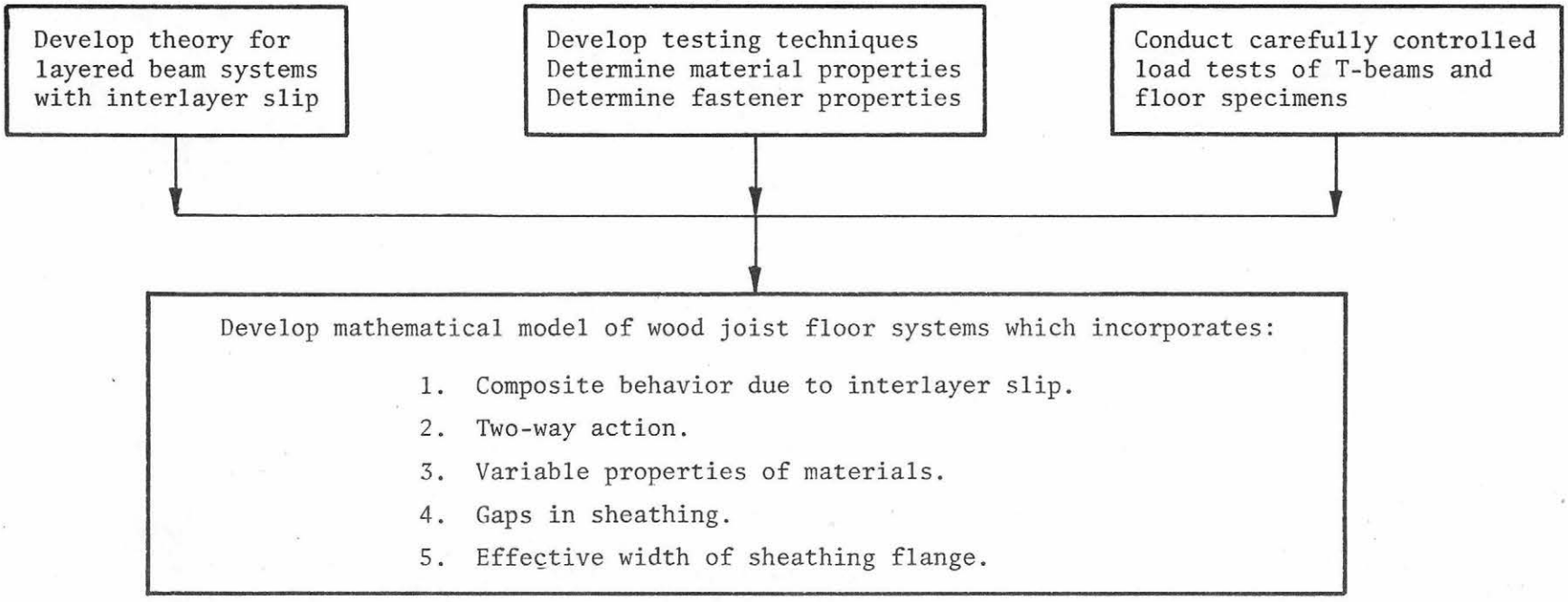

Fig. 1.1 Scope of Research on Wood Joist Floor Systems

in the sheathing, the composite behavior of the layers acting together is one of incomplete composite action. The joist and sheathing layers do not act together as efficiently as a rigidly connected T-beam, but are considerably stiffer than the joist acting alone.

The beneficial effects of the sheathing layer or layers on the performance of the floor system can be conveniently divided into those arising from two-way action and composite or T-beam action. Both effects are highly dependent upon the magnitude of the slip modulus and the presence of gaps.

Sheathing perpendicular to the joists acts to minimize deflection differences between adjacent joists and consequently can transfer loads between the joists (load sharing). This results in a two-way action allowing the system to act as an orthotropic plate.

1.3 Brief Review of the State-of-the-Art for T-beam and Floor Analysis

Work done or in progress at the time of the beginning of the project is reviewed briefly herein. Detailed reviews of the literature and research activities of other investigators can be found in the several papers, theses and dissertations produced during the duration of the project and listed in Section 1.4 below.

A theoretical basis for the analysis of one of the components of the system, the layered beam, has been developed previously by several authors. Clark (16) developed a theory for layered systems connected by spaced rigid connections. Granholm (34) presented a theory for doubly symmetric cross sections which included effects of interlayer slip. Pleshkov (62) developed a theory for multilayer systems which generalized the work of Granholm. Newmark, Siess, and Viest (55) considered the problem of incomplete interaction between the steel beam and composite concrete slab of composite I-beam systems. Test results for this system were presented in a later paper (68). A method based on sandwich theory for beams was developed by Norris, Ericksen, and Kommers (57), and extended by Kuenzi and Wilkinson (44). An extensive treatment of interlayer slip problems for beams, plates, and shell structures has been made by Goodman (26,27,28,32). Goodman also conducted a series of experiments with layered wood beams and plates which showed good agreement with the developed theory. Other studies

on layered beams have been performed by Amana and Booth (1,2,3,4). Reported theoretical and experimental studies on floor systems include those by Polensek (63,64,65) and Sliker (69,70). Field-glued plywood T-beams and floors were tested by Rose (66), wherein up to a 66 percent increase in calculated floor stiffness was noted due to composite behavior. Experimental work on floors has also been reported by the NAHB Research Foundation (49). Atherton and Corder (13) reported on tests of wood joists floors which showed a factor of safety of 3.9 to 5.5 using ultimate load to working load as the measure of safety. Onysko reviewed the literature on floor studies (59) and generally concluded that although the strength of floors is more than adequate, the entire problem of deflections, which includes computation of stiffness and deflections for concentrated and uniformly distributed loads, required definitive study.

Thus the current state-of-the-art for design and analysis of wood floor systems is clearly inadequate to meet the challenges of the future requirements for housing. The research described in this report is a concentrated effort to develop new methods of rational analysis which will lead to a general increase in the knowledge of the behavior of wood joist systems. Such knowledge has broad implications for upgrading design methods, insuring adequate performance, and improving efficient use of critical natural resources.

1.4 List of Publications to Date - NSF Grant No. GK-30853

The following publications have been completed or are in progress as a result of the work of the research staff of the project.

Papers:

Vanderbilt, M. D., J. R. Goodman, and M. E. Criswell, "Service and Overload Behavior of Wood Joist Floor Systems," Presented at the ASCE Structural Engineering Meeting, San Francisco, California, April 1973. (Published in Journal of the Structural Division, Vol. 100, No. ST1, January 1974.)

Goodman, J. R., M. D. Vanderbilt, M. E. Criswell, and J. Bodig, "Composite and Two-Way Action in Wood Joist Floor Systems," Presented at the Forest Products Research Society Annual Meeting, June 1973. (Published in Wood Science, Vol. 7, No. 1, July 1974.)

Goodman, J. R., M. E. Criswell, M. D. Vanderbilt, and J. Bodig, "Implications of Rational Analysis of Wood Joist Housing Floor Systems," Accepted for publication and presentation, Third International Symposium of International Association for Housing Science, May 1974, Montreal, Canada.

Vanderbilt, M. D., J. R. Goodman, M. E. Criswell, and J. Bodig, "Development and Verification of a Mathematical Model of Wood Joist Floors Using Computer Analysis and Closed-Loop Structural Testing," Closed-Loop Magazine, MTS Corporation, Fall/Winter 1973.

McLain, T. E. and J. Bodig, "Determination of Elastic Parameters of Full Size Wood Composite Boards," Presented at the Forest Products Research Society Annual Meeting, Anaheim, California, June 1973. (Published in Forest Products Journal, Vol. 24, No. 4, April 1974.)

Theses:

Penner, B., "Experimental Behavior of Wood Flooring Systems," M.S. Thesis, Civil Engineering Department, Colorado State University, January 1973.

Ko, M. F., "Layered Beam Systems with Inter-layer Slip," M.S. Thesis, Civil Engineering Department, Colorado State University, January 1973.

Patterson, D. W., "Nailed Wood Joints Under Lateral Loads," M.S. Thesis, Forest and Wood Sciences Department, Colorado State University, March 1973.

McLain, T. E., "Determination of Elastic Parameters of Full Size Wood Composite Boards," M.S. Thesis, Forest and Wood Science Department, Colorado State University, June 1973.

Kuo, M. L., "Verification of a Mathematical Model for Layered T-Beams," M.S. Thesis, Civil Engineering Department, Colorado State University, March 1974.

DeBonis, A. L., "Combined Loading Effects on Nailed Wood Joints," M.S. Thesis, Forest and Wood Sciences Department, Colorado State University, June 1974.

Liu, J. S., "Verification of a Mathematical Model for Wood Joist Floor Systems," Ph.D. Dissertation, Civil Engineering Department, Colorado State University, August 1974.

Dawson, P. R., "Variability Simulations of Joist Floor Systems," M.S. Thesis, Civil Engineering Department, Colorado State University, September 1974.

Tremblay, G. A., "Nonlinear Analysis of Layered T-Beam with Interlayer Slip," Civil Engineering Department, Colorado State University, September 1974.

Several papers based on studies reported in the theses and dissertations above are in progress.

2. DEVELOPMENT OF MATHEMATICAL MODELS

2.1 Introduction

The wood joist floor is an extremely complex structural system. Not only is it usually multilayered with each layer made of orthotropic materials, but in nailed and elastomerically-glued systems there exists an interlayer slip of sufficient magnitude to significantly affect the deflection behavior of the system. These factors, coupled with the variability of the material in each element and the presence of gaps, require a sophisticated analysis procedure to successfully predict the system performance. The objective of this section is to describe the development of mathematical models for wood joist T-beam and floor systems. Only a summary of the key features of the theoretical work is given. For more detailed discussions of each subject area, the reader is referred to the papers and theses on individual topics listed in Section 1.4. Specific references are made to previous work by the investigators and other researchers.

2.2 Theoretical Studies of Layered T-Beams

The basic theory for a two-layered beam with mechanical connectors or nonrigid glued connections as shown in Fig. 2.1a,b is reviewed here. A more detailed treatment of the theory can be found elsewhere (42,45,73). This theory forms the basis for all the analysis methods used in the development of the mathematical models.

The following assumptions are made in the analysis:

1. Materials are linearly elastic,
2. Deflections are small,
3. Shear deformations are neglected,
4. Strains over the depth of each layer are linear,
5. The slip modulus is linear,
6. Friction between layers is negligible, and
7. Each layer is bent to the same radius of curvature.

Based on these assumptions, the curvature for each layer of the element in Fig. 2c, from elementary beam theory, is given by

$$\frac{d^2y}{dx^2} = -\frac{M_i}{EI_i} \qquad [1]$$

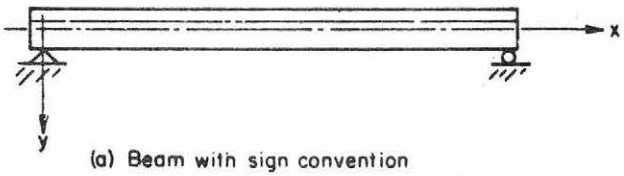

(a) Beam with sign convention

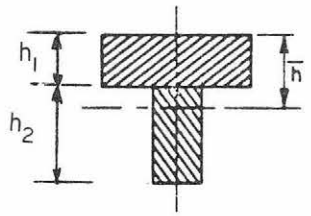

(b) Cross section

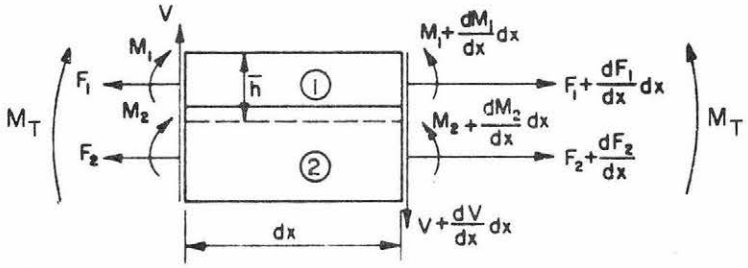

(c) Beam element

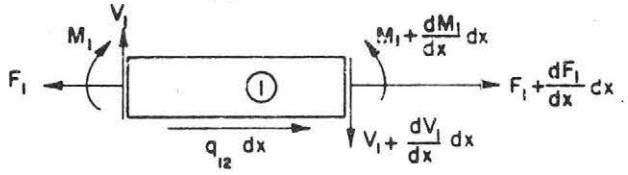

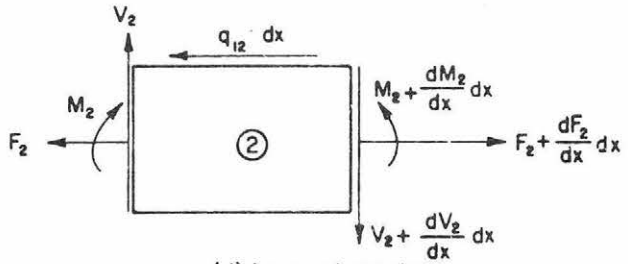

(d) Layer elements

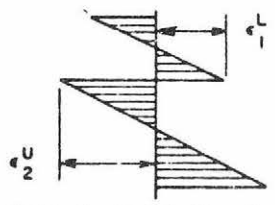

(e) Strain distribution in layers

Fig. 2.1 Two Layer Beam System

where I_i = the transformed moment of inertia of the ith layer about its own centroidal axis (in.^{4}) and E = Young's modulus for the reference layer (the joist E in most applications). Applying the equations of equilibrium to the beam element of Fig. 2.1c and utilizing Eq. [1] leads to

$$\frac{d^2y}{dx^2} = -\frac{M_T + C_{12}F}{\sum EI_i} \qquad [2]$$

where $F = -F_1 = +F_2$ and $C_{12} = \frac{h_1 + h_2}{2}$.

The second equation in the two basic variables, y and F, is found from the slip relationship between the layers. Figure 2.1d shows the interlayer shear flow, q_{12}, which must be resisted by the connectors. Since the connectors are not considered to be rigid, the resulting slip is a function of the stiffness of the connectors. For mechanical connectors, the effective interlayer connection is given by the equation

$$\Delta_{s_{ij}} = (s/kn)_{ij}\, q_{ij} \qquad [3]$$

where $\Delta_{s_{ij}}$ = the interlayer slip (in.),

q_{ij} = interlayer shear flow (lb/in.) (Fig. 2b),

s = spacing of connectors (in.),

n = number of connectors per row (usually n = 1 for floors),

k = slip modulus of connector (lb/in.).

For a glued system, the term s/kn is modified to account for the area on which the glue acts.

The interlayer shear flow is evaluated by considering horizontal equilibrium for the top layer of Fig. 2.1d which gives

$$q_{12} = \frac{dF}{dx} \qquad [4]$$

Combining Eqs. [3] and [4] results in

$$\Delta_{s_{12}} = \frac{s}{kn}\frac{dF}{dx}. \qquad [5]$$

The strains shown in Fig. 2.1e are evaluated by considering the effects of the moments and axial forces giving

$$\varepsilon_1^L = \frac{M_1}{EI_1}\frac{h_1}{2} - \frac{F}{EA_1}$$

$$\varepsilon_2^U = -\frac{M_2}{EI_2}\frac{h_2}{2} + \frac{F}{EA_2} \qquad [6]$$

where, with tensile strain taken as positive,

ε_1^L = the strain at the lower surface of the first layer,

ε_2^U = the strain at the upper surface of the second layer, and

A_i = the transformed area of the ith layer.

The interlayer slip over a length x is obtained by integration of the strains in Eq. [6] to give

$$\Delta_{s_{12}} = \int_o^x \varepsilon_2^U \, dx - \int_o^x \varepsilon_1^L \, dx \qquad [7]$$

Substituting Eqs. [6] and [1] into Eq. [7], equating the result to Eq. [5], and differentiating to remove the integration in Eq. [7], leads to

$$\frac{s}{kn}\frac{d^2F}{dx^2} = \left(\frac{1}{A_1} + \frac{1}{A_2}\right)\frac{F}{E} + C_{12}\frac{d^2y}{dx^2} \qquad [8]$$

Equations [2] and [8] represent the governing equations of the beam system for static loading. These equations may be rewritten in operator form with a change in variable, $z = x/L$, introduced to give

$$\begin{bmatrix} \left\{\frac{\Sigma E_i}{L^2} - D^2\right\} & \left\{-C_{12}\right\} \\ \left\{C_{12}\frac{D^2}{L^2}\right\} & \left\{-\frac{s}{kn}\frac{D^2}{L^2} + \frac{1}{E}\left(\frac{1}{A_1} + \frac{1}{A_2}\right)\right\} \end{bmatrix} \begin{Bmatrix} y \\ F \end{Bmatrix} = \begin{Bmatrix} -M_T(z) \\ 0 \end{Bmatrix} \qquad [9]$$

where $D^2 = d^2/d^2z$.

Solving Eq. [9] simultaneously for F and simplifying the results leads to

$$\frac{d^2F}{dz^2} - C_1 F = - C_2 M_T(z) \qquad [10]$$

where

$$C_1 = \frac{knL^2}{sE} \left(\frac{1}{A_1} + \frac{1}{A_2}\right) + \frac{C_{12}^2}{(I_1 + I_2)} \qquad [11]$$

and

$$C_2 = \frac{knL^2}{sE} \frac{C_{12}}{(I_1 + I_2)} \qquad [12]$$

Solving Eq. [9] for y and simplifying leads to

$$\frac{d^2y}{dz^2} = - \frac{M_T(z)L^2}{EI_s} + \frac{L^2}{C_1} \frac{C_{12}}{\Sigma EI_i} \frac{d^2F}{dz^2} \qquad [13]$$

where I_s = moment of inertia if the cross section of Fig. 2.1b acts as a solid section. Direct integration of Eq. [13] for a simply supported beam results in

$$y = y_s + \frac{L^2}{C_1} \frac{C_{12}}{\Sigma EI_i} F \qquad [14]$$

Deflections of any simply supported, two-layer T-beam can be computed by solving Eqs. [10] and [14]. This analysis forms the basic theory used throughout the study. An extension of this theory, to allow solution of three-layer beams has been presented in theses by Ko (42) and Kuo (45). Numerical methods of solution must be employed to handle conditions encountered in solving real beams. In particular, gaps in the sheathing layers present discontinuities in the layers of the T-beam or floor and must be handled by other than closed-form solution techniques. Two methods of treating variation of mechanical properties and gaps were developed, a finite difference and a finite element technique. Details of these methods are discussed in subsequent sections.

2.3 Mathematical Models for T-beam Analysis

As discussed in Sec. 2.2, basic theoretical methods of analysis have been developed for layered beams which account for incomplete

composite action due to interlayer slip between the layers. Since closed-form solutions cannot be obtained for real beams which have variable material properties and discontinuities at joints in sheathing layers, it was necessary as a basic part of the research project to develop the numerical methods of solution described in this section.

The first numerical method considered utilized finite differences. Based on the basic equations as developed for the case of a two-layered T-beam in Sec. 2.2, this solution technique leads to a set of simultaneous equations which can be written as

$$[H]\{F\} = \{C_2 L^2 M\} \qquad [15]$$

where [H] = square matrix combining all finite difference operators,
L = length of the simply-supported beam,
M = moment, and
{F} = vector of axial forces in the layers.

The deflections at the node points of a rigidly connected beam, $\{y_s\}$, can be obtained from

$$[R]\{y_s\} = \{-\frac{6qL^4}{n^2 EI_s}(1 - z)z\} \qquad [16]$$

where [R] = square matrix combining all finite difference operators, and
$z = x/L$, $0 \leq z \leq 1$.

Once {F} and $\{y_s\}$ are solved from Eqs. [15] and [16], the total beam deflection y can be computed from Eq. [14].

Numerous beam solutions were calculated by this method and were presented by Ko (42). Attempts were made to incorporate the effect of gaps in sheathing layers on the behavior of beams using this method. It was found that this technique was not satisfactory and solution of the problems of gaps required further development using the finite element method.

Thus, the limitations of the closed-form and finite difference approaches, required the development of a more versatile technique to allow consideration of the properties displayed by real floors and beams including gaps in the sheathing.

Thompson (72) developed a finite element method using the methods of potential energy and the same mathematical model and basic assumptions presented in Sec. 2.2. Energy expressions from the following sources are evaluated for the solution of the layered beam problem:

1. pure bending of each layer,
2. axial elongation of each layer,
3. slip deformation of the connectors between each layer, and
4. external loads on the beam.

By including all the potential energy resulting from the forces above, the total potential energy of an m-layered beam is

$$J = \sum_{i=1}^{m} \int_{o}^{L} \{\tfrac{1}{2} E_i I_i \left(\frac{d^2y}{dx^2}\right)^2 + \tfrac{1}{2} E_i A_i \left(\frac{du}{dx}\right)^2\} \, dx$$

(bending) (axial loads)

$$+ \sum_{i=1}^{m-1} \int_{o}^{L} \tfrac{1}{2} \left(\frac{k_i n_i}{s_i}\right) \left[(u_{i+1} - u_i) - \tfrac{1}{2} (h_{i+1} + h_i) \frac{dy}{dx}\right]^2 dx$$

(slip deformation)

$$- \int_{o}^{L} qy \, dx \qquad [17]$$

(external loads)

where J = total energy, in.-lbs, and

u_i = axial displacement in ith layer, in.

Equation [17] is valid for positive y directed upwards.

The principle of virtual work requires that the potential energy reach a stationary value at the equilibrium position of the layered beam. Using the variational principle, this requirement may be expressed as

$$\delta J = 0 \qquad [18]$$

where δ = variational operator.

The deflection and axial displacements of the layered beam must satisfy Eq. [18] and can be approximated with the finite element form of the Rayleigh-Ritz procedure. This method allows direct solution of the differential equation using an approximate minimization of the

functional (72). Formulation of the finite element solution technique is presented in detail by Kuo (45) and Liu (46).

The three solution methods discussed yield nearly identical answers when the limitations of the methods are met. This can be demonstrated by comparing the deflections predicted by each method for the same problem. As an example, consider a two-layer beam with the following properties:

Joist MOE = 2.43×10^6 psi
Plywood MOE = 5.50×10^5 psi
Slip modulus k = 30,000 lb/in.
Nail spacing = 8 in.
Concentrated load at midspan = 500 lb.

Midspan deflections for this example obtained by each method using separate computer programs are listed in Table 2.1 along with a comparison of the predicted deflections. Because of its closeness to the exact (closed form) solution and its many earlier cited advantages, the finite element method was used to compute the theoretical deflections in all the subsequent verification studies of the research project. This method forms the basic solution method for the beam analysis part of the floor model. Results of the verification studies to prove the usefulness of the mathematical model for T-beams are presented in Section 5.2.

Table 2.1 Comparison of Solution Techniques

Technique	Closed Form	Finite Difference	Finite Element
Centerline Deflection	0.1980"	0.1985"	0.1978"
Difference, %	-	0.24	0.10

2.4 Mathematical Models for Wood Joist Floor Systems

The wood joist floor is a highly indeterminate and complex structural system. Proper analysis methods must include effects of incomplete composite action, two-way behavior, effect of gaps in sheathing layers, and numerous other variables as described previously.

Simplification of this complex system is required to allow development of a practical analysis method. Any such simplification must be carefully chosen so as to represent a conservative approximation to the complete behavior of the system.

The basic scheme chosen for the analysis of wood joist floor systems is the idealization of the complex system as a set of crossing beams. A schematic for this method is shown in Fig. 2.2 for a two-layer system. Each of the T-beam strips consists of a joist plus a sheathing flange usually taken to be equal in width to the joist spacing, although any effective width may be used. Each of the sheathing strips for a two-layer system consists of a beam of sheathing spanning in the transverse direction of the joist and of any chosen width. While a two-layer system is illustrated, the analysis method is valid for n-layered systems.

Assuming the floor to be represented by a system of crossing beams ignores the contribution of the torsional stiffnesses of the sheathing and T-beams. As the G/E ratio for plywood is small, neglect of its torsional stiffness is felt to represent a small error. Likewise the torsional stiffness of a T-beam section is small compared to its bending stiffness. Deflections computed using the crossing-beam model may be expected to be slightly greater and therefore conservative, than if torsional stiffnesses were included.

The solutions of the layered beam theory discussed in Sec. 2.1 - 2.3 can now be applied to each system of crossing beams. Each system of beams is first considered separately and then a set of compatibility equations are written insuring equal deflections at the intersections of each system of beams. Both finite difference and finite element schemes were employed using this basic analysis procedure and each are outlined in this report. More details of each method are given by Liu (46).

A finite difference form of the solution of the physical representation of the floor system as a crossing beam problem was developed by Vanderbilt, et al. (77). For this solution a matrix theory was used in the form of the flexibility approach (76). Variability of material properties and beam geometry were incorporated in this method. However, it was found that the problem of gaps in the sheathing

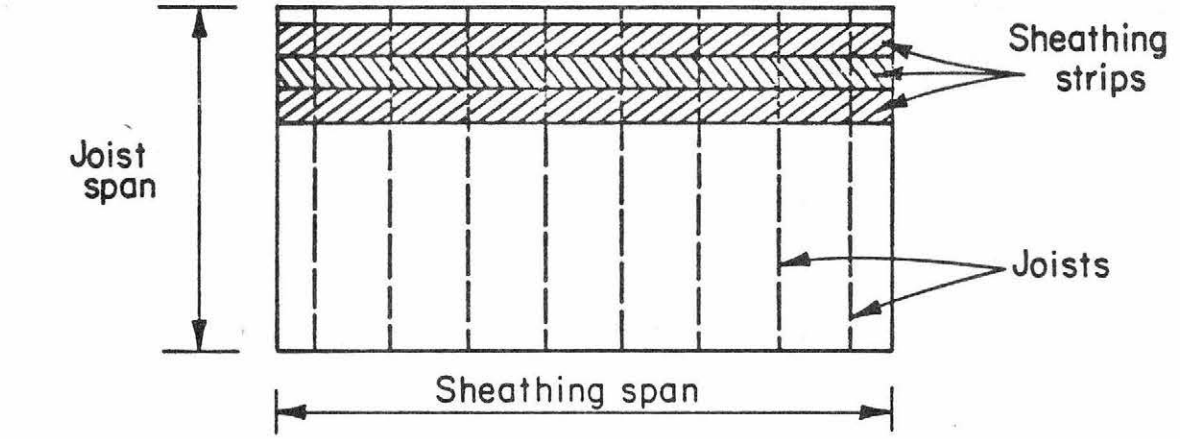

(a) Plan view of floor system

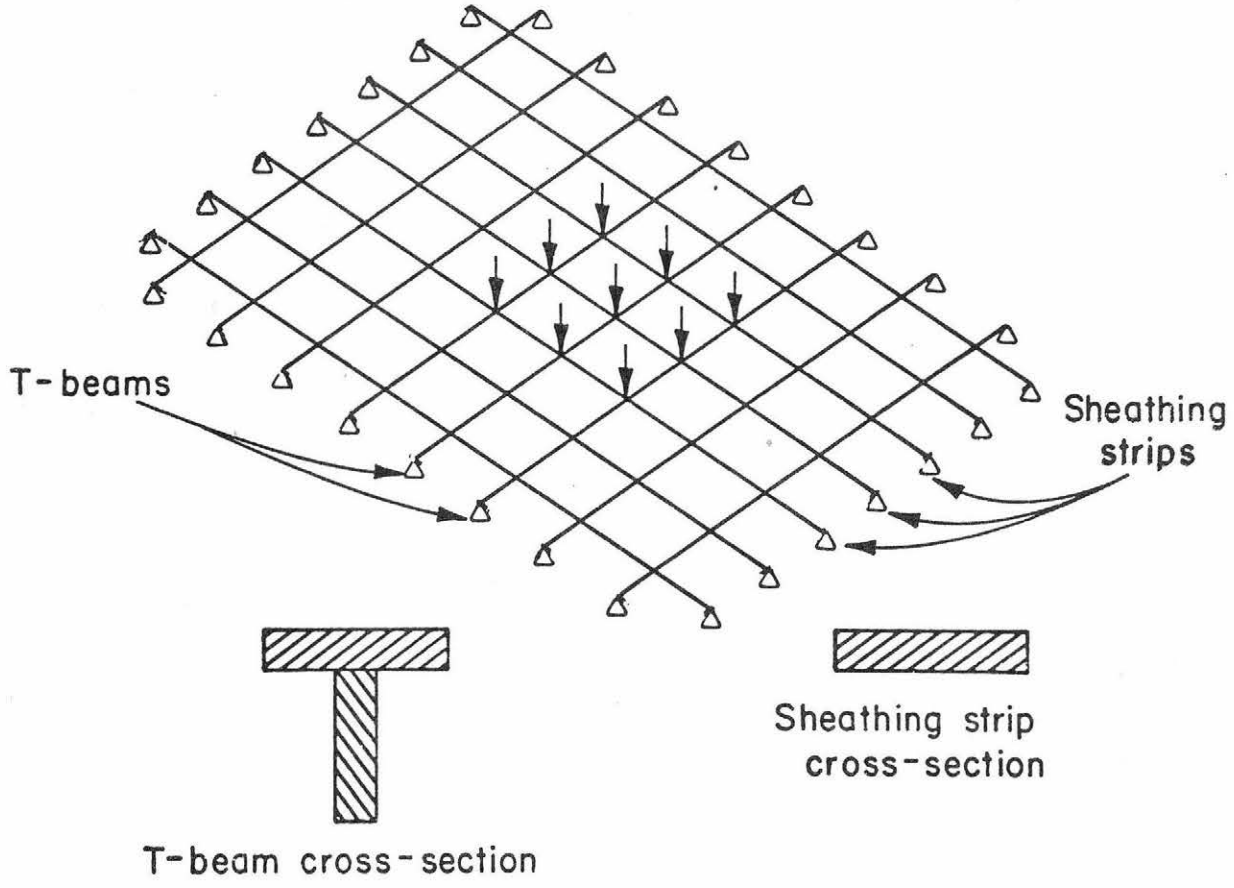

(b) Schematic of crossing beam idealization

Fig. 2.2 Idealization of Floor System

layers could not be adequately treated by use of this procedure, which necessitated the development of a finite element procedure.

The steps involved in the flexibility approach using the finite difference method are as follows.

The load-deflection behavior of the set of T-beams acting alone is given by

$$DT = FT * AT \qquad [19]$$

where DT = matrix of deflections of T-beams, FT = flexibility matrix of T-beams, and AT = matrix of loads carried by joists. The flexibility matrix FT is calculated by applying a unit load successively at each nodal point on each beam using the analysis procedure described in the preceeding section. Similarly for the sheathing strips acting alone

$$DS = FS * AS \qquad [20]$$

Equilibrium of the system requires that

$$AT + AS = A \qquad [21]$$

where A = matrix of loads applied at nodal intersection points.

Compatibility of deflections is satisfied by requiring that the two beams crossing at each node point undergo the same deflection, thus

$$DS = DT = D \qquad [22]$$

where D = matrix of nodal deflections.

Substituting Eqs. [19], [20], and [21] into Eq. [22] and simplifying the result gives

$$(FT + FS) * AT = (FS*A) \qquad [23]$$

from which

$$AT = (FT + FS)^{-1} (FS*A) \qquad [24]$$

Finally with AT determined from Eq. [24], the deflections, D, may be computed using Eq. [19]. Since large matrices are involved in each of these computations, a high speed computer with adequate storage is essential to efficiently handle the computations necessary.

A finite element model using the same basic assumptions of the crossing-beam analogy was developed by Thompson (72) to provide the required sophistications of analysis needed to handle actual floor

systems. In particular, it was found that the problem of gaps in the sheathing layers was best modeled by this procedure. Gaps are treated by the insertion of an element representing the gap which has zero length and may be either flexible or of zero axial stiffness depending on the physical character of the gap being modeled. Methods of treating various gaps were developed by Kuo (45) and extended to use in the floor model by Liu (46).

2.5 Effective Flange Width and Sheathing Modulus Considerations for Mathematical Models

The basic mathematical model for T-beams or floors developed during the course of the research project assumes the use of ordinary beam theory in calculations of deflection behavior of the system. For certain cases of joist spacing in floors, the width of the assumed sheathing flange may be such that shear lag may occur in the flange. To insure that ordinary beam theory may be correctly used in the analyses, computations for effective flange width were made by Liu (46). A series of parameter studies on the effects of the variables involved were conducted to determine the individual influence of each on the effective flange width. Liu (46) reported on the results of these studies which show that the primary variable involved is the width of available flange (joist spacing in a floor). While other variables have minor influence and the effective flange actually varies along the length of the beam element, the practical results may be summarized as shown in Table 2.2.

Table 2.2 Recommended Effective Flange Width for Uniform Load on a Wood Joist Floor System

Joist Spacing (in.)	Effective Flange Width (in.)
16	16
24	22.5
36	31
48	37

Use of plywood sheathing requires special handling in the mathematical models. To simplify the model, the gross cross-sectional dimensions of the sheathing element were used. Since the effective MOE in bending and in axial loading are not equivalent for plywood if the gross section is used as a homogeneous element, adjustments to properly compensate for this effect were made. A parameter defined as K* was introduced as follows:

$$E_{ea} = K^* E_{eb} \qquad [25]$$

where E_{ea} = effective modulus of plywood in axial load based on gross section, and

E_{eb} = effective modulus of plywood in bending based on gross section.

The parameter, K*, may be calculated from the following equation:

$$K^* = \frac{I_g}{I_t} \frac{A_t}{A_g} \qquad [26]$$

where I_g = moment of inertia of the plywood based on the gross section,

A_g = area of the plywood based on the gross section,

I_t = moment of inertia of the plywood based on transformed section,

A_t = area of the plywood based on the transformed section.

Further details of the development of the parameter K* are given by Liu (46). Calculations of K* can easily be made for any commercial plywood by referring to the Plywood Design Specification (7).

2.6 Example Results of the Application of Mathematical Models to a Wood Joist Floor System

Deflections of a typical example floor were calculated using the finite difference and finite element forms of the mathematical model. The details of the assumed floor are shown in Fig. 2.3. A uniform MOE for all the 2 x 8 joists was used to illustrate the difference between the current design method of considering only the joists to carry the floor loads. Results of the analysis are shown in Table 2.3.

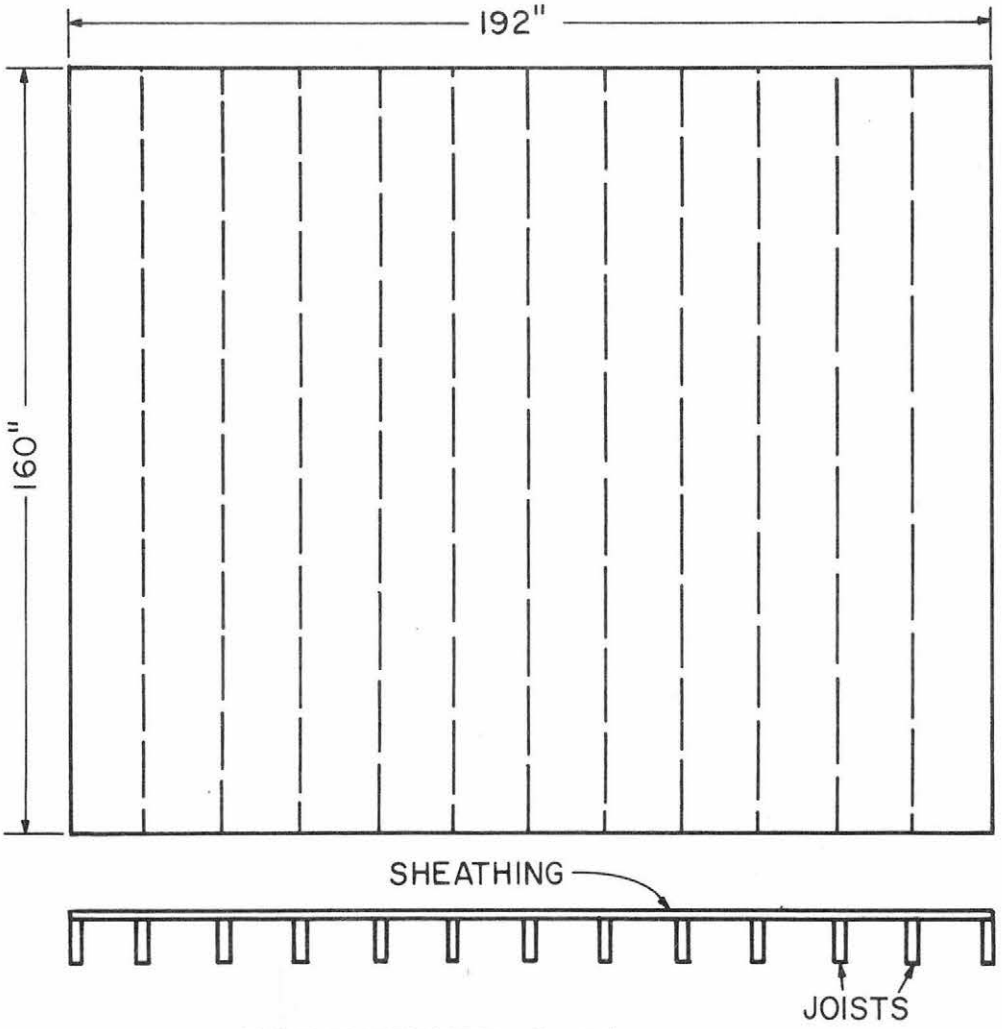

NOMINAL JOIST DIMENSION = 2 × 8 in.
SHEATHING THICKNESS = 0.75 in.
SLIP MODULUS = 30,000 lb/in.
NAIL SPACING = 8 in.
SHEATHING MOE
    ∥ TO SURFACE GRAIN = 1,361,000 psi
    ⊥ TO SURFACE GRAIN = 523,000 psi
UNIFORM LOAD = 40 psf

Fig. 2.3 Configuration and Data for Floor Example

Table 2.3 Calculation of the Deflection Behavior of an Example Wood Joist Floor System for Uniform Load

	Mathematical Model and Assumed Gap Conditions				
	Finite Dif. No Gaps	Finite Element No Gaps	Finite Element Flexible Gaps[1]	Finite Element Open Gaps	Joist Only[2]
Maximum Floor Deflection (in.)	0.266	0.244	0.315	.386	.422

[1]Represents tightly butted T & G joints, MOE of gap = 5000 psi.

[2]Joist only = current design method. L/360 deflection = 0.44 in. where L = span

The influence of gaps in the sheathing is clearly evident in this example as are the differences between the behavior of the floor as predicted by the model and the current method of design. Differences between current design and the predicted deflection are more striking for concentrated loads since current methods assume all the load acts on a single joist whereas the mathematical models properly account for the two-way composite action of the floor system.

To demonstrate the full effects of composite and two-way action, the deflections of an example floor were computed using the finite difference form of the mathematical model for the case of uniform load. Floor data include 2 x 8 nominal joist sizes, nail spacing of 8 in. with 1 nail per row, and floor dimensions of a 12 ft span and 16 ft width. The face grain of the sheathing was assumed to be perpendicular to the joist span. The effect of gaps in the sheathing was not included in this example. The floor contained 11 T-beam and 11 sheathing strip components. Simple supports were assumed at all edges of the floor. This example was analysed for four conditions: 1) joists only carrying loads which is the current design assumption, 2) distribution of loads by two-way action but neglecting composite or T-beam action, 3) composite action due to 8 in. nail spacing and k = 30,000 lbs/in. with no two-way action, and

4) complete composite and two-way action as predicted by the complete mathematical model. In addition, the MOE values of the joists were varied as shown to simulate a possible actual case.

The results of these analyses, shown in Fig. 2.4, clearly demonstrate the importance of the composite and two-way behavior of wood joist floor systems. The differences in deflections as predicted by the various assumptions range up to greater than 100 percent when deflections of the joists acting alone are compared with those predicted by the complete mathematical model. Since design of wood joist floors is currently based on neglecting the contributions of the composite and two-way actions, the deflections predicted are greatly overestimated. In addition, the smoothing out of deflection behavior by two-way action is demonstrated to be significant as evidenced by comparison of the various cases. This example shows the need for recognition of the complete behavior of the system including full recognition of both composite and two-way action.

Verification studies of the use of the models for T-beams and floors are presented in Chapter 5. The fully verified mathematical model provides a tool with great promise for development of new design procedures which properly account for the observed behavior of wood joist floor and beam systems.

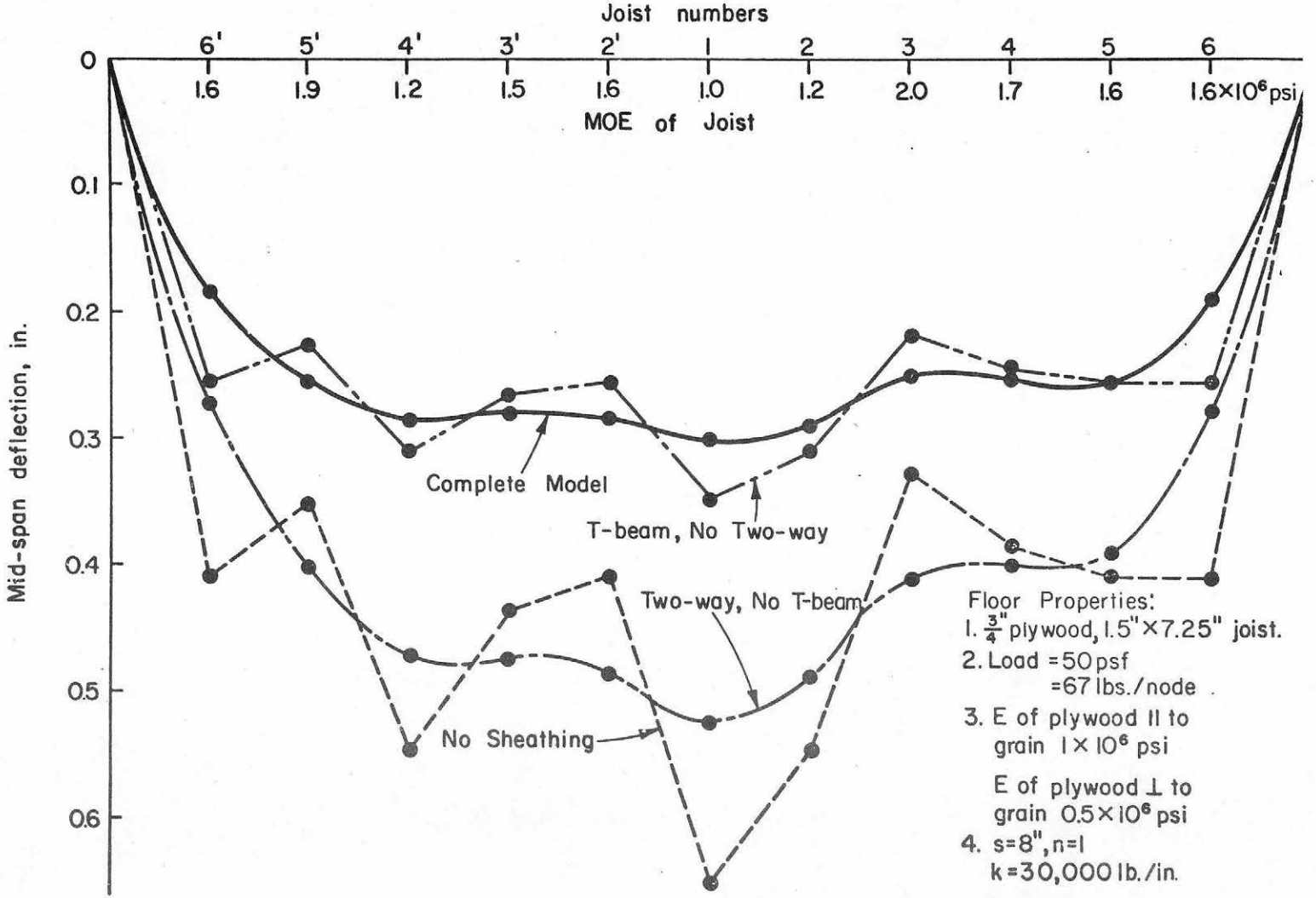

Fig. 2.4 Composite and Two-Way Behavior of Wood Joist Floor System with Varying Joist Moduli.

3. MATERIALS RESEARCH

3.1 Introduction

The mathematical model of the wood-joist floor system predicts the performance of floors utilizing the principles of mechanics and the properties of the materials composing the structure. Thus, both for the verification of the model and for its future use as a design tool, knowledge of material properties is essential.

For the first phase of the study, the model was developed to predict the deflections of T-beams and floors within the elastic range. Thus, knowledge of some of the elastic parameters of the joist and the sheathing materials are needed. Since the tests on the floor systems were carried out to destruction, the elastic parameters of the materials had to be evaluated in advance using nondestructive testing techniques. For each joist the modulus of elasticity along its length was determined by bending each member as a plank. For the sheathing material two moduli of elasticity in the plane, one parallel and the other perpendicular to the long axis of the sheathing were evaluated. During the course of the materials research other properties and testing techniques were also evaluated for the wood components.

Due to the nature of the fasteners used in floors, slippage occurs between the layers. The magnitude of this slip depends on the stiffness of the connection, which in turn determines the degree of interaction between the layers. Therefore, the measure of this stiffness, the slip modulus of the connector and the connected layers, must be evaluated to allow proper analysis of the systems.

Research done on material properties and slip moduli is discussed in more detail in the following sections. Complete accounts of the methods used and results obtained are available in individual papers, theses and dissertations (20,47,48,58,60,61).

3.2 Joist Properties

Two species of joist material, Douglas-fir and Engelmann spruce, were selected for use in the experimental verification of the mathematical model phase of the research. Douglas-fir was chosen because of the large volume of its use in residential floor systems and because it represents the upper range of strength and stiffness for softwood lumber. Engelmann

spruce was selected because it represents a lower range of strength and stiffness of softwood lumber used in construction. By the selection of these two species, the effects of extreme cases of material properties could be investigated.

A total of 420 pieces of 2 x 8 and 2 x 12, sixteen-foot long joist material were used in the study. Select Structural and No. 3 grades were the two qualities represented. The moisture content of the material was that commonly found in dimension lumber, ranging from 8 to 12 percent. The moisture content was determined for each piece by an electrical resistance moisture meter, both before and after testing of the floor and T-beam specimens.

Each piece of dimension lumber was first tested nondestructively as a plank on a continuous deflection machine. A schematic of this test setup is shown in Fig. 3.1 and has been described previously (58,61). The span between the supports was 3 ft allowing the evaluation of the MOE along the length of the joist for all but the end 1.5 ft of the member. The MOE values were obtained at each one foot interval. The average MOE and its standard deviation for each species, size and grade are summarized in Table 3.1.

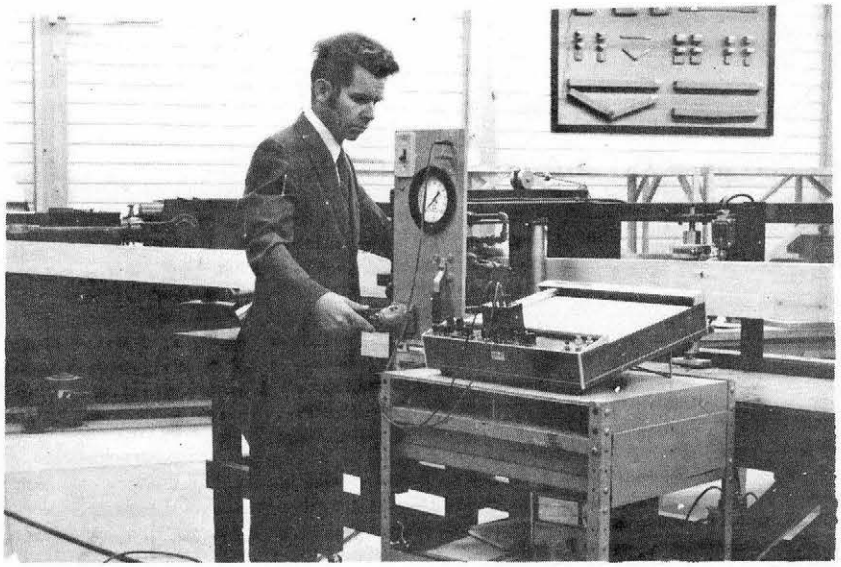

Fig. 3.1 Continuous Deflection Device for MOE of Joists

Table 3.1 Flatwise Modulus of Elasticity and its Variation for Joist Material

Species	Grade	Nominal Dimensions, in.	Sample Size	Mean (10^6 psi)	Stand. Dev. (10^6 psi)	Coeff. of Variation (%)
Douglas-fir	Select Struct.	2 x 8	90	1.707	0.3674	21.5
		2 x 12	64	1.486	0.2754	18.5
	No. 3	2 x 8	96	1.482	0.3806	25.7
		2 x 12	62	1.308	0.2230	24.3
Engelmann Spruce	Select Struct.	2 x 8	28	1.132	0.2040	18.1
		2 x 12	27	1.062	0.1690	16.0
	No. 3	2 x 8	72	1.024	0.1910	18.7
		2 x 12	46	0.890	0.1430	16.1

The lumber was cut to 12 ft - 2 in. lengths by removing equal amounts at each end of the 16 foot long pieces. This center portion was used to construct the test floors. The end pieces from the 2 by 8 material were used for the load-slip study, described in Section 3.4.

Additional testing was conducted for each joist used in construction of T-beam and floor specimens. To insure accurate MOE values for the verification studies of the mathematical model, each joist was also tested as a simple beam in an edge-wise configuration just prior to beam or floor construction. Details of this in-place testing are described in Sections 4.3 and 4.4.

3.3 Sheathing Material Properties

Nondestructive testing of full-size sheathing materials had not been reported in the literature when the project began. As a consequence, a testing technique had to be developed to obtain the needed elastic parameters of full-size sheathing materials.

The method developed permitted the evaluation of the two moduli of elasticity for each piece of sheathing, parallel to long and short axes of the sheathing material, under both static and dynamic loading. Further, the in-plane modulus of rigidity of the sheathing material also was evaluated. Complete details of the testing method are described elsewhere (47,48).

The MOE's were evaluated on the basis of beam bending using the arrangement shown in Fig. 3.2. The following equation was used to compute the moduli of elasticity in each direction

$$E = \frac{Pb^2L}{3I\Delta} \qquad [27]$$

where:

Δ = deflection (in.),
P = applied line load (lb),
b = length of overhang (in.),
L = length of beam (in.),
E = modulus of elasticity (psi), and
I = effective moment of inertia ($in.^4$).

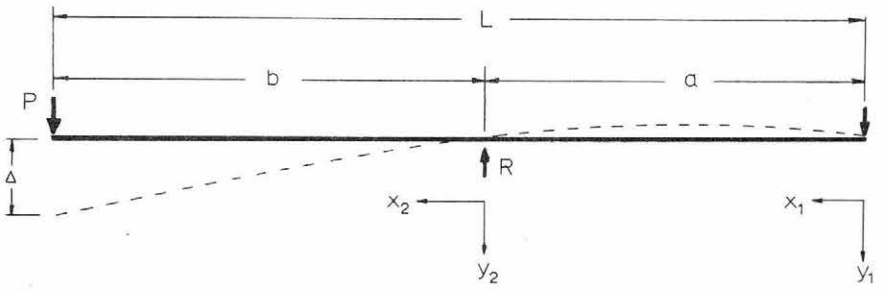

Figure 3.2 Overhanging Beam Arrangement used for the Evaluation of Static and Dynamic Moduli of Elasticity of Sheathing Materials

The dynamic modulus of elasticity E_d was evaluated by the same setup considering the beam to be in free vibration. The following equation to compute the dynamic modulus of elasticity was derived on the basis of potential and kinetic energies:

$$E_d = \frac{24\pi^2 f^2}{gI_t[P^2(b^3+b^2a)+6W^2(D)]}\left[WP^2(A+B)+P^3C+\frac{W^3}{2}(H+F)\right] \quad [28]$$

where:

E_d = dynamic MOE (psi),
P = applied load at end of overhang (lb),
a = length of the span of the beam (in.),
b = length of the overhang (in.),
W = weight of beam per unit length (lb/in.),
f = fundamental frequency (cycles/sec),
g = acceleration due to gravity (in./sec^2),
I_t = transformed moment of inertia (in.^{4}),

$$A = \frac{2b^2a^5}{945},$$

$$B = \frac{b^5a^2}{27} + \frac{11b^6a}{180} + \frac{33b^7}{1260},$$

$$C = \frac{b^4a^2 + 2b^5a + b^6}{18},$$

$$D = \frac{a^5 - 5b^2a^3 + 10ab^4}{34560},$$

$$F = \frac{a^2b^7}{108} - \frac{a^4b^5}{216} + \frac{13ab^8}{1080} - \frac{13a^3b^6}{4320} + \frac{589b^9}{90720} + \frac{a^6b^3}{1728}, \text{ and}$$

$$H = \frac{31a^9}{360880} - \frac{51a^7b^2}{120960} + \frac{a^5b^4}{1890}.$$

The test frame with which the elastic parameters were evaluated is shown in Fig. 3.3.

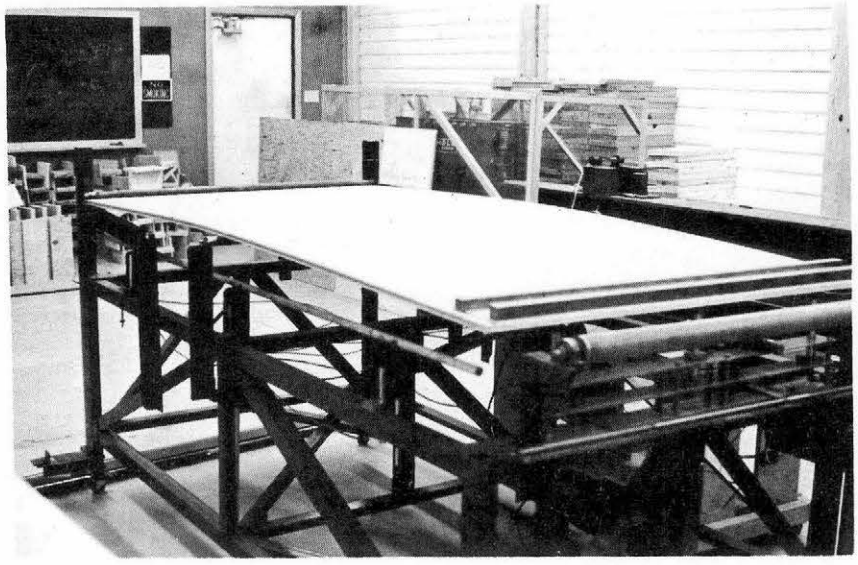

Fig. 3.3 Test Frame for the Evaluation of Elastic Parameters of Full-Size Sheathing Materials

The determination of the modulus of rigidity utilized the plate twisting principle. This test proved to be size dependent in some cases unrealistic values were obtained. Values needed in the theoretical

study were obtained from standard references in these cases. Further details are given in (47,48).

A total of 219 pieces of 4 ft by 8 ft panels of 3/4-in. and 1/2-in. Douglas-fir plywood, Engelmann spruce plywood and 1/2-in. Douglas-fir particleboard were evaluated. For the verification of the model, the individual elastic parameters of each piece of sheathing were needed. Table 3.2 presents a summary of resulting data showing the mean, standard deviation, range and standard error of the mean for each species, size, material, and elastic parameter evaluated.

Table 3.2 Statistics of Average Values of MOE in Bending and Modulus of Rigidity in Plate Twist for Sheathing Materials (10^6psi)[1]

Species-thickness group	n*	Parameter	Static MOE		Dynamic MOE		Modulus of rigidity
			Lengthwise	Crosswise	Lengthwise	Crosswise	
3/4 in. Douglas-fir plywood	39	Mean	2.140	1.667	2.498	1.745	0.222
		Std. deviation	0.182	0.152	0.185	0.147	0.019
		Range	0.822	0.619	0.764	0.603	0.095
		Std.error of mean	0.029	0.024	0.029	0.023	0.002
1/2 in. Douglas-fir plywood	50	Mean	1.906	1.647	2.195	1.908	0.366
		Std. deviation	0.202	0.127	0.231	0.131	0.036
		Range	0.907	0.581	1.046	0.690	0.160
		Std.error of mean	0.029	0.017	0.033	0.019	0.004
3/4 in. Engelmann spruce plywood	45	Mean	1.826	1.563	1.999	1.776	0.252
		Std. deviation	0.105	0.102	0.105	0.109	0.018
		Range	0.587	0.329	0.490	0.386	0.085
		Std.error of mean	0.016	0.015	0.016	0.016	0.002
1/2 in. Engelmann spruce plywood	40	Mean	1.602	1.485	1.826	1.738	0.487
		Std. deviation	0.084	0.087	0.100	0.126	0.077
		Range	0.398	0.385	0.449	0.535	0.459
		Std.error of mean	0.013	0.014	0.016	0.020	0.008
1/2 in. Douglas-fir particleboard	45	Mean	0.524	0.398	0.607	0.451	0.465
		Std. deviation	0.071	0.057	0.075	0.065	0.048
		Range	0.214	0.205	0.229	0.222	0.203
		Std.error of mean	0.106	0.086	0.112	0.098	0.005

[1]Average of four measurements per panel.

*Number of specimens.

The use of plywood sheathing requires special handling for input to the mathematical models of T-beam and floor systems. As discussed in Sec. 2.5, the gross cross-sectional dimensions are used in the model

and adjustments of MOE are made to compensate for this effect. A list of values of the parameter, K*, along with the area and moment of inertia values developed for sheathing used in verification testing are shown in Table 3.3. Other details concerning the use of sheathing in the experimental studies are discussed in sections dealing with each test program.

3.4 Fastener Properties

Nails and elastomeric adhesives used in floor construction produce semi-rigid connections. This characteristic results from the interlayer slip effect which is evaluated using the load-slip characteristic of the fastener-wood combination. The slope of the curve, i.e. the slip modulus k, may be defined on a curvilinear, tangent, or secant basis as shown in Fig. 3.4.

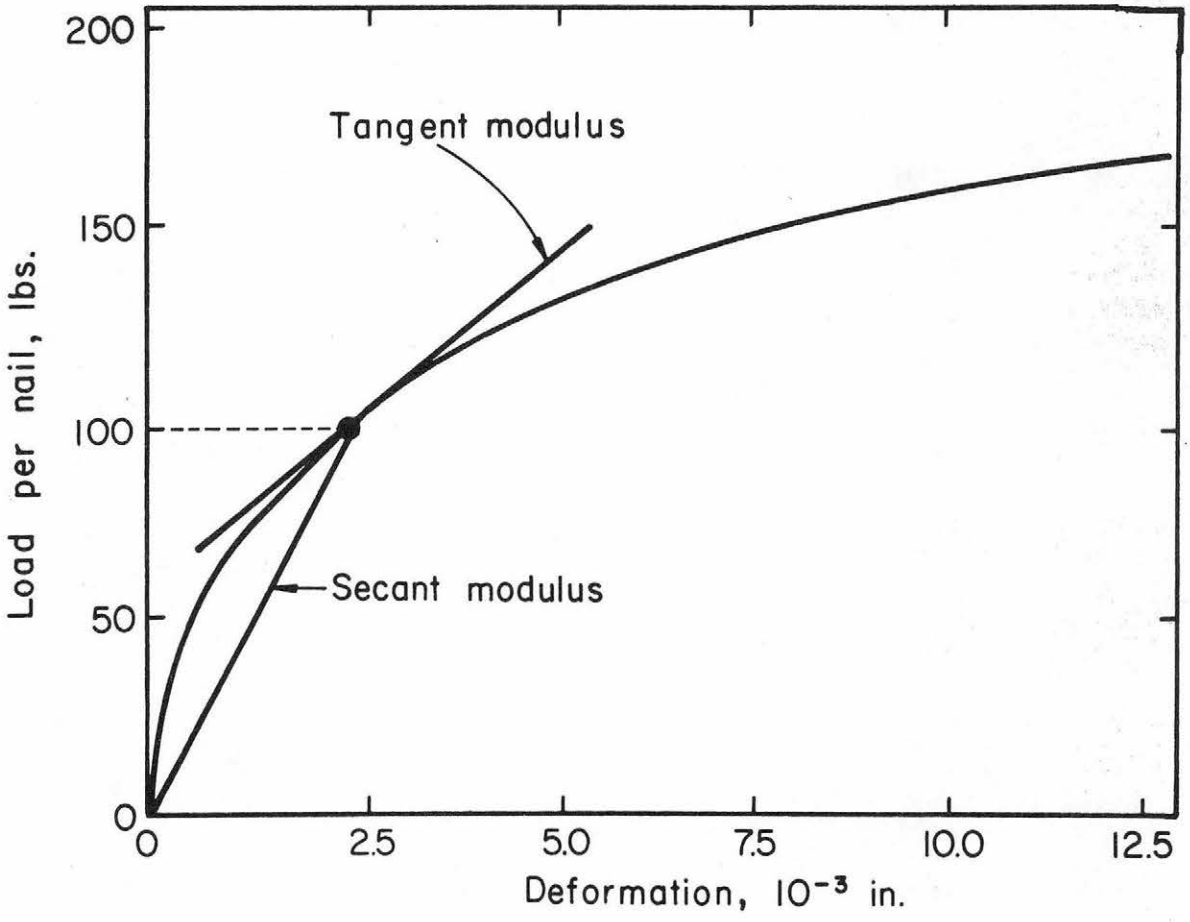

Fig. 3.4 Typical Load-Slip Curve

The load-slip curves for the various combinations of joists, sheathing, and fasteners were determined by a double shear test

Table 3.3 Values of MOE Transformation Constants for Plywood used in Verification Testing of Mathematical Models

Plywood Species	Nominal Thickness, in.	Surface Ply	A_t $in.^2/ft$	A_{gr} $in.^2/ft$	I_t $in.^4/ft$	I_{gr} $in.^4/ft$	$K^* = \frac{A_t . I_{gr}}{A_{gr} . I_t}$
Douglas-fir	1/2	$\parallel$	3.060	6.0	0.1072	0.125	0.5947
		$\perp$	3.060	6.0	0.0183	0.125	3.4836
	3/4	$\parallel$	4.435	9.0	0.2682	0.422	0.7753
		$\perp$	4.563	9.0	0.1301	0.422	1.6445
Engelmann Spruce	1/2	$\parallel$	2.641	6.0	0.0781	0.125	0.7045
		$\perp$	2.641	6.0	0.0120	0.125	4.5850
	3/4	$\parallel$	3.998	9.0	0.2105	0.422	0.8905
		$\perp$	2.728	9.0	0.0794	0.422	1.6110

Note: MOE_{axial} = K* times $MOE_{bending}$

arrangement as depicted in Fig. 3.5. A side study indicated no significant difference for average ultimate load per connector between this test set-up and the single shear arrangement specified by ASTM.

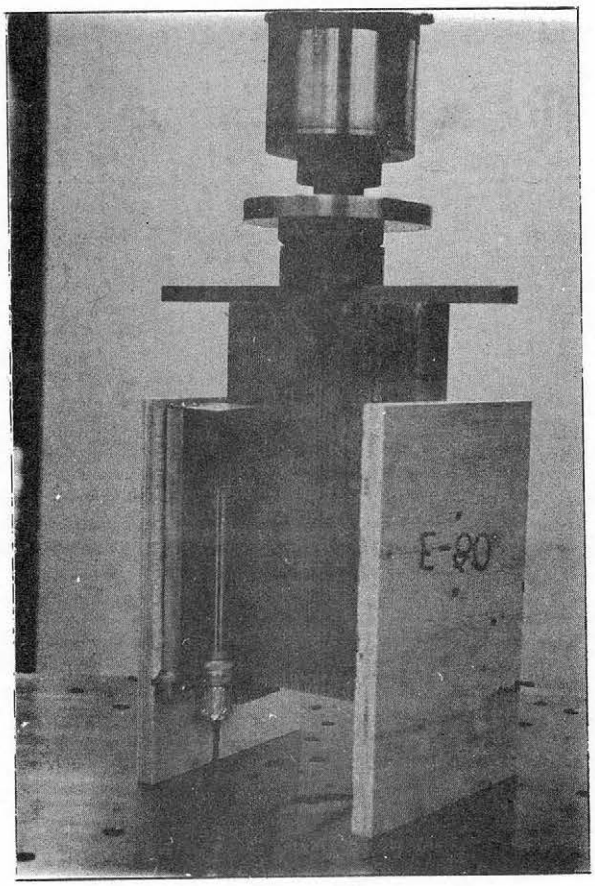

Fig. 3.5 Photo of Test Set-up for Determining Load-Slip Relationship for Connectors

The material used was cut from the ends of the 16 foot-long pieces of 2 x 8 joists. The plywood side pieces were either nailed or glued to the lumber. The nails were 8d size except when the slip modulus was evaluated for the plywood-particleboard combination used in three-layer systems. In this case 6d nails were used in connecting the particleboard to the plywood.

The joist specimens were selected with varying MOE values to evaluate possible correlation with measured slip moduli. For the materials studied, these correlations were significant in most cases, but for simplicity and practicality, only average slip moduli values were used in the verification studies of the mathematical models.

The test results are based on the double-shear test set-up with a total of eight nails used to fasten the side plates. The slip moduli were evaluated for conditions where the load was applied parallel to the grain direction of the joist and perpendicular to the surface grain of the plywood, and for the case where the cross-machine direction of the particleboard was perpendicular to the joist length.

Continuously recorded load-slip curves were taken and used in formulating a mathematical expression for the load-slip characteristics. Values for constants C_1, C_3 and C_5 for the equation given below were determined:

$$\Delta = C_1(e^{C_2F} - 1) + C_3(e^{C_4F} - 1) + C_5(e^{C_6F} - 1) \qquad [29]$$

where:

Δ = deformation (in.),

F = load per connector (lb),

$C_2 = 0.01$,

$C_4 = 0.002$, and

$C_6 = 0.0002$.

The values of C_2, C_4 and C_6 were assumed.

The tangent modulus, KT, can be derived from Eq. [29] by differentiating the slip equation with respect to force and taking the inverse of the result. This gives

$$KT = \frac{1}{C_1C_2e^{FC_2} + C_3C_4e^{FC_4} + C_5C_6e^{FC_6}} \qquad [30]$$

where the tangent slip modulus is evaluated at a given force F. The secant modulus, KS, is simply

$$KS = \frac{F}{\Delta} \qquad [31]$$

The tangent and secant moduli were evaluated at 25, 50, 100 and 150 pound levels. These values are summarized in Table 3.4. Further details on the evaluation of the slip modulus values are given by Patterson (60). Tabulations of values used in the individual verification tests are given in the appropriate sections of this report.

Table 3.4 Average Connector Slip Moduli Values

Load Level lb.	Douglas-fir Joist		DF Joist	DF Joist	ES Joist	ES Joist	DF Joist	ES Joist	1/2" DF Particle board		DF Joist
	Douglas-fir Plywood		3/4" DF	3/4" ES	3/4" ES	3/4" DF	1/2" DF	1/2" ES	1/2" DF	1/2" ES	DF Plywood
	Parallel to veneer	Perpendicular to veneer	Plywood	Plywood	Plywood	Plywood	Plywood	Plywood	Plywood	Plywood	
	8d cement-coated		8d common						6d common		Glue
	lb/in.		lb/in.						lb/in.		lb/in./in.^{2}
			Average tangent moduli								
KT 25	93,200	3,280	69,800	59,400	36,300	48,000	29,025	32,900	3,920	3,900	46,800
KT 50	58,900	3,540	56,400	33,700	32,500	25,500	15,070	13,800	3,870	3,930	36,700
KT 100	16,200	3,570	27,300	10,500	10,300	14,200	3,300	3,620	3,370	2,340	7,810
KT 150	6,080	2,890	20,000	4,160	3,700	4,900	1,217	2,300	2,460	1,010	2,750
			Average secant moduli								
KS 25	---	---	75,900	56,800	52,700	63,100	29,475	31,120	4,000	3,780	39,400
KS 50	83,400	3,260	73,500	53,700	39,000	45,200	23,900	21,360	3,900	3,810	37,300
KS 100	41,900	3,420	49,200	25,300	23,000	30,100	9,583	8,922	3,780	3,450	24,000
KS 150	---	---	31,200	12,200	11,300	12,800	3,958	4,502	3,480	2,560	8,440

Note: All values from tests conducted by the Wood Science Laboratory. The slip modulus is divided by the nail spacing to obtain the effective slip modulus per linear inch of joist length. For glued connections the value given is multiplied by joist width to obtain the slip modulus per linear inch of joist length.

Additional work was conducted to evaluate the effects of combined loading on nailed joints during the project by DeBonis (20). In particular, his research showed that the combined action of withdrawal and lateral load on a nailed wood joint does not reduce the capacity of the joint to resist lateral or interlayer shear deformation. In fact, the presence of withdrawal load, which has been shown to exist in floors (77) when the sheathing pulls up on joists adjacent to the loaded joist, helps to prevent bending of the nail due to lateral loading. The slip modulus values may be, therefore, increased somewhat over those obtained under lateral load only.

4. DESCRIPTION OF EXPERIMENTAL STUDIES OF T-BEAMS AND FLOORS

4.1 Introduction

With few exceptions, research on wood and wood structures has been developed from the viewpoint of testing of materials or systems having unknown properties to determine statistical data on their behavior. Generally, in this approach, a number of variables are isolated, several levels of each variable are chosen, replications are made, and a large number of tests are conducted. The testing is then followed by statistical analyses and conclusions are drawn.

While this method is probably the only method suitable for the determination of say, strength properties of wood, it is clearly inappropriate for wood structural systems. In the first place, the inordinate amount of testing required makes the method financially impossible. For example, it is estimated that a reasonably complete test program for wood joist floors could require several million specimens. Secondly, the concept of empirical testing of structural systems is obsolete. Analysis procedures now available make the derivation of a mathematical model of such systems a realizable goal. Thus, only verification testing of a developed mathematical model is needed. Once this has been accomplished, the model may then replace the physical machine as the tool for evaluating of newly-developed configurations, material combinations, etc.

To this end, a series of carefully controlled T-beams and floors were constructed to provide the required verification data for comparison with the predicted results using the developed mathematical models. Results of these tests are described and comparisons made with predicted values in Chapter 5. A general description of the test methods and facilities utilized in the structural testing phase of the project is presented below.

4.2 Description of Structural Testing Equipment

Facilities used for the structural testing are located in the Structural Engineering Laboratory at the Colorado State University Engineering Research Center. A 55 kip-capacity MTS hydraulic actuator and its associated control equipment were used to load all the T-beam and floor specimens included in this study. Penner (61) has presented an extensive description of the construction of these facilities.

The MTS closed-loop structural testing system is essentially a self-controlled hydraulic loading system composed of three major components: the power supply, the control console, and the actuator. The actuator is mounted on a movable steel beam which in turn is attached to the supporting frame by trolleys such that the actuator can be quickly moved to any point over the test area (see Figs. 4.1 and 4.2). An elevated reinforced concrete frame provides the support for the floor and T-beam specimens over a 12-ft span and allows widths up to 16 ft. Along the top face of each 16 ft span of the frame, a nominal 2 x 6 in. Engelmann spruce sill plate was fastened to the concrete frame with bolts. The bottom of the sill plate was grouted with mortar having a thickness of about one-quarter in. The joists of the floor and T-beam specimens rested upon this sill plate.

A load cell with a capacity of either 2.5 or 50 kips is mounted on the actuator, depending on the desired load level. The control console can operate the actuator in either a load control or stroke control mode. In addition to its static loading capability, a function generator in the console allows cyclic loading with a specific function. Sine, haversine, square, haverquare, and ramp and other functions can be generated.

The ram of the MTS hydraulic loading system was used to apply a concentrated load transmitted to the specimen by a 4 in. square steel pad through a ball and socket bearing. The thickness of the steel pad and the diameter of the ball bearing varied with the load cell capacities chosen.

A twin T-beam configuration was used for the beam tests to obtain the necessary stability. To allow each joist to be equally loaded, a load distribution beam was used to divide the load equally and transmit it to each joist. For floor specimen loading, the 4 in. square steel pad was placed directly over the joist to be loaded.

Deflection measurements were obtained at the various load levels using dial gages, a surveying level, and LVDTs (linear variable differential transformers) connected to an X-Y plotter.

Dial gages with ranges of one or two in. were used to obtain most of the deflection data in the working load range. The deflection dials

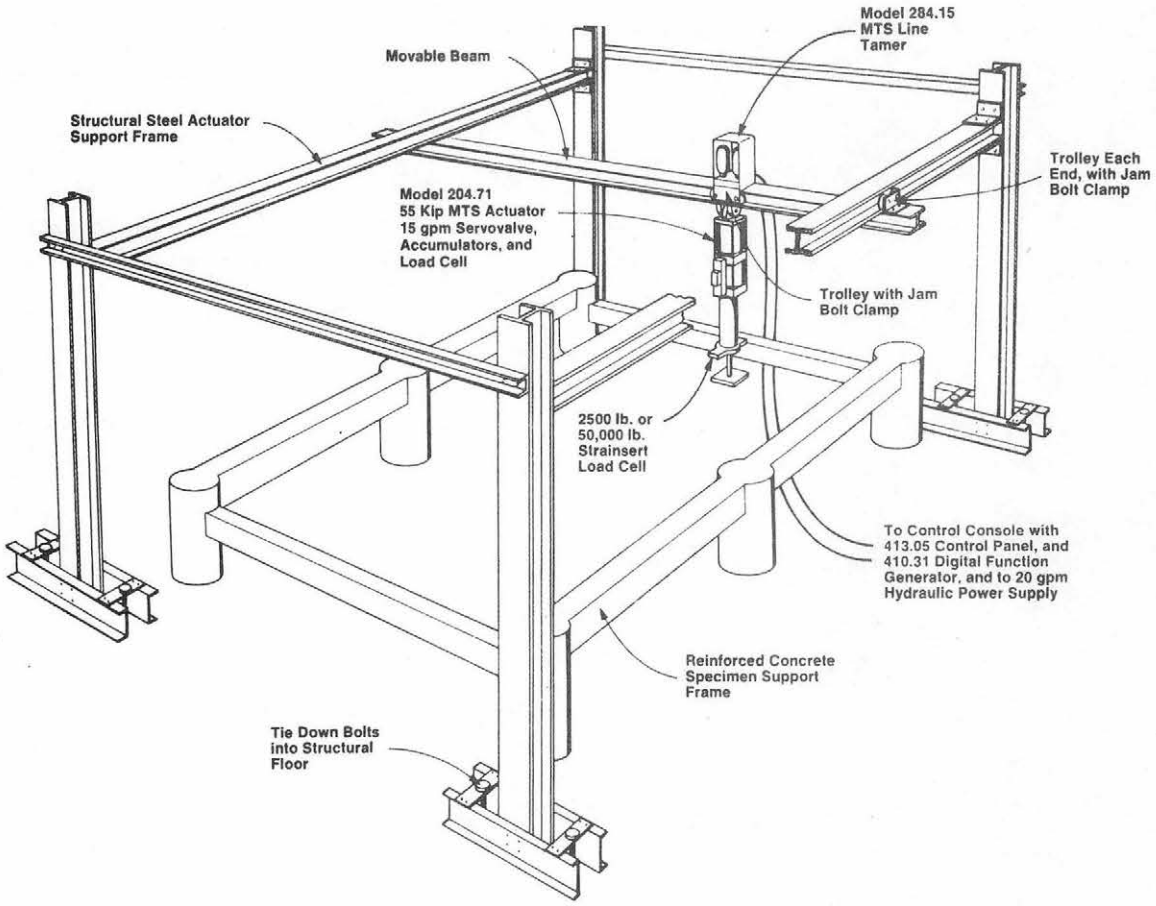

Fig. 4.1 55 Kip Loading Actuator and Support Frame

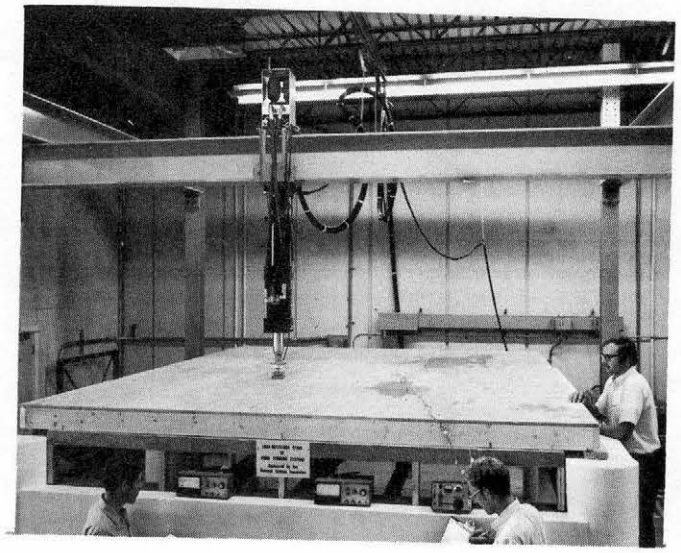

Fig. 4.2 Photo of Structural Testing System

were read to the nearest .001 in. They were placed underneath the joists at selected points across the span and were fastened to punched steel angles attached to a supporting bridge across the span of the test area. Detailed descriptions of the arrangement of the dial gages for each specimen have been given by Penner (61), Kuo (45) and Liu (46).

During a test to failure, engineering scales with 50 divisions per in. were attached to the joists at points where deflections were to be measured. A surveying level was used to read these scales for the deflections after the application of each load increment.

The LVDTs were used for some tests to obtain a continuous plot of load versus deflection. An LVDT contained within the load actuator was also used to plot the load-deflection curve, to failure, at the point of load application.

4.3 General Description of T-Beam Test Specimens

An alphanumeric identifying system was used to describe each specimen. This system was constructed as follows to allow easy recognition of the specimen characteristics:

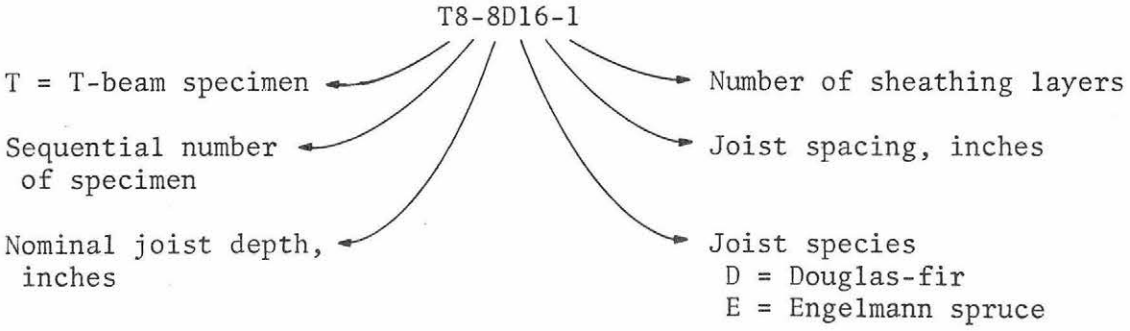

Sixteen individual T-beams were built and tested. In some cases, tests were conducted on the beams as both two and three layer systems. Thus nineteen verification specimens are available for study. These full-size specimens were constructed using joists with plywood and/or particleboard sheathing of Douglas-fir and/or Engelmann spruce, or a combination of these materials. One-half in. thick particleboard was added to selected two-layered systems to form the three-layered specimens. The nominal dimensions of the joists were 2 x 8 in. or 2 x 12 in. with a total length of 12 ft and 2 in. The plywood selected had nominal thicknesses of 1/2 and 3/4 inches. Each piece of joist and sheet of plywood or particleboard was numbered according to the alphanumeric identifying system shown below:

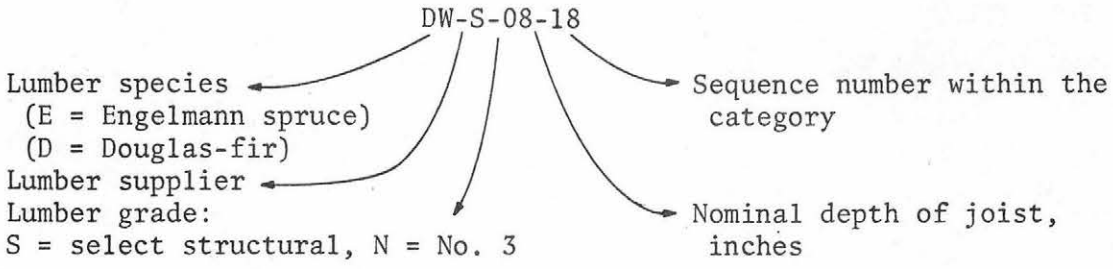

For the plywood and particleboard:

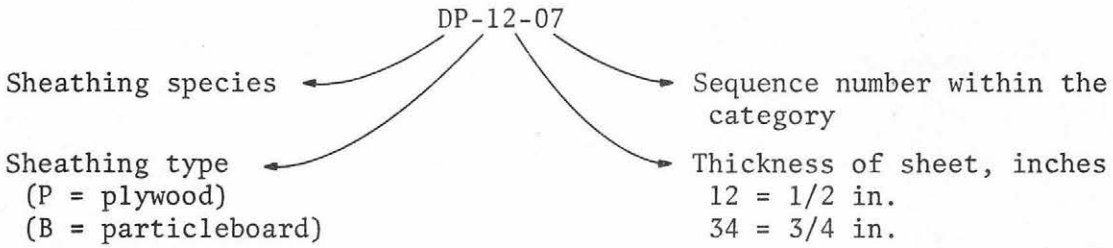

Six- and eight-penny common nails at varying nail spacings (from 2 in. to 8 in.) were used as connectors. An elastomeric glue was also used as the interlayer connection in the fabrication of some specimens. Joist spacings were 16, 19.2 or 24 in. A more detailed description of selected individual specimen configurations is presented in Chapter 5.

Several methods of selecting the materials were considered prior to starting the specimen construction. Two schemes were adopted for the selection of joists. In the first method, joists were selected from within a predetermined range of average MOE values using data provided by the Wood Science Laboratory. After these preselected joists were located, those joists found to have excessive crookedness or abnormal cracks or knots were discarded. Joists for most T-beam specimens were selected using this first method. For a few T-beams, random selection was used, i.e., both joists needed were randomly selected from the lumber supply of the desired size, grade, and species without regard to their measured stiffness. Again, excessively crooked or abnormally cracked joists were discarded.

Plywood and particleboard sheets were selected from the top of the supply pile in order as needed.

All joists and sheathing materials were covered with plastic sheets to help maintain a stable moisture content. Moisture content

was checked after testing to insure that no significant changes had occurred during storage.

The construction procedures for all T-beams were essentially the same. Each joist was placed edgewise across the concrete frame and seated on the sill plate. Normal construction practice was followed: the crowned edge was usually placed upward and whenever a large knot was present at the edge of a joist, it was placed on the top edge.

Prior to attaching the sheathing, each joist was evaluated for edgewise MOE after a header plate was attached at the ends of the twin joist configuration. These edgewise MOEs provided an accurate measure of the effective modulus of the joist component of the T-beam specimens.

For the two-layered T-beam systems, the plywood was sawed into the required sizes and then placed with the face grain perpendicular to the joists. Eight penny common nails were used to connect the plywood and joist in all nailed specimens. Nail spacings differed from specimen to specimen, ranging from 2 in. to 8 in. apart. One row of nails was used per joist.

An elastomeric adhesive (Franklin Construction Adhesive) was used to connect the plywood to the joist of some specimens. The glue was applied with a caulking gun in two one-quarter in. wide beads placed continuously along the upper joist face. The glue was then spread evenly. After the plywood was placed at the desired position, double-headed common nails were driven into the joist at a spacing of about 8 in. to insure a tight contact between the plywood and joist. The glued specimens were allowed to cure about two weeks. The double-headed nails were pulled out immediately before load testing began.

Details of the sheathing joints varied. Usually the tongue-and-groove joints were butted tightly by forcing the unnailed sheathing to the nailed one until the gap was closed at several points along the joist. Small variations in the straightness of the sheathing edge resulted in some small gap opening remaining along part of the joint length in some cases. For some specimens, joints were left with a 1/16 in. wide gap. For others, the joints were glued and tightly butted.

One layer of particleboard was added to several of the joist-plywood specimens systems to form a three-layered system. The

particleboard was selected as previously described and sawed into the same sizes as those of the plywood in the two-layered system. The particleboard sheathing joints were staggered from the plywood joints. Six penny common nails were typically used to attach the particleboard. Nail spacings varied from specimen to specimen, with an 8 in. spacing most commonly used. Nails were driven through the particleboard and plywood into the joist with the nail spacings staggered from the nails previously driven through the plywood layer in most cases.

The location and identification of all joists, plywood and particleboard used in the test specimens were recorded using the numbering systems described in the previous section. A summary of the specimen configurations, gap locations, and nail spacings is presented in the appendix.

4.4 Description of Floor Test Specimens

An alphanumeric identifying notation was assigned to each floor specimen to indicate the type of joist material and the value of several major parameters. This notation, created to allow easy recognition of the specimen characteristics, is illustrated by the following example:

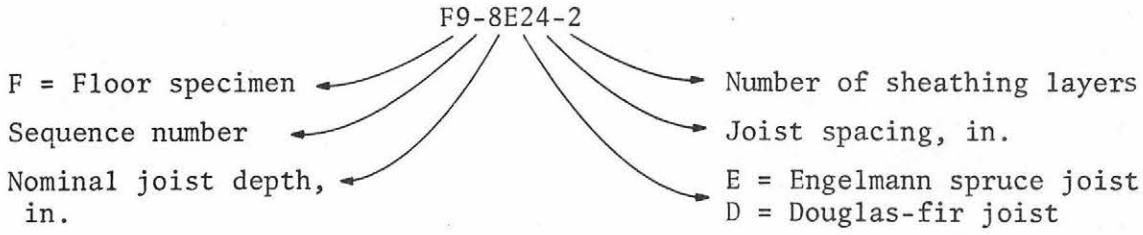

Eleven individual floors were built and tested. The first floor was used to develop construction and testing techniques and is not further considered. Six of the remaining floors were tested in both a two-layer and a three-layer configuration. Thus results of 16 floors representing a wide range of stiffnesses, joist spacings, and joist-sheathing arrangements are available for verification of the mathematical models.

Of the sixteen floor specimens studied, 2 x 8 in. joists were used for all but two floors specimens where 2 x 12 in. joists were used. Douglas-fir joists were used in nine floors and Engelmann spruce joists were used in seven floors. The floor specimens tested each had one of

three different joist spacings, 16, 19.2 or 24 in. Each joist and sheet of plywood or particleboard used in the floors was numbered using the alphanumeric identifying notation described in Sec. 4.3.

Six and eight-penny common nails at varying spacings, from 4 in. to 8 in., were used as connectors with two exceptions. Cement coated nails were used in one specimen and an elastomeric glue (Franklin Construction Adhesive) was used in another.

In floor construction, joists are placed edgewise. Because of this configuration, the preliminary MOE values of joists obtained from flatwise measurement only approximate the MOE of the joists as actually used. Therefore, the edgewise MOE values of joists were determined during the construction of the floor specimen just prior to attachment of the sheathing. It should be noted that shear deformation occurring in the joists due to the concentrated load applied at the center acts to reduce the effective modulus since simple beam theory was used in obtaining the MOE values. Calculation of the MOE on this basis was acceptable because the mathematical model does not explicitly include beam-shear deformations. This effect is introduced by using the effective MOE of each joist which includes the shear deformations.

While careful construction practice was followed in building the floor specimens, no special effort was made to obtain a "laboratory" specimen. Gaps in sheathing were staggered for the three-layer specimens and varied from open to tightly-butted or glued joints.

The general testing procedures for the floor specimens have been discussed in detail by Penner (61). A summary of the testing procedure follows.

A concentrated load was applied at the desired location directly over one of the joists in the floor specimen being tested. Load increments of 50, 100, 200 or 250 pounds were used in the range of service load depending on the size of the joists and the arrangement of the components of the floor. The service load level was assumed as 800 or 1000 pounds. One exception was specimen F7-12D24-1 which was loaded to 2000 pounds corresponding to a maximum deflection of 1/360th of the 12 ft span, or 0.4 in.

For each of the three-layered floors, load tests were conducted after each layer of sheathing was properly constructed. Only loads in

the elastic range were applied to the two-layered specimen so that a valid test could be conducted after the third layer was added. After the top particleboard sheathing was added for each three-layered specimen, load tests up to the service load level were performed in two steps. First, the nails were driven into the bottom sheathing layer until they touched the top face of joists. Second, the nails were driven to their maximum penetration into the joists. Thus additional test data were obtained concerning the added stiffness due to the effect of nailing the third layer.

Finally, each specimen was tested to failure with the load applied at the center of the floor. The 50-kip capacity load cell was installed, and engineering scales were used to replace the dial gages for the measurement of deflections. A concentrated load was applied in 500 pound increments and deflections, obtained with a surveying level, were recorded. The LVDT from the actuator was connected to the X-Y plotter to obtain a continuous load-deflection plot.

A number of variables were examined during the experimental research on the floor specimens. However, since the main purpose of this study was the verification of the mathematical model for floor systems, discussion in this report centers on that objective. For further details concerning the experimental work on T-beams and floors the reader is referred to theses by Penner (61), Kuo (45) and Liu (46).

A summary of the general data of all the floor specimens constructed and tested is presented in the appendix. The detailed data for each selected floor specimen is given in Chapter 5 as part of the discussion of verification results.

5. RESULTS OF VERIFICATION TESTING OF T-BEAMS AND FULL-SCALE FLOORS

5.1 Introduction

The goal of the research described in this report was to develop a mathematical model for the behavior of wood joist floor systems and to verify its use through a series of carefully controlled full-scale tests. The experimental details of these tests are described in Chapter 4. Comparisons of measured vs. computed (predicted) deflections are presented in this chapter for both T-beam components and full-scale floor systems.

As discussed in Chapter 2, the development of the mathematical model was done in several stages. A finite element procedure was finally chosen for the verification studies since this method has sufficient flexibility to allow inclusion of the effects of gaps in sheathing layers and variability of material properties. Analysis of each specimen required the preparation of data cards describing the geometry, material properties, and slip modulus for each element, plus gap and load data. Results of the analysis included the computed deflections at each node point, plus moments and interlayer forces. Measured and predicted deflections are compared in detail for selected test specimens to show the degree of verification obtained. A tabulation of all results is given showing comparison of measured and calculated deflections. Further details can be found in (45,46).

5.2 Comparisons of Measured and Predicted T-Beam Deflections

Computed and measured deflections were obtained for fourteen two- and three-layered T-beam specimens. The favorable comparisons of these results form the basis for the verification of the developed mathematical model. While considerable additional data were taken for each specimen, load-deflection plots at the midspan of each joist are used to assess the degree of verification. The load, placed at the T-beam midspan, is equally shared by the two joists unless otherwise noted. Typical results are discussed in detail and a table showing all comparisons of measured vs. predicted values is presented.

The slip moduli values used in the calculations (Table 5.1) were obtained from Table 3.4 using the secant definition corresponding to average nail loads of about 100-500 lbs per nail. Working loads

Table 5.1 Values of Slip Modulus, k, Used for T-beam Specimens

Connector	8d common nails				Elastomeric glue	6d nails, common and cement-coated		Connector Spacing
Joist	Douglas-fir		Engelmann spruce		Both D.F. & E.S.	------		
Sheathing	D.F.	E.S.	D.F.	E.S.	Both D.F. & E.S.	Particleboard D.F. Plywood	Particleboard E.S. Plywood	
k, lb/in.	30,000	-	30,000	18,000	-	4,500	3,500	8"
k, lb/in.	38,000	-	-	23,000	-	-	-	6"
k, lb/in.	-	35,000	-	-	-	-	-	4"
k, lb/in.	50,000	-	-	-	-	-	-	2"
k, lb/in./ in.^{2}	-	-	-	-	16,000	-	-	continuous

Note: These values are for 8 in. nail spacing. Adjustment is made in the values for other nail spacing due to the difference in nail loads.

sufficient to produce beam deflections near L/360 were used. Adjustments of the slip modulus are required, due to changes in nail forces, for spacings other than the 8 in. spacing which was used as a reference for the nailed beams. Slip moduli values for glue are reported on the basis of force per unit area and thus are not divided by the spacing as are the nailed values.

Figure 5.1 shows the layout and properties for specimen T4-8D16-1. Computed vs. measured deflections for the load at midspan are shown in Fig. 5.2. As can be seen, good agreement exists between computed and measured deflections when the appropriate gap situation is modeled. Joints in sheathing were tightly butted allowing a limited transfer of force at the gap. This situation was modeled by inserting a flexible gap with small MOE into the finite element model of the beam. The use of open gaps, as shown in Fig. 5.2, underestimates the stiffness of the beam.

A typical example showing the results of adding a third layer, in this case particleboard, is illustrated using the results for specimens T15-8E19.2-1 and T15-3E19.2-2 (the last number indicates one and two layers of sheathing, respectively, for the same specimen). Properties of the two and three-layer versions of this beam are given in Figs. 5.3 and 5.4. Computed vs. measured deflections are presented in Fig. 5.5 for each case. As can be seen, the model properly accounts for the presence of each layer with its individual gaps and gives good agreement with the measured deflections. As indicated, a considerable stiffness increase is obtained by adding the layer of particleboard, particularly if the gaps are staggered, as they were in this case. While not directly a part of this study, it should be noted that the concentrated midspan load required to fail the three-layer specimen was a fairly high value of 4500 lbs.

The sheathing-joist surfaces of several T-beams were connected with an elastomeric adhesive. Specimen T9-8D16-1 was a typical glued T-beam. The properties and loading conditions for this beam are shown in Fig. 5.6. Figure 5.7 shows its load-deflection behavior. A substantial composite action was obtained which may be seen by comparing the measured deflection in Fig. 5.7 with the deflection computed assuming the joist only was loaded. Again good agreement between measured

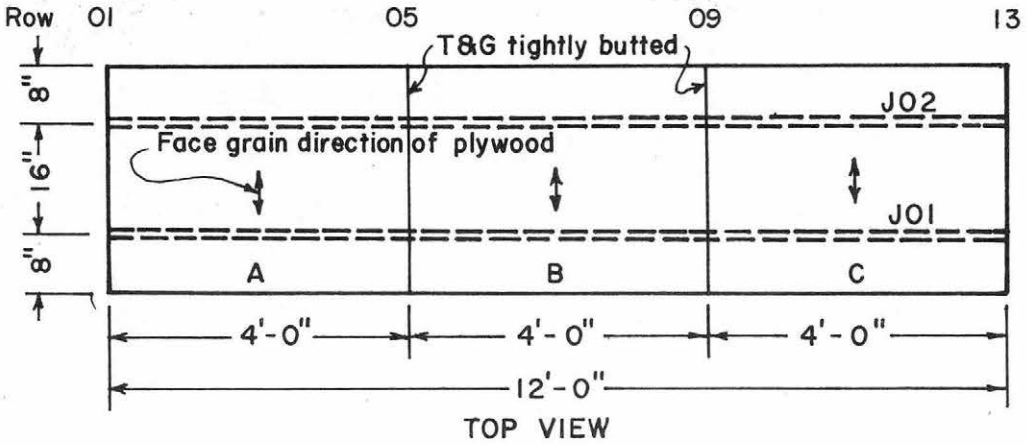

TOP VIEW

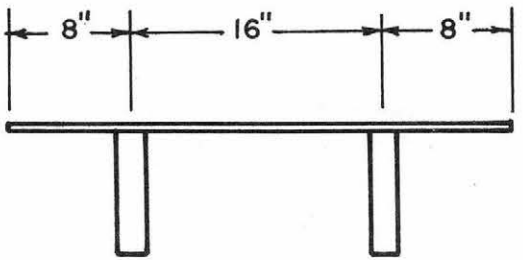

CROSS SECTION

Description of Specimen:

Joist: 2x8 Douglas fir

J01	DW-S-08-37	$E = 2.429 \times 10^6$ psi
J02	DW-S-08-43	$E = 1.694 \times 10^6$ psi

Sheathing: 3/4" D. F. Plywood

A	DP-34-25	$E_\perp = 5.50 \times 10^5$ psi
B	DP-34-25	
C	DP-34-25	

Connector: 8d common nails spaced at 8"

Sheathing joints: Tongue & groove, tightly butted.

Slip modulus: k = 30,000 lb/in.

Test sequence:

1. Loaded at midspan (row 07) with ΔP = 250 lb up to P = 1000 lbs
2. Loaded at row 09 with loads same as in 1
3. Loaded at row 11 with loads same as in 1
4. Cut gaps at rows 05 and 09; repeated tests 1, 2 and 3
5. Failure test: loaded at row 07; J02 failed at P = 4000 lbs.

Note: Rows are spaced one ft apart

Fig. 5.1 Configuration and Properties of Specimen T4-8D16-1

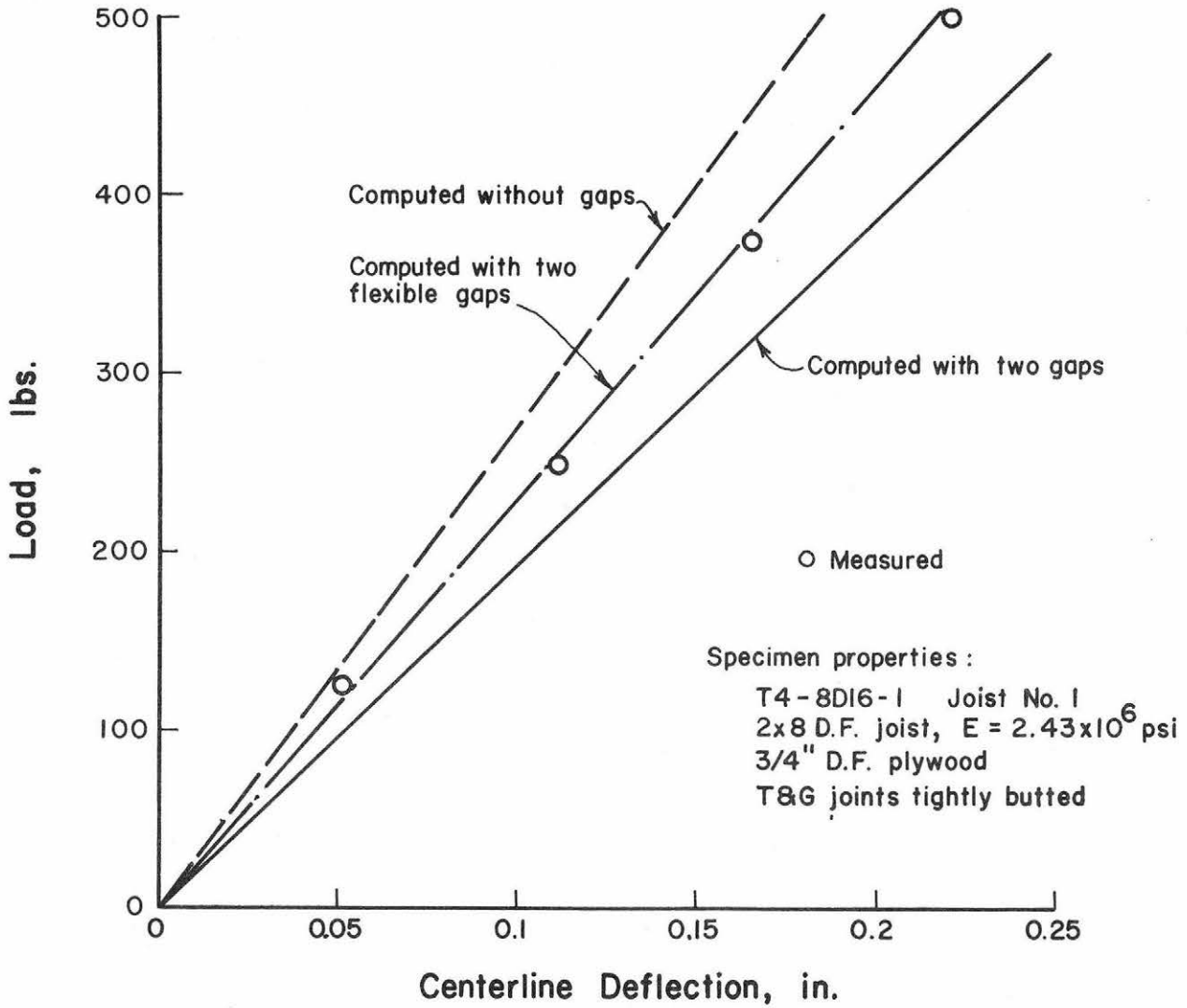

Fig. 5.2 Computed and Measured Deflections at Midspan for T-Beam T4-8D16-1

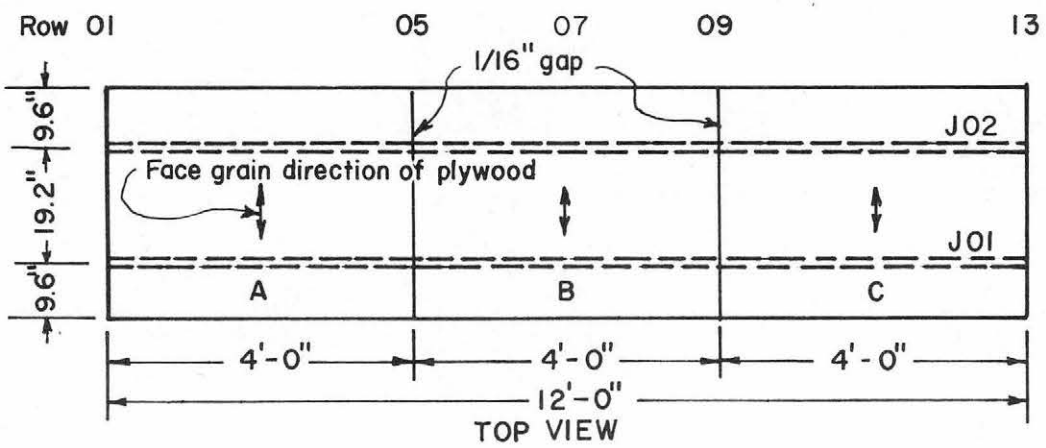

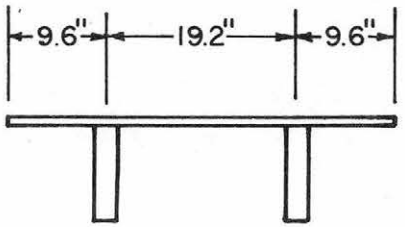

CROSS SECTION

Description of specimen:

Joist: 2x8 Engelmann spruce

	Joist Mark	
J01	EK-S-08-01	$E = 1.191 \times 10^6$ psi
J02	EK-S-08-09	$E = 1.151 \times 10^6$

Sheathing: 1/2" E.S. Plywood

	Sheathing Mark	
A	EP-12-03	$E_{\perp} = 2.221 \times 10^5$ psi
B	EP-12-02	$E_{\perp} = 2.157 \times 10^5$
C	EP-12-02	

Connector: 8d common nails spaced at 8"

Sheathing Joints: left open with 1/16" gaps

Slip Modulus: k = 18,000 lb/in.

Test sequence

1. Loaded at midspan (row 07) with ΔP = 250 lb up to P = 750 lbs
2. Repeated 1 with ΔP = 100 up to P = 600 lbs
3. Loaded at row 05 with ΔP = 100 lb up to P = 700 lbs
4. Loaded at row 03 with loads same as in 2

Fig. 5.3 Configuration and Properties of Specimen T15-8E19.2-1

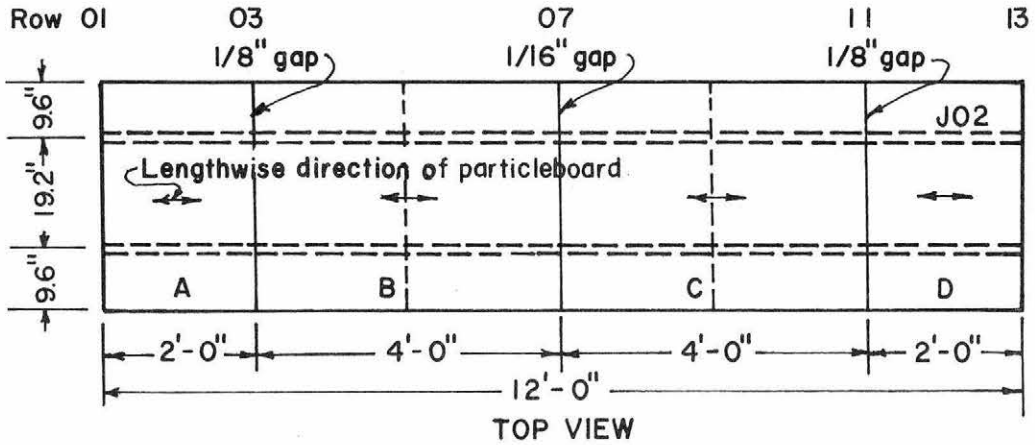

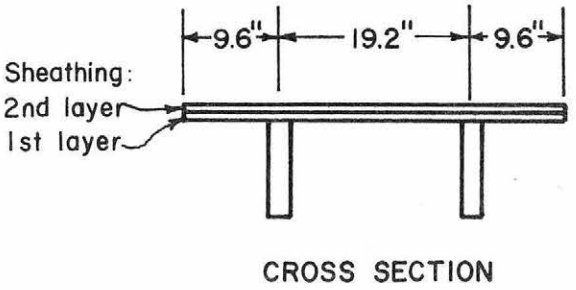

Description of specimen:

Joist: 2x8 Engelmann spruce (see T15-8E19.2-1)

Sheathing: 1st layer (see T15-8E19.2-1)
2nd layer 1/2" particleboard

Sheathing mark		
A	DB-12-20	E_{11}= 5.837×10^5 psi
B	DB-12-21	E_{11}= 5.447×10^5
C	DB-12-21	E_{11}= 5.447×10^5
D	DB-12-19	E_{11}= 5.782×10^5

Connector: 1st layer (see T15-8E19.2-1)
2nd layer 6d cement-coated nails spaced at 6"

Sheathing Joints: left with 1/16" and 1/8" gaps

Slip Modulus: k = 5000 lb/in.(2nd layer)
k = 45,000 lb/in.(1st layer), assuming nails in second sheathing layer driven into joist

Test sequence

1. Loaded at midspan(row 07) with ΔP = 100 lb up to P = 800 lbs
2. Loaded at row 05 with ΔP = 200 lb up to P = 1000 lbs
3. Loaded at row 03 with loads same as in 2
4. Test to failure: loaded at row 07 with ΔP = 500. J01 failed at P = 4500 lbs.

Fig. 5.4 Configuration and Properties of Specimen T15-8E19.2-2

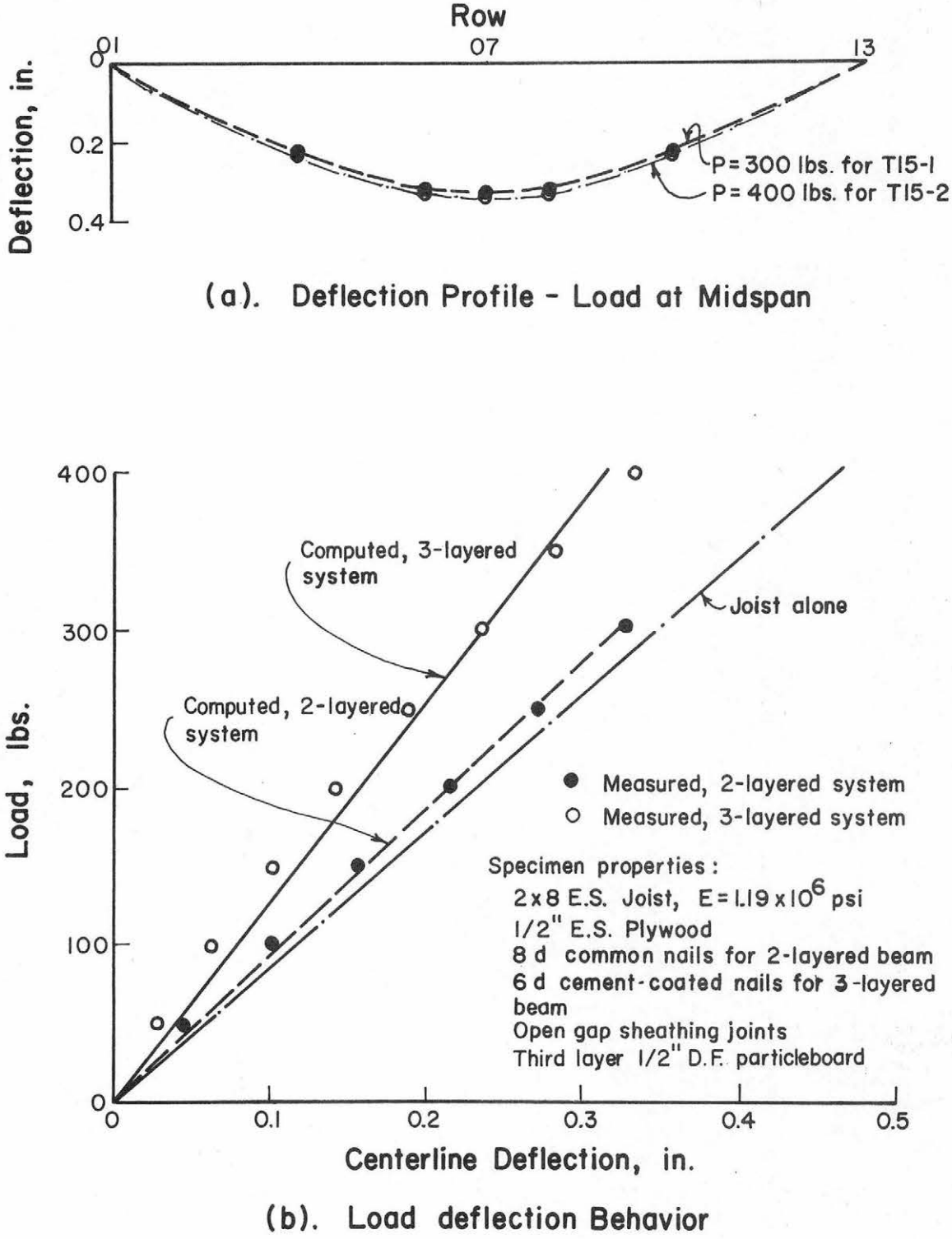

Fig. 5.5 Computed and Measured Deflection at Midspan for T-Beams T15-8E19.2-1 and T15-8E19.2-2

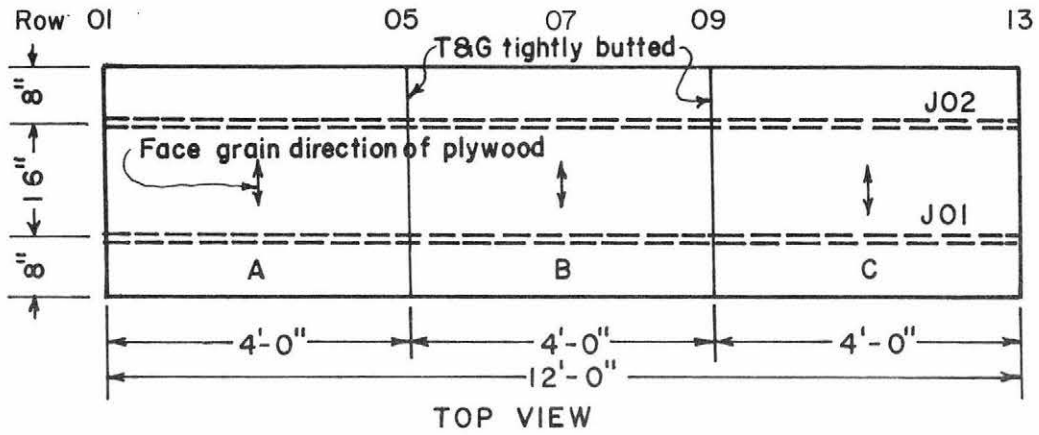

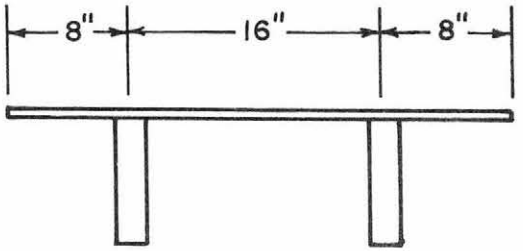

Description of specimen:

Joist: 2x8 Douglas-fir

J01	DW-S-08-12	$E = 2.269 \times 10^6$ psi
J02	DW-S-08-05	$E = 2.566 \times 10^6$

Sheathing: 3/4" D.F. Plywood

A	DP-34-18	$E_{\perp} = 5.352 \times 10^5$ psi
B	DP-34-18	$E_{\perp} = 5.352 \times 10^5$ psi
C	DP-34-18	$E_{\perp} = 5.352 \times 10^5$ psi

Connector: Franklin Construction Adhesive

Sheathing Joints: T&G tightly butted

Slip Modulus: $k = 16{,}000$ lb/in.^{2}

Test sequence

1. Loaded at row 07 with $\Delta P = 500$ lbs up to $P = 2500$ lbs
2. Repeated test 1 for five times
3. Cut gaps at rows 05 and 09; reloaded same as in 1
4. Gaps fiiled with wood strip; repeated test 1
5. Gaps filled; repeated test 1 up to $P = 4000$ lbs
6. Test to failure: P at row 07; J02 cracked and completely failed at $P = 10{,}000$ lbs.
7. Test to failure for single T, J01 failure load = 5000 lbs

Fig. 5.6 Configuration and Properties of Specimen T9-8D16-1

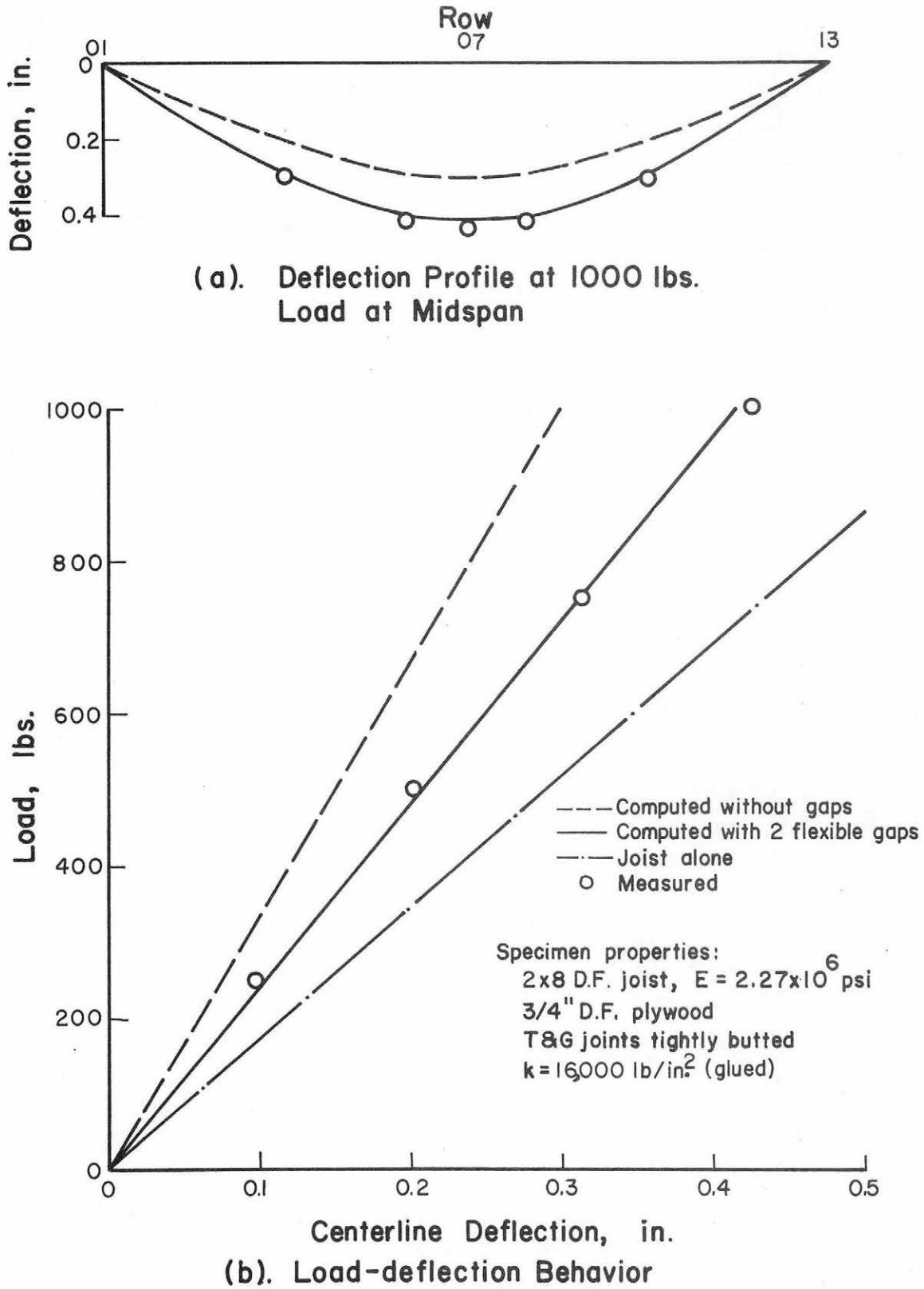

Fig. 5.7 Computed and Measured Deflections for T-Beam T9-8D16-1

deflections and deflections computed assuming composite action is achieved, indicating that the model is capable of properly predicting T-beam behavior for a wide range of beam types.

To further illustrate the use of the mathematical model and the ability of the solution technique to approximate various sheathing joint conditions, the deflections observed for Specimen T12-8D16-1 (Fig. 5.8) were compared with computed results. This specimen was tested several times after successively cutting additional gaps in the sheathing layer perpendicular to the joists at desired intervals. The specimen was tested first without any gaps, except the two flexible joints (glued) between the four foot wide sheathing elements. The sheathing was then cut at midspan and the T-beam reloaded. This procedure was repeated until the gaps were located at one foot intervals. All loads were applied at the midspan of the specimen and were shared equally by each joist.

For clarity, Fig. 5.9 shows only a portion of the experimental and computed results. The predicted values show good agreement with the measured deflections, even with five cuts in the sheathing. For this extreme case of many gaps, the applied load may be considered to be carried primarily by joists alone and the effect of composite action is greatly reduced as expected.

Table 5.2 shows comparisons of predicted and observed midspan deflections for all the T-beam specimens tested. The comparisons are arbitrarily based on conditions corresponding to an experimental midspan deflection of about L/500. The data for each specimen at the load level nearest this deflection are shown. The last column shows the ratio of computed to observed deflections. Good agreement was generally obtained, with the predicted deflection generally within four percent of the observed values. Additional work evaluating the use of the model for uniformly loaded beams tested by a beam manufacturer is discussed by Kuo (45). The verification of the mathematical model provides a workable method to predict the behavior of the T-beam component of floors at working load levels. Incorporation was made of the basic features of this model into the floor analysis procedure and results of its use in predicting the behavior of floors is discussed next.

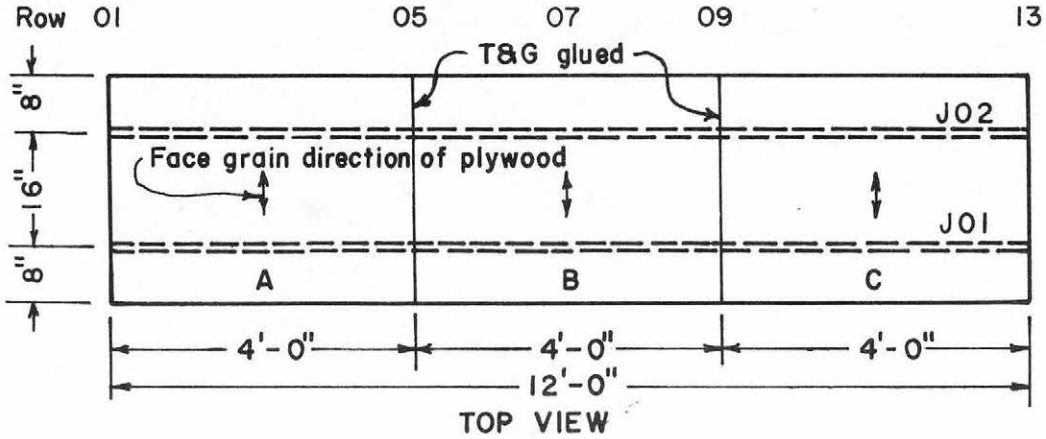

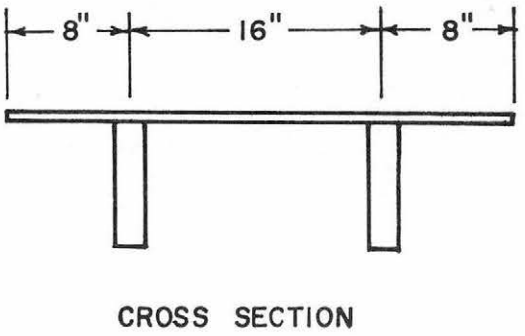

Description of specimen:

Joist: 2x8 Douglas-fir

J01	DW-N-08-51	$E = 1.249 \times 10^6$ psi
J02	DW-N-08-55	$E = 1.261 \times 10^6$

Sheathing: 3/4" D.F. Plywood

A	DP-34-12	$E_{\perp} = 5.581 \times 10^5$ psi
B	DP-34-12	$E_{\perp} = 5.581 \times 10^5$ psi
C	CP-34-12	$E_{\perp} = 5.581 \times 10^5$ psi

Connector: 8d common nails spaced at 6"

Sheathing Joints: T&G glued

Slip Modulus: k = 38,000 lb/in.

Test sequence

1. Loaded at row with ΔP = 250 lb up to P = 1250 lbs. Repeated three times.
2. Cut gap at row 07 and tested as in 1
3. Cut gaps at rows 05 and 09 (total 3 cuts), loaded at row 07 with ΔP = 250 lb up to P = 1000 lbs
4. Loaded at rows 03 and 04 with center gap filled; P_{max} = 1000 lbs
5. Cut gaps at 2-foot intervals and loaded as in 3
6. Cut gaps at 1-foot intervals and loaded at row 07 with P = 750 lbs
7. Cut gaps at 6 in intervals and loaded as in 6.

Fig. 5.8 Configuration and Properties of Specimen T12-8D16-1

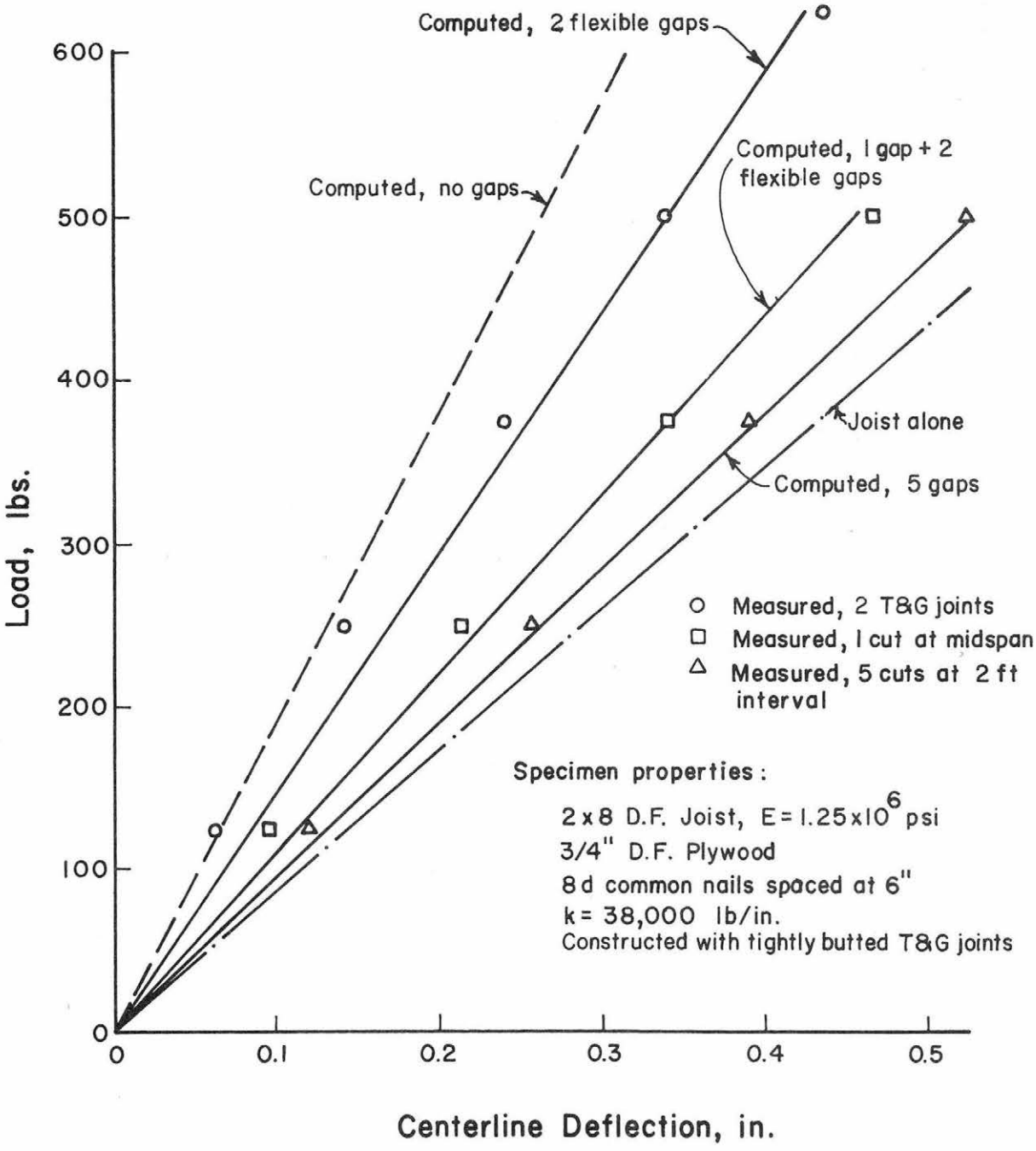

Fig. 5.9 Example of Beam Verification T12-8D16-1 Joist No. 1

Table 5.2 Comparison of Measured and Predicted Midspan Deflections for All T-Beams Tested

Specimen	Joist No.	Load Level (lbs.)	Observed Deflection Δm (in.)	Computed Deflection Δc (in.)	Δc/Δm	Remarks
T4-8D16-1	1	500	.232	0.258	1.11	2 flexible
	2	500	.309	0.361	1.17	gaps
T4-8D16-1	1	500	.262	0.262	1.00	2 open gaps
	2	500	.353	0.349	0.99	2 open gaps
T5-8D16-1	1	500	.338	0.332	0.98	2 open gaps
	2	500	.354	0.341	0.96	2 open gaps
T6-8D16-1	1	640	0.300	0.280	0.93	2 flexible
	2	640	0.282	0.288	1.02	gaps
T7-8D16-1	1	770	0.300	0.300	1.00	2 flexible
	2	770	0.282	0.306	1.08	gaps
T8--8D16-1	1	750	0.373	0.364	0.98	2 flexible
	2	750	0.352	0.378	1.07	gaps
T8-8D16-1	1	750	0.399	0.370	0.93	2 open gaps
	2	750	0.386	0.384	0.99	2 open gaps
T9-8D16-1	1	750	0.314	0.312	0.99	2 flexible
	2	750	0.317	0.302	0.95	gaps
T9-8D16-1	1	750	0.336	0.317	0.95	2 open gaps
	2	750	0.340	0.307	0.91	2 open gaps
T10-12E24-1	1	1000	0.215	0.194	0.90	2 flexible
	2	1000	0.197	0.194	0.98	gaps
T10-12E24-1	1	1000	0.252	0.253	1.00	2 open gaps
	2	1000	0.242	0.253	1.04	2 open gaps
T10-12E24-1	1	1000	0.259	0.272	1.05	5 open gaps
	2	1000	0.253	0.271	1.07	5 open gaps
11-8D16-1	1	375	0.371	0.361	0.97	1 open gap
	2	375	0.348	0.353	1.01	at centerline
T12-8D16-1	1	500	0.322	0.342	1.06	2 flexible
	2	500	0.316	0.316	1.00	gaps
T12-8D16-1	1	375	0.340	0.341	1.00	1 open gap at
	2	375	0.325	0.313	0.96	centerline
T12-8D16-1	1	375	0.390	0.386	0.99	3 open gaps
	2	375	0.362	0.353	0.98	3 open gaps
T12-8D16-1	1	375	0.391	0.398	1.02	5 open gaps
	2	375	0.386	0.364	0.94	5 open gaps
T13-8D16-1	1	375	0.307	0.288	0.94	2 open gaps
	2	375	0.346	0.337	0.97	2 open gaps
T14-12D24-1	1	1000	0.184	0.181	0.98	2 open gaps
	2	1000	0.205	0.194	0.95	2 open gaps

Table 5.2 (Continued)

Specimen	Joist No.	Load Level (lbs.)	Observed Deflection Δm (in.)	Computed Deflection Δc (in.)	Δc/Δm	Remarks
T14-12D24-2	1	1000	0.154	0.157	1.02	3 open gaps
	2	1000	0.167	0.166	0.99	3 open gaps
T15-8E19.2-1	1	300	0.327	0.318	0.97	2 open gaps
	2	300	0.332	0.319	0.96	2 open gaps
T15-8E19.2-2	1	400	0.335	0.313	0.94	5 open gaps
	2	400	0.318	0.314	0.99	5 open gaps
T16-8E19.2-1	1	400	0.339	0.351	1.04	2 flexible
	2	400	0.368	0.384	1.04	gaps
T16-8E19.2-2	1	500	0.357	0.367	1.03	3 flexible
	2	500	0.392	0.396	1.01	gaps
Average:					0.996	

5.3 Comparisons of Measured and Predicted Floor Deflections

Verification studies using the results of the full-scale floor tests were conducted for 22 cases using 16 basic floor specimens. Deflections computed using the finite element form of the crossing beam mathematical model were compared with measured values for working load levels. A concentrated load ranging from 600 to 1000 lbs maximum acting over the midspan of the center joist was applied to each floor. Measured deflections at selected positions along the centerline of each floor specimen were plotted against the computed results. While data were taken at other load positions, for the sake of brevity, only the center loading is reported herein. Percentage errors of the predicted versus the measured deflection are given below for all cases. Selected examples are treated in detail. Complete results are available elsewhere (46).

The theoretical analysis of the behavior of each floor requires certain input data to the mathematical model. These data include floor span, floor length, numbers of T-beams and sheathing strips, dimensions and MOE values of all components, slip modulus values, data on gaps in sheathing layers, and load data.

While the joist span and floor length were held constant at 144 and 192 in. respectively, other physical and geometric properties varied widely. An attempt was made to study a divergent set of specimens to fully test the applicability of the mathematical model.

Material properties for each component of the floor were determined prior to ordering construction of each specimen. The MOE values of joists used where those determined by loading each joist after the header had been connected as previously described for T-beam tests. The MOE values of plywood and particleboard sheathing pieces used were those obtained by the Wood Science Laboratory (See Chapter 3). Flexible gap evaluations were used for those gaps which were tightly butted or glued while open gaps were assumed where the sheathing panels were not butted or glued. Examples of the detailed arrangement of typical floors are given later in this section. A summary of basic data for all floor specimens tested is given in Table 5.3.

Slip moduli values were developed for each case using the basic data cited previously in Table 5.1. Adjustments were made for nail

Table 5.3 Basic Data for Floor Test Specimens

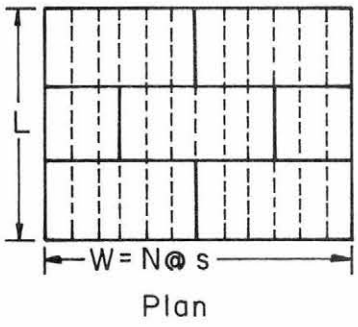

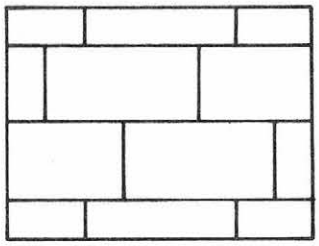

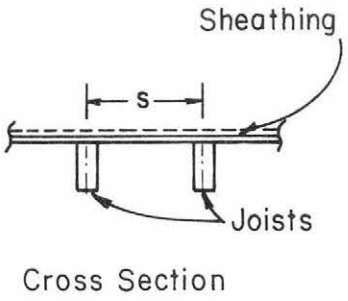

Specimen No.	Joist Size in.	Sheathing	Floor Dimension in. L	W	N	S	Connector	Sheathing Joint	Sheathing face grain direction
F2-8D16-1	2x8 D.F.	3/4" D.F. Plywood	144	192	12	16	8d cement coated @ 8"	T & G	Transverse
F3-8D16-1	2x8 D.F.	3/4" D.F. Plywood	144	192	12	16	8d common @ 8"	T & G	Transverse
F4-12E16-1	2x12 E.S.	3/4" E.S. Plywood	144	192	12	16	8d common @ 6"	T & G	Transverse
F5-8D16-1	2x8 D.F.	3/4" D.F. Plywood	144	192	12	16	8d common @ 4"	T & G glued	Transverse
F6-8E16-1	2x8 E.S.	1/2" E.S. Plywood	144	192	12	16	8d common @ 8"	T & G 1/16" gap	Transverse
F6-8E16-2	2x8 E.S.	1/2" E.S. Plywood 1/2" Particle-board	144	192	12	16	6d common @ 8"	Butted No gap	Stagger joints
F7-12D24-1	2x12 D.F.	1/2" D.F. Plywood	144	192	8	24	8d common @ 4"	Butted 1/16" gap	Transverse
F7-12D24-2	2x12 D.F.	1/2" D.F. Plywood 1/2" P.B.	144	192	8	24	6d common @ 4"	Butted No gap	Double stagger joints
F8-8D19.2-1	2x8 D.F.	1/2" D.F. Plywood	144	192	10	19.2	8d common @ 8"	Butted 1/16" gap	Transverse
F8-8D19.2-2	2x8 D.F.	1/2" D.F. Plywood 1/2" P.B.	144	192	10	19.2	6d common @ 8"	Butted No gaps	Double stagger joints
F9-8E24-1	2x8 E.S.	1/2" E.S. Plywood	144	192	8	24	8d common @ 8"	Butted 1/16" gap	Transverse
F9-8E24-2	2x8 E.S.	1/2" E.S. Plywood 1/2" P.B.	144	192	8	24	6d common @ 8"	Butted No gap	Double stagger joints
F10-8E24-1	2x8 E.S.	1/2" D.F. Plywood	144	192	8	24	8d common @ 4"	Butted 1/16" gap	Transverse
F10-8E24-2	2x8 E.S.	1/2" D.F. Plywood 1/2" P.B.	144	192	8	24	6d common @ 4"	Butted No gap	Double stagger joints
F11-8D16-1	2x8 D.F.	1/2" D.F.	144	192	12	16	Glued	Glued	Transverse
F11-8D16-2	2x8 D.F.	1/2" D.F. Plywood 1/2" P.B.	144	192	12	16	6d common @ 8"	1/16" gap	Double stagger joints

spacing attachment of a third floor layer, and other special features of each specimen. A listing of the slip moduli values used in each case is given in Table 5.4.

The theoretical floor deflections at all nodal points were obtained for each floor in this study. Each three-layer floor specimen produced two cases for the verification study since the specimen displayed different performances depending upon whether the top layer of nails attaching the second sheathing layer were driven or not driven into the joists. Therefore, the verification study of the mathematical floor model is comprised of 22 testing cases from 16 floor specimens.

Examples showing comparisons of computed with measured deflections are shown in Fig. 5.11 through 5.13 for specimens F6-8E16-1 (a two-layer floor) and F6-8E16-2 (a three-layer floor with top layer nails driven and not driven into the joists). A description of these floors is given in Fig. 5.10. The plots of computed and measured results for the remaining specimens are presented in the Appendix.

A comparison of measured and computed midfloor deflections is given in Table 5.5. In general, good results were obtained. The errors ranged from less than one percent to a maximum of 12 percent. The computed deflections fluctuated above and below the measured deflections (a positive percentage error means the mathematical model overpredicts the deflections and a negative percentage error means the mathematical model underpredicts the deflection). For the three-layer specimens, a general trend showed that the percentage error was less when the top layer nails were not driven into joists than when the nails were driven into joists. This indicates that the assumed increase in the value of slip modulus due to this effect was generally not enough when the top layer nails were also driven into the joists.

The average absolute error of the computed deflections with respect to the corresponding measured deflections for all the floor specimens is 6.44 percent, whereas the average algebraic error is +3.24 percent. Thus, deflections at the center of floor (directly under the concentrated load) predicted by the mathematical floor model were generally slightly greater than the corresponding measured deflections and are therfore conservative. The torsional stiffness of the sheathing is not included in the mathematical model and thus computed results were expected to exceed measured results by a small amount.

Table 5.4 Slip Moduli Used for Floor Specimens

Floor Specimen	Joists	Sheathing	Connectors	Nails of Top Layer Not into Joist		Nails of Top Layer Driven into Joist	
				k, lbs/in.	k/s lbs/in./in.	k, lbs/in.	k/s, lbs/in./in.
F2-8D16-1	2x8 DF	3/4 DF Plywd	8d @ 8" (Cement coated)	-	-	30,000	3,750
F3-8D16-1	2x8 DF	3/4 DF Plywd	8d @ 8" (Common nails)	-	-	30,000	3,750
F4-8E16-1	2x12 ES	3/4 ES Plywd	8d @ 6" (Common nails)	-	-	23,000	3,833
F5-8D16-1	2x8 DF	3/4 DF Plywd	8d @ 4" (Common nails)	-	-	45,000	11,250
F6-8E16-1	2x8 ES	1/2 ES Plywd	8d @ 8" (Common nails)	-	-	18,000	2,250
F7-12D24-1	2x12 DF	1/2 DF Plywd	8d @ 4" (Common nails)	-	-	45,000	11,250
F8-8D19.2-1	2x8 DF	1/2 DF Plywd	8d @ 8" (Common nails)	-	-	30,000	3,750
F9-8E24-1	2x8 ES	1/2 ES Plywd	8d @ 8" (Common nails)	-	-	18,000	2,250
F10-8E24-1	2x8 ES	1/2 DF Plywd	8d @ 4" (Common nails)	-	-	45,000	11,250
F11-8D16-1	2x8 DF	1/2 DF Plywd	Glued	-	-	24,000	24,000
F6-8E16-2	2x8 ES	1/2 ES Plywd	8d @ 8" (Common nails)	30,000	3,750	3,000	375
		1/2 ES Plywd	8d @ 8" (Common nails)	18,000	2,250	35,000	8,750
F7-12D24-2	2x12 DF	1/2 DF DB	6d @ 4" (Common nails)	4,500	1,125	4,500	1,125
		1/2 DF Plywd	8d @ 4" (Common nails)	45,000	11,250	50,000	25,000

Table 5.4 Slip Moduli Used for Floor Specimens (continued)

Floor Specimen	Joists	Sheathing	Connectors	Nails of Top Layer Not into Joist		Nails of Top Layer Driven into Joist	
				k, lbs/in.	k/s lbs/in./in.	k, lbs/in.	k/s, lbs/in./in.
F8-8D19.2-2	2x8 DF	1/2 DF PB	6d @ 8" (Common nails)	4,000	500	4,000	500
		1/2 DF Plywd	8d @ 8" (Common nails)	3,000	3,750	45,000	11,250
F9-8E24-2	2x8 ES	1/2 DF PB	6d @ 8" (Common nails)	3,000	375	3,000	375
		1/2 ES Plywd	8d @ 8" (Common nails)	18,000	2,250	35,000	8,750
F10-8E24-2	2x8 ES	1/2 DF PB	6d @ 4" (Common nails)	4,500	1,125	4,500	1,125
		1/2 DF Plywd	8d @ 8" (Common nails)	45,000	5,625	50,000	18,750
F11-8D16-2	2x8 DF	1/2 DF PB	6d @ 8" (Common nails)	4,000	500	4,000	500
		1/2 DF Plywd	Glued	24,000	24,000	54,000	27,750

Note: DF = Douglas-fir
ES = Engelmann spruce
Plywd = Plywood
PB = Particle board
k = Slip modulus
s = Nail spacing

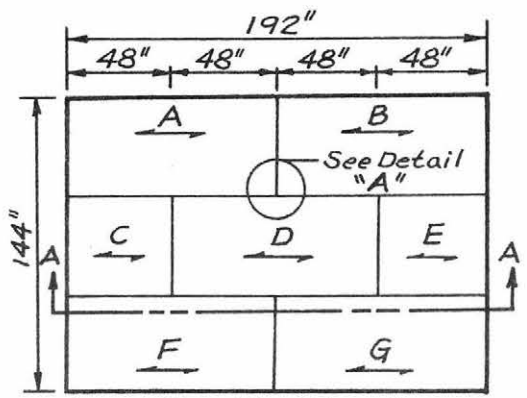

Plan of Top Sheathing Layer

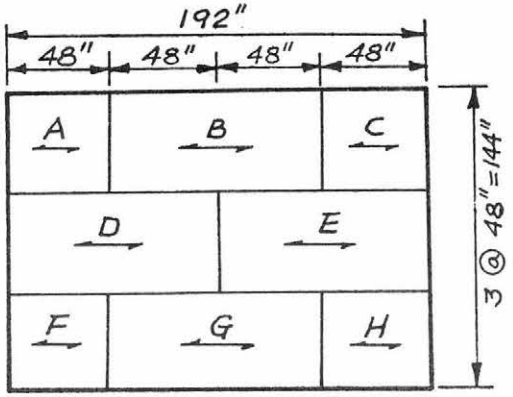

Plan of Bottom Sheathing Layer

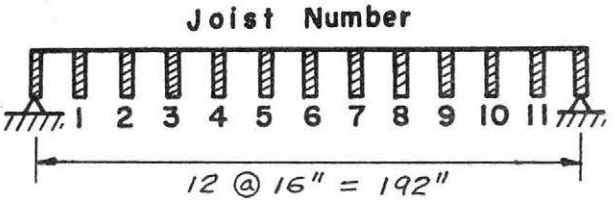

Section A-A

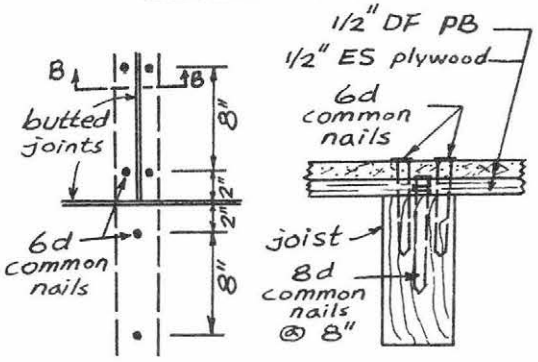

Detail "A" Section B-B

Material	Property	Joist Number										
		1	2	3	4	5	6	7	8	9	10	11
2×8 ES joist	Actual Size, in (width x depth)	1.51 × 7.20	1.50 × 7.20	1.54 × 7.38	1.47 × 7.24	1.50 × 7.23	1.48 × 7.26	1.51 × 7.19	1.54 × 7.15	1.50 × 7.23	1.51 × 7.19	1.50 × 7.27
	Average MOE ∥ Grain, 10^6 psi	1.16	1.12	1.13	1.14	1.06	1.67	1.24	1.21	1.18	1.23	1.27

Joist Data

Layer	Material	Thickness in.	Gap	Connector	Average MOE, 10^6 psi															
					A		B		C		D		E		F		G		H	
					∥	⊥	∥	⊥	∥	⊥	∥	⊥	∥	⊥	∥	⊥	∥	⊥	∥	⊥
Bottom	1/2 ES plywood	3/8	1/16" T&G	8d nails @ 8"	1.36	0.21	1.36	0.20	1.36	0.21	1.41	0.23	1.40	0.23	1.45	0.23	1.43	0.24	1.45	0.23
Top	1/2 DF PB	1/2	butted no gap	6d nails @ 8"	0.42	0.31	0.53	0.41	0.45	0.35	0.46	0.33	0.45	0.35	0.42	0.33	0.51	0.40	—	—

Sheathing Data

Fig. 5.10 Layout and Data of Specimens F6-8E16-1 and F6-8E16-2

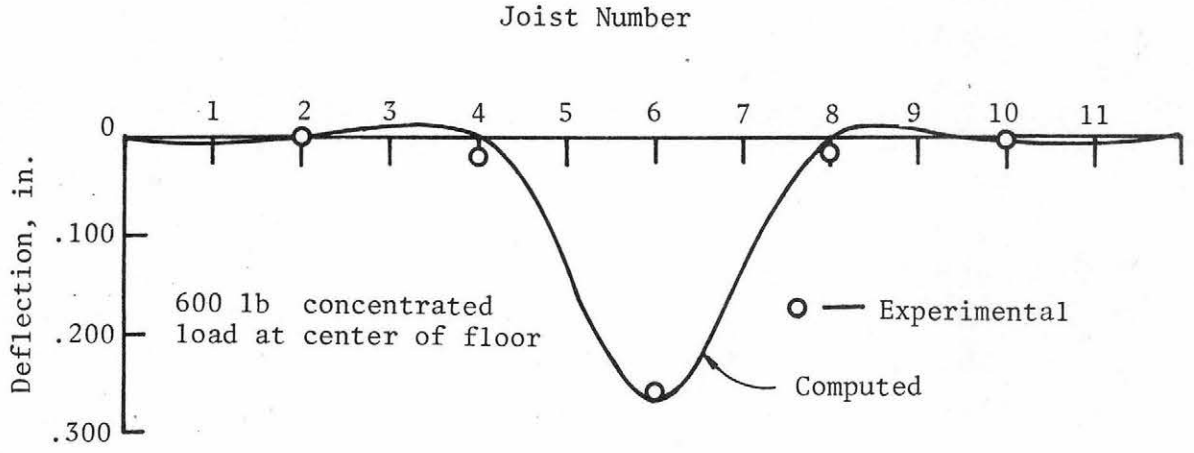

(a) Deflection Profile at Centerline of Joists

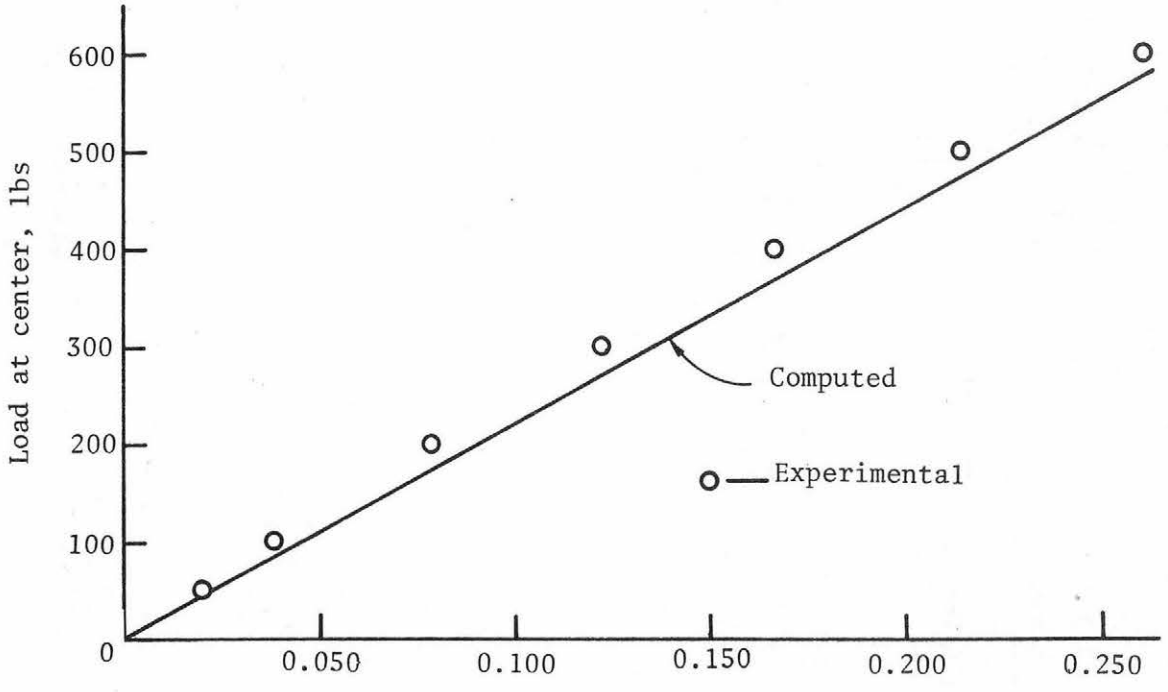

(b) Load-Deflection Behavior

Fig. 5.11 Computed vs Measured Results of Floor Specimen F6-8E16-1

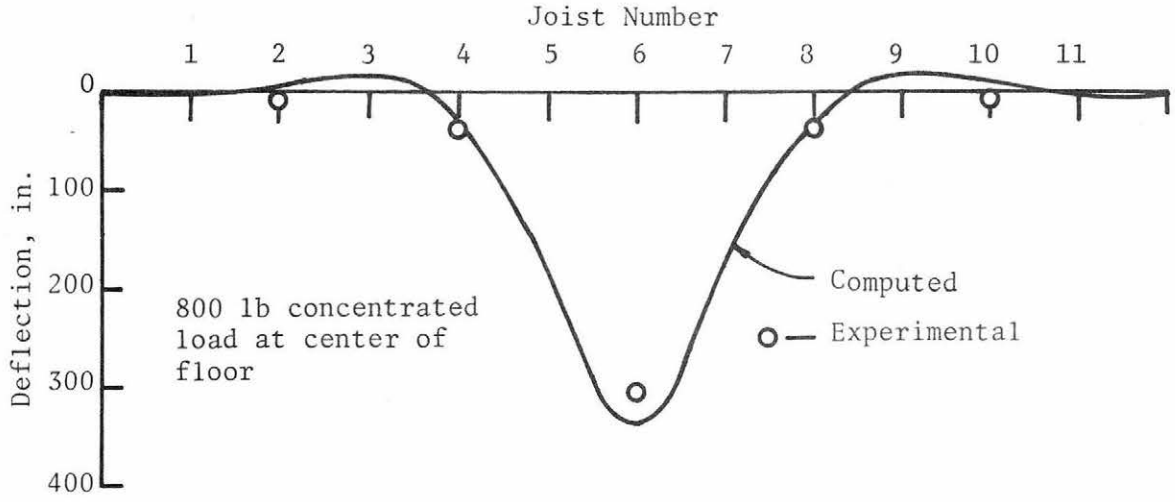

(a) Deflection Profile at Centerline of Joists

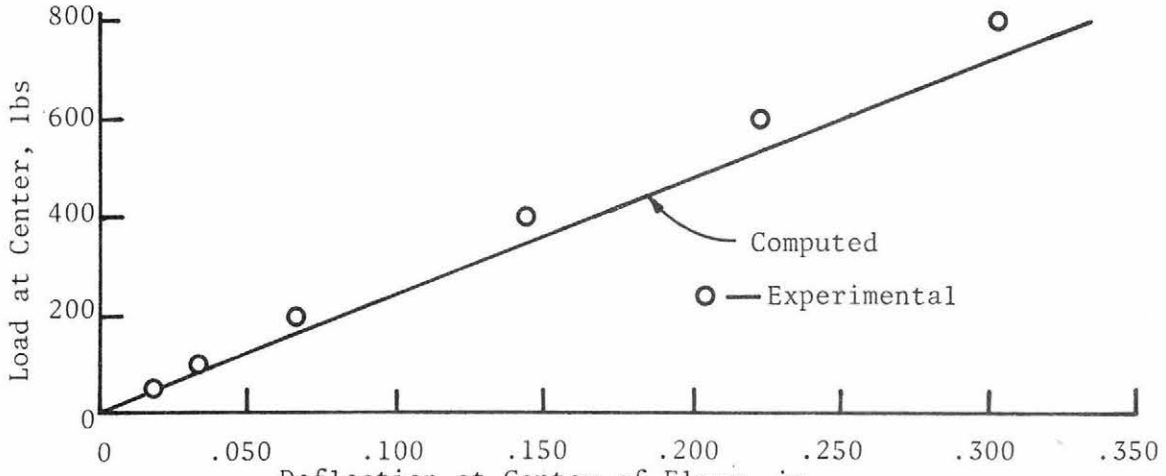

(b) Load-Deflection Behavior

Fig. 5.12 Computed vs Measured Results of Floor Specimen F6-8E16-2 (Nails of Top Layer Not Driven into Joists)

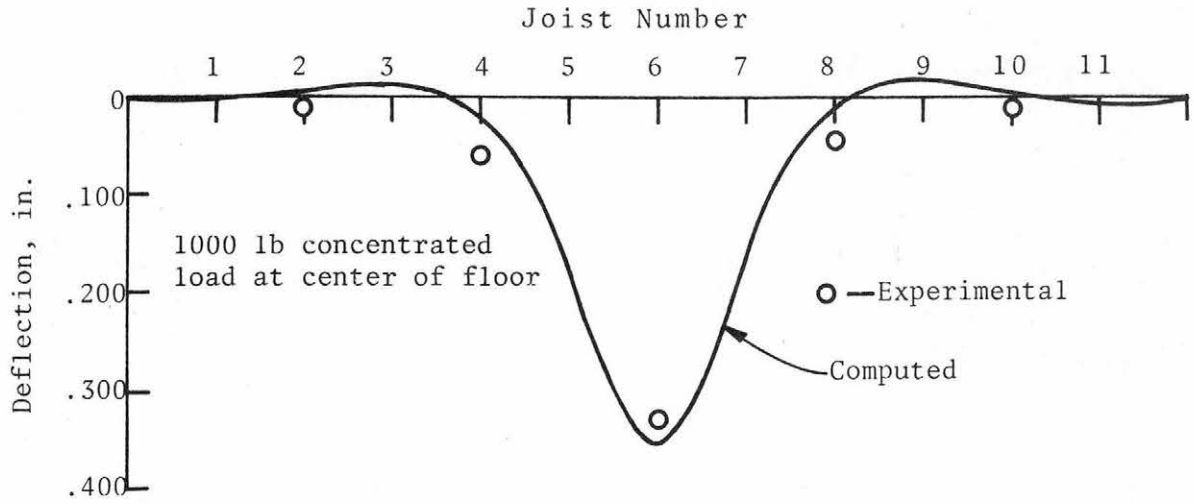

(a) Deflection profile at centerline of joists

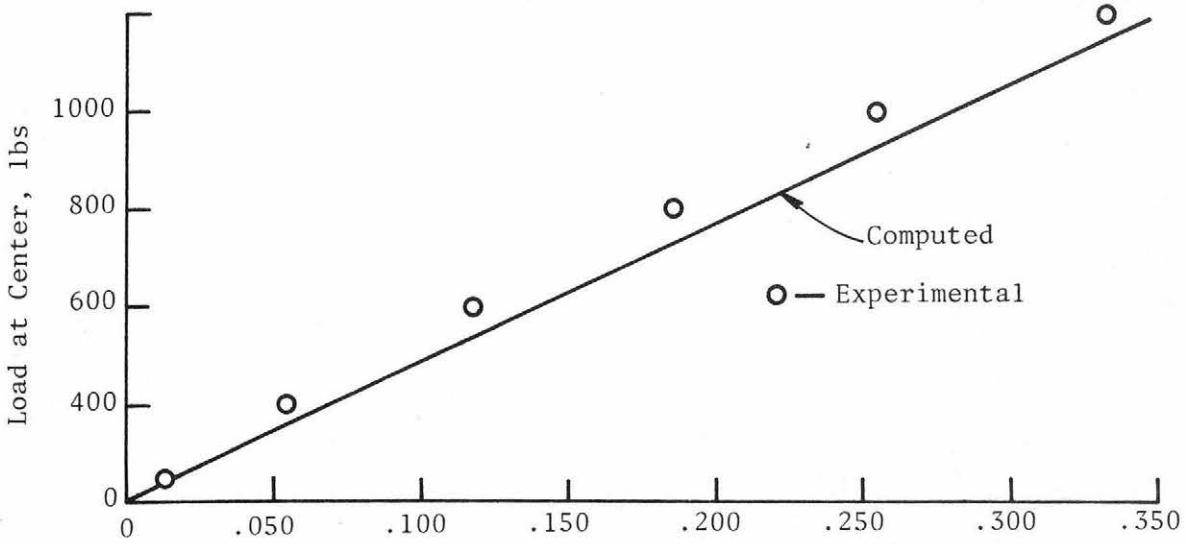

(b) Load-deflection behavior

Fig. 5.13 Computed vs Measured Results of Floor Specimen F6-8E16-2 (Nails of Top Layer Driven into Joists)

Table 5.5 Comparison of Computed and Experimental Results

Floor Specimen	Computed Deflection at Center of Floor, (in.)	Experimental Deflection at Center of Floor, (in.)	Load Level (lbs)	Error, %
F2-8D16-1	0.278	0.261	1,000	+6.51
F3-8D16-1	0.251	0.269	1,000	-6.69
F4-12E16-1	0.112	0.127	1,000	-11.81
F5-8D16-1	0.236	0.217	1,000	+8.76
F6-8E16-1	0.270	0.260	600	+3.85
F7-12D24-1	0.168	0.165	1,000	+1.82
F8-8D19.2-1	0.296	0.337	1,000	-12.17
F9-8E24-1	0.417	0.395	600	+5.57
F10-8E24-1	0.366	0.359	800	+1.95
F11-8D16-1	0.209	0.215	1,000	-2.78
F6-8E16-2 (Nails of top layer not into joists)	0.336	0.303	800	+10.89
F6-8E16-2 (Nails of top layer driven into joists)	0.352	0.326	1,000	+7.98
F7-12D24-2 (Nails of top layer not into joists)	0.146	0.141	1,000	+3.55
F7-12D24-2 (Nails of top layer driven into joists)	0.144	0.132	1,000	+9.09
F8-8D19.2-2 (Nails of top layer not into joists)	0.284	0.278	1,000	+2.16

Table 5.6 Comparison of Computed and Experimental Results (continued)

Floor Specimen	Computed Deflection at Center of Floor, (in.)	Experimental Deflection at Center of Floor, (in.)	Load Level (lbs)	Error, %
F8-8D19.2-2 (Nails of top layer driven into joists)	0.274	0.250	1,000	+9.60
F9-8E24-2 (Nails of top layer not into joists)	0.413	0.410	800	+0.73
F9-8E24-2 (Nails of top layer driven into joists)	0.387	0.394	800	-1.78
F10-8E24-2 (Nails of top layer not into joists)	0.367	0.352	1,000	+4.26
F10-8E24-2 (Nails of top layer driven into joists)	0.361	0.321	1,000	+12.46
F11-8E16-2 (Nails of top layer not into joists)	0.206	0.195	1,000	+5.64
F11-8E16-2 (Nails of top layer driven into joists)	0.199	0.183	1,000	+8.74

Average Absolute Error = 6.44%

Average Algebraic Error = +3.24%

Overall, the errors of the computed deflections with respect to the measured midfloor deflections are relatively small. Therefore, the mathematical floor model developed in this study is regarded as having a very good accuracy in predicting the behavior of wood joist floor systems of widely divergent types.

6. USES OF VERIFIED MATHEMATICAL MODELS

6.1 Introduction

With few exceptions, research in wood and wood structures has been developed from the viewpoint of testing unknown materials or systems to obtain statistical data on their behavior. Typically, a wood research project is conducted by isolating the variables thought to affect a particular behavior, establishing the test levels of each variable, choosing the number of replications and then testing the large number of specimens resulting. This testing is followed by statistical analyses and conclusions are then drawn.

While this method is well suited to establishing strength properties of wood or other similar types of basic information, it is clearly inappropriate for determining behavior of wood structural systems for at least three reasons. First, the inordinate amount of testing required makes the method financially impossible. Second, the procedure is obsolete for application to structural systems, and third, it is often very difficult to construct wood specimens identical except for one variable so that the effect of a chosen parameter can be isolated. The approach of this research has been the development and verification of a mathematical model of the system based on rational analysis. Now that the model has been verified, as the previous chapter shows has been due, a computer may be used as the "testing machine" to study many important behavior, design, and application questions for wood joist structural systems.

To demonstrate the capabilities of the verified mathematical model of wood joist floor systems, a pilot series of parameter studies was conducted. The parameter studies isolate the effects of specific variables on floor performance and thus can form the bases for the development of rational design procedures and future studies of the effects of material variability on floor performance.

6.2 Floor Configuration Used in Parameter Studies

A two-layer floor specimen was selected as the basic floor for the parameter studies on the floor behavior. Fixed data included a 144-in. joist span, 192-in. floor length, 2 x 8 in. nominal joist sizes, 16-in. joist spacings, 8-in. nail spacings and one row of nails per joist. Basic data included a 3/4 in. sheathing thickness, a sheathing MOE of

2,000,000 psi parallel to grain and of 1,000,000 psi perpendicular to grain, joist MOE values of 2,000,000 psi, and a connector slip modulus of 30,000 lbs/in.

The face grain of the sheathing was oriented perpendicular to the joist span in all cases. The floor was assumed to have no gaps in the sheathing and was idealized as containing 11 T-beams and 11 sheathing strips crossing each other at right angles. Simple supports were assumed at all edges of the floor.

Two loading pattern examples were considered. The first was a single concentrated load of 1100 pounds applied at the center of floor. The second was a uniform load of 120 psf, which is equivalent to a concentrated load of 160 lbs at each nodal point. These load magnitudes were chosen such that if no two-way or composite action occurred, the midspan joist deflections would be nearly the same for each loading.

The floor configuration was chosen to represent a fairly typical floor so that the results would be meaningful and within the range expected for most floor systems. The numerical results for floors with different properties and configurations from those chosen will, of course, differ from those resulting for the floor selected.

6.3 Effects of Parameters on Floor Behavior

In this section the isolated effects of connector slip modulus, joist MOE values, and effective flange width on floor behavior are examined. The isolated effects were obtained by varying only one parameter at a time, while holding all other input data constant.

6.3.1 Effect of Slip Modulus

The effect of slip modulus on composite action is shown in Fig. 6.1 for the concentrated loading case. Midspan joist deflections are plotted versus slip modulus values. For slip modulus values less than about 1000 lbs/in., the effect of sheathing as a T-beam flange is negligible. Rather, the sheathing and the joist carry all of the load in the joist direction through nearly independent action. This represents the region of insignificant composite action. While little composite action is present for low values of slip modulus, the deflections of the adjacent joists shown in Fig. 6.1 indicate that two-way action exists. For slip modulus values greater than 10^6 lbs/in., essentially complete composite action is present and the joist plus effective

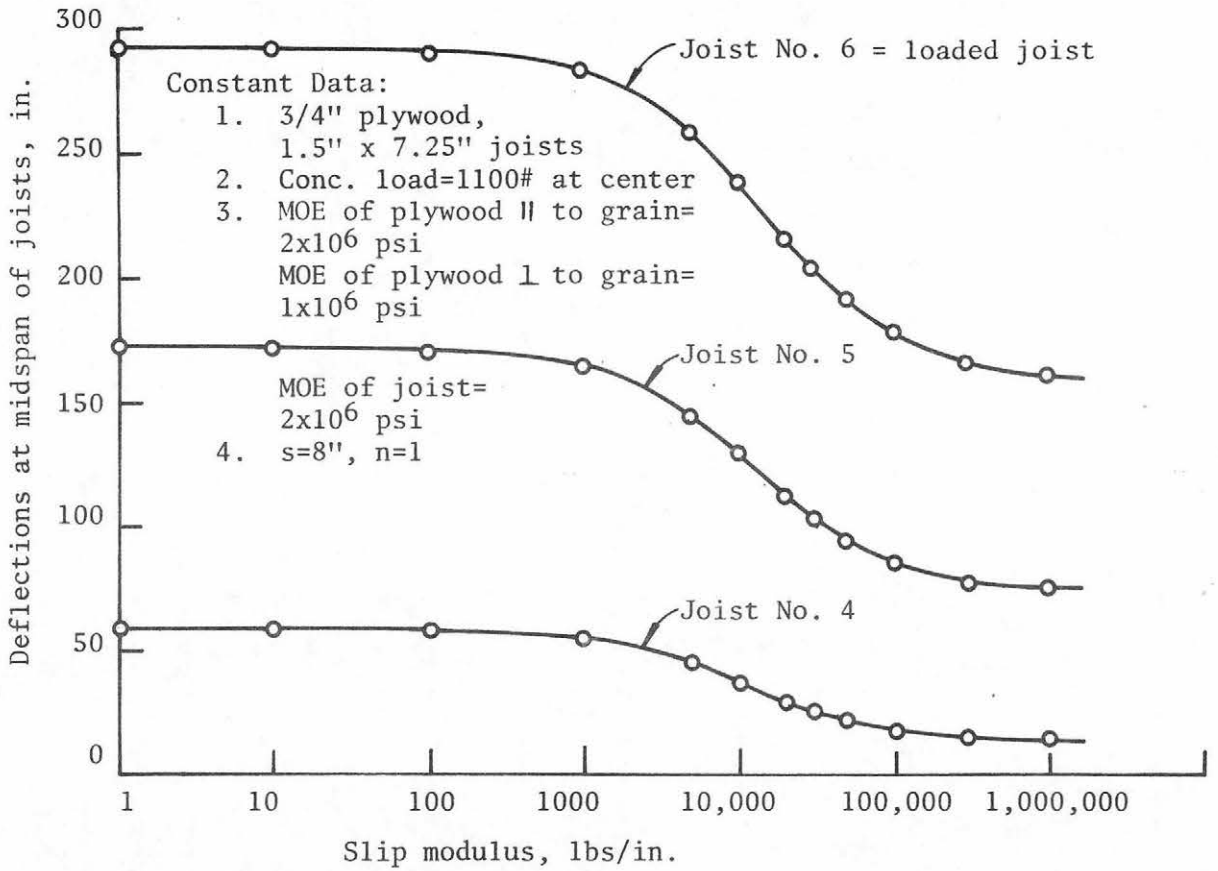

Fig. 6.1 Deflections vs Slip Modulus, k, Concentrated Load

flange behave nearly as a rigidly-connected beam. Consequently, the deflections are reduced by a substantial amount compared to the region of low slip modulus. Slip modulus values between 10^3 and 10^6 lbs/in. represent the region of incomplete composite action. Both significant composite action and interlayer slip occur in this region. The slip moduli of most currently used structural connectors, except very rigid glues, fall in this range. Thus, either the neglect of interlayer slip or the assumption of full composite behavior for the commonly used connectors can lead to gross error.

Similar behavior is observed for the same floor subjected to uniform load, as shown in Fig. 6.2. Fairly uniform deflections are noted for the joists. The small differences in joist deflections are due to the fact that while the same load is applied to each joist, the sheathing carries a portion of the load to the supports at the ends of sheathing strips.

6.3.2 Effect of Joist MOE

One of the major parameters affecting floor behavior is the average joist MOE value. Figure 6.3 shows the effect of MOE on floor deflections for the case of a concentrated load at midfloor. The deflection curves are seen to be very sensitive to changes in MOE in the low joist MOE range (less than 10^6 psi). As the joist MOE increases from 10^6 psi to 2×10^6 psi with all other parameters held constant, the midspan deflection of the loaded joist decreases by 40 percent. The MOE values of the Douglas-fir and Engelmann spruce joists used in the experimental program of this study generally fell between 10^6 and 2×10^6 psi. Deflections vary less slowly with MOE values than the normal inverse relationship between deflections and MOE values because of the two-way interaction of T-beams and sheathing strips. Similar behavior is observed for the same floor subjected to uniform load as seen in Fig. 6.4.

6.3.3 Effect of Effective Flange Width

The plot of floor deflections versus the effective flange width for the case of a concentrated load at midfloor is given in Fig. 6.5. The 16-in. flange width corresponds to the joist spacing. It is seen from Fig. 6.6 that the deflections are relatively insensitive to the effective flange of the loaded T-beam. Reducing this value by 50 percent,

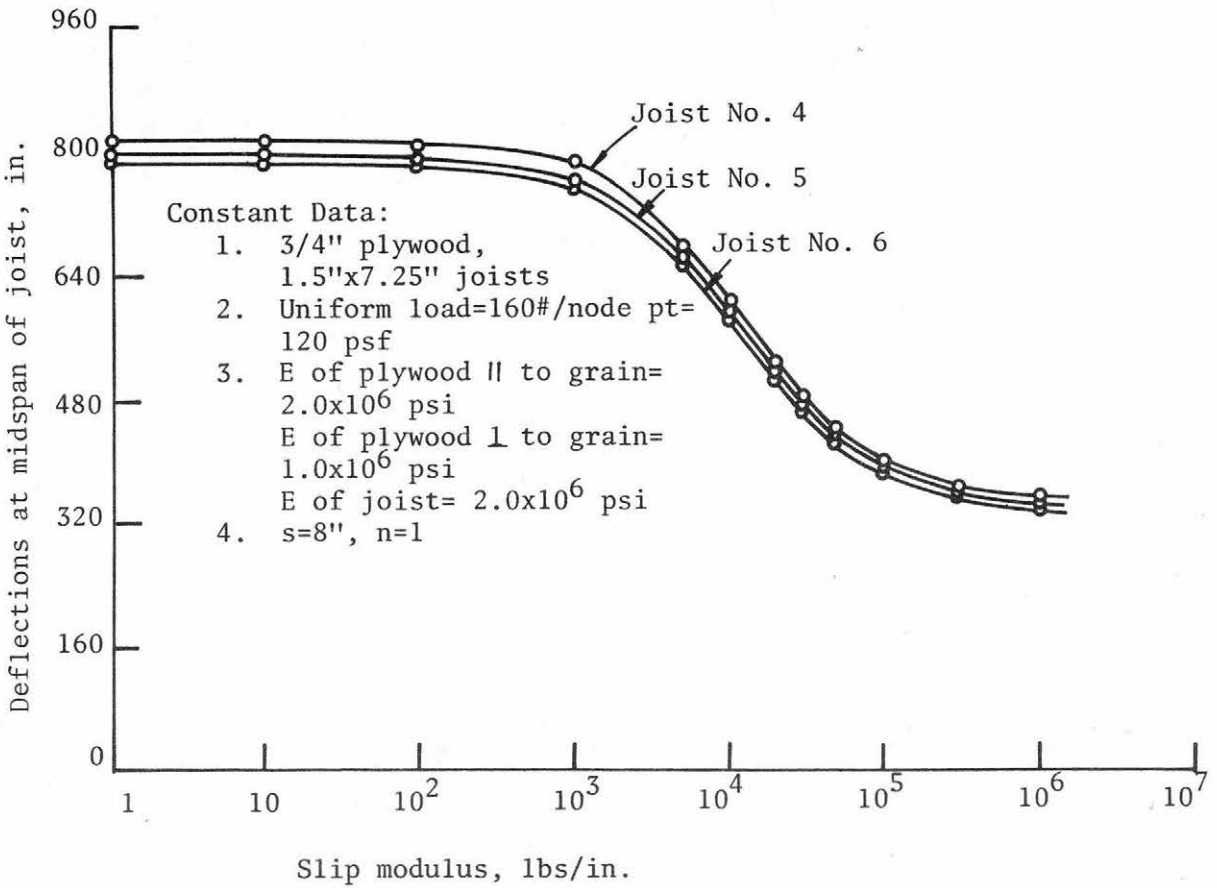

Fig. 6.2 Deflections vs Slip Modulus of Floor Joists with Uniform Load

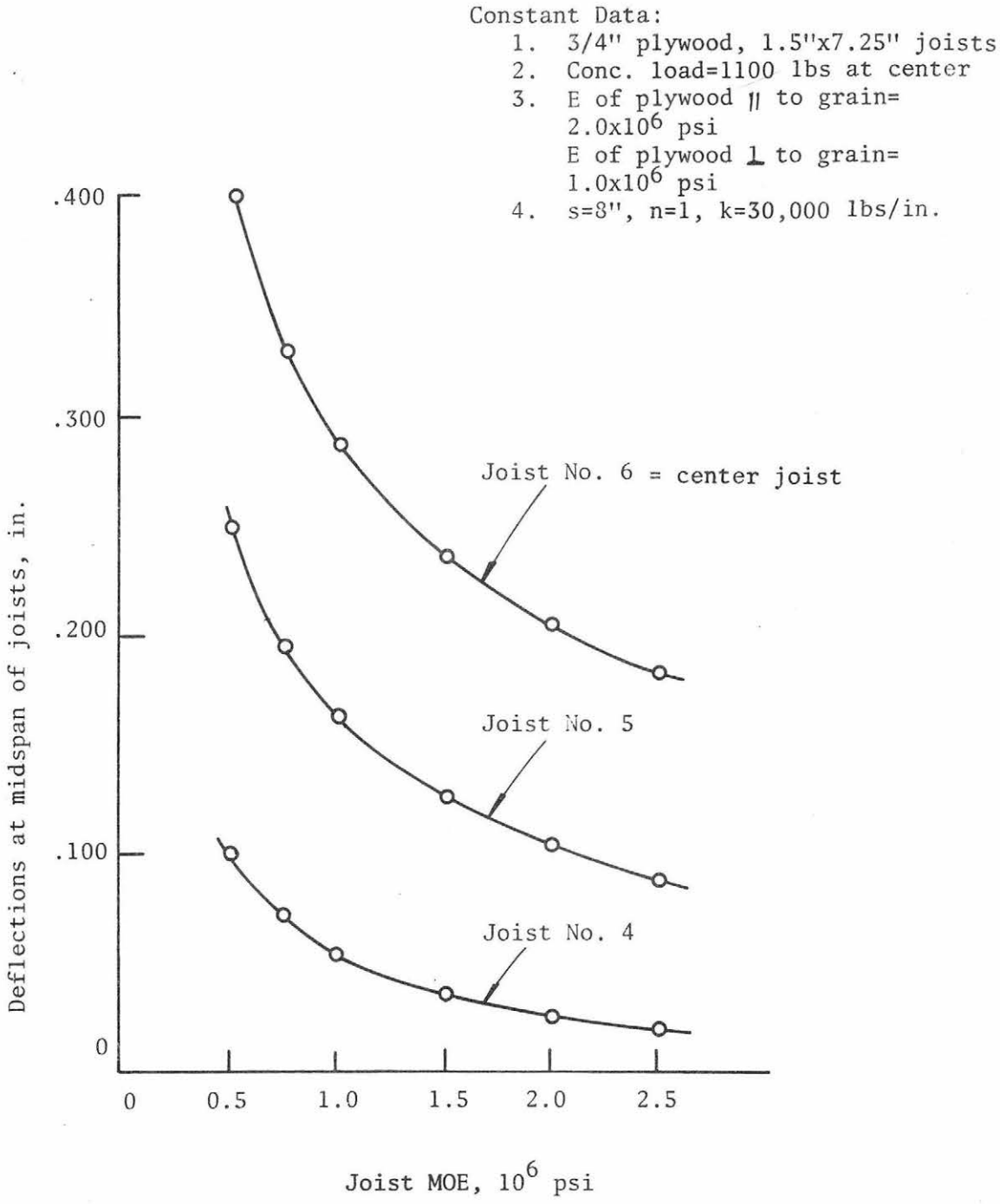

Fig. 6.3 Joist MOE vs Joist Deflections

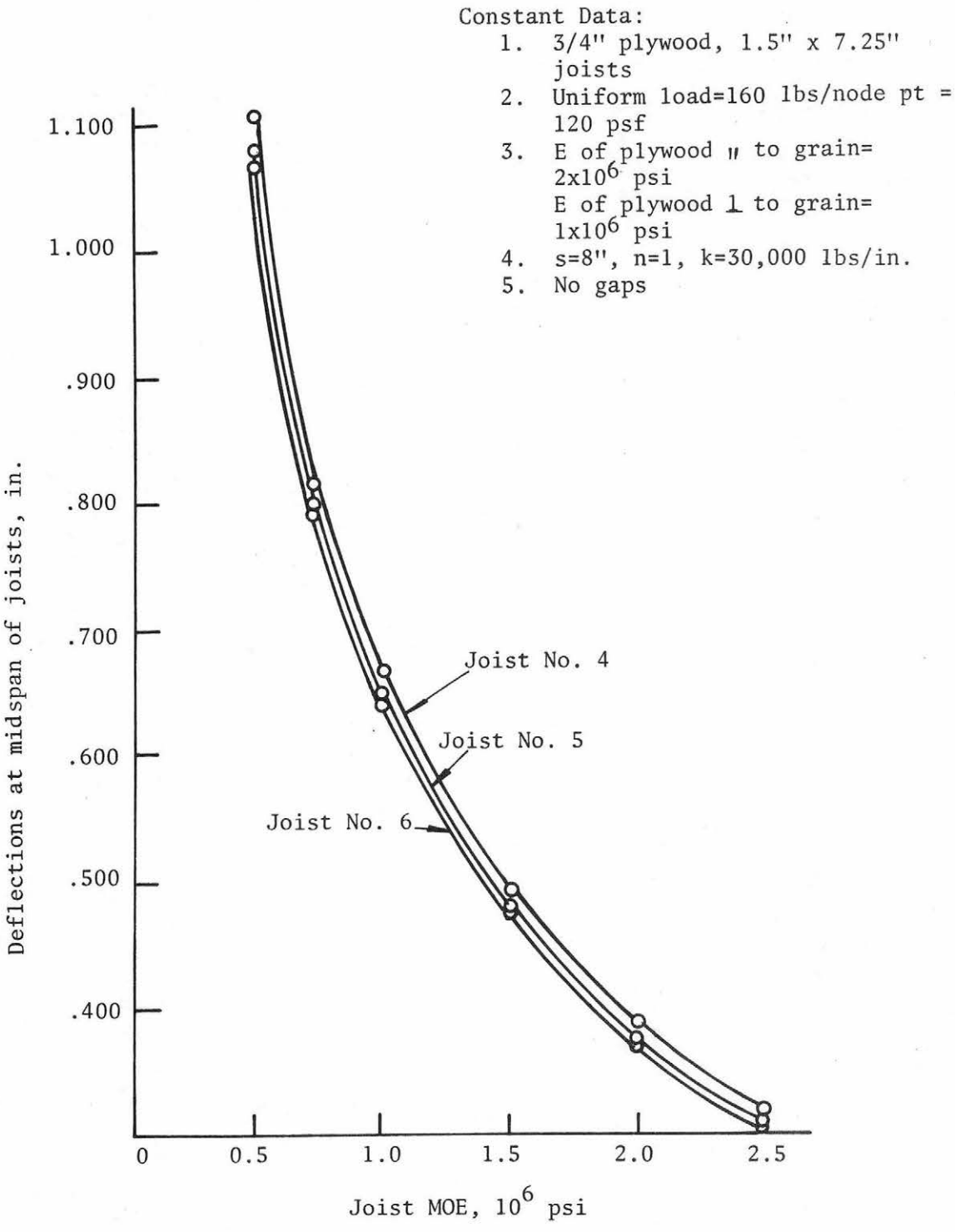

Fig. 6.4 Joist MOE vs Joist Deflections with Uniform Load

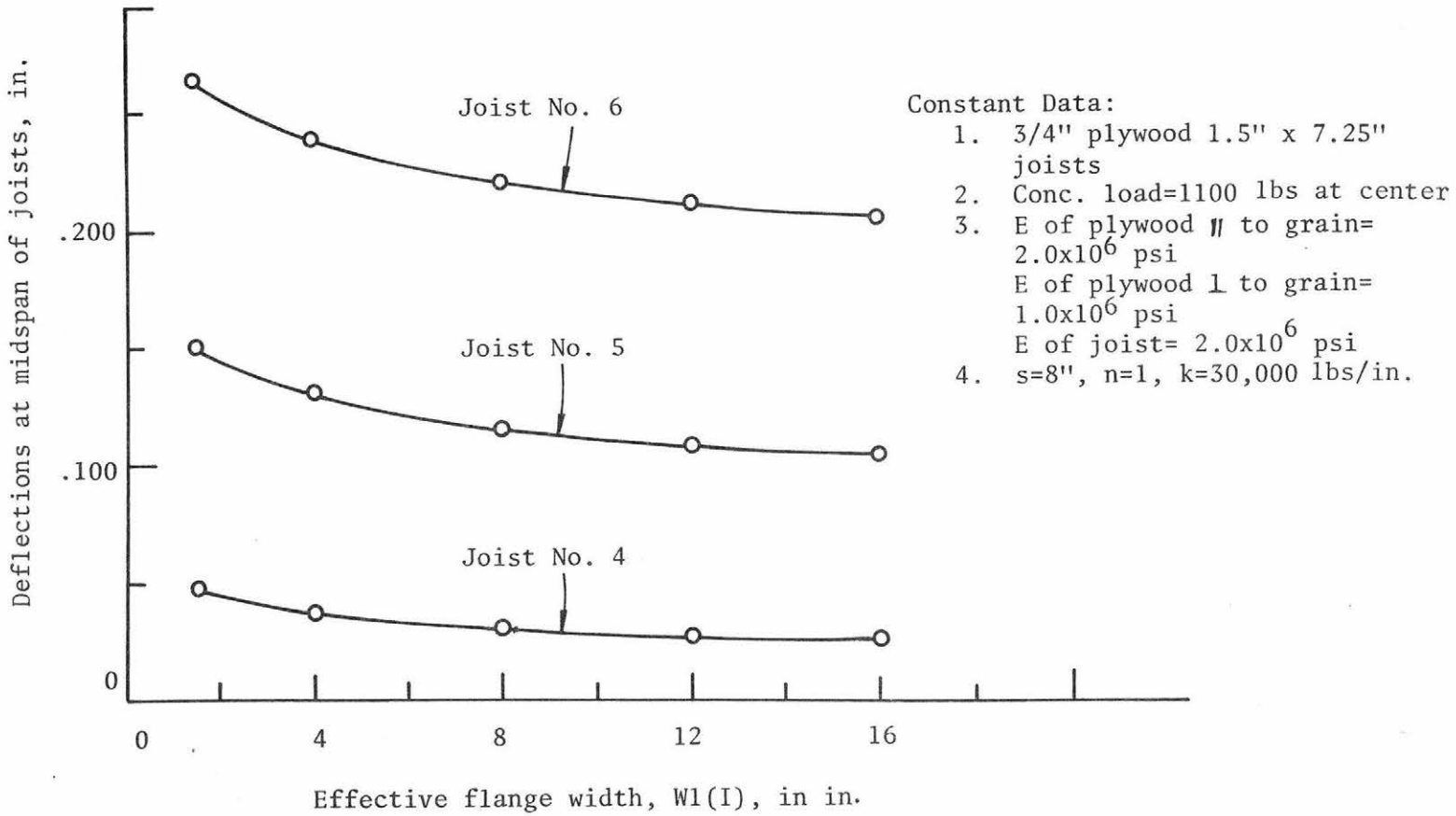

Fig. 6.5 Effective Flange Width vs Joist Deflections with Concentrated Load at Midspan of Joist No. 6

from 16 to eight in., which is equivalent to assuming that only 50 percent of the available flange is effective in carrying load, results in only an eight percent increase in deflection of the loaded joist when the other parameters are held constant. Even smaller percentage increases are noted for the other joists. Results of the study of effective flange width indicate that for the range of parameters studied, the flange is fully effective at some distance away from the ends and gaps in sheathing, for normal joist spacings.

A similar trend for the behavior of the effective flange width versus the floor deflections for the uniform load case is illustrated in Fig. 6.6.

6.4 Simulation Studies of the Effects of Component Variability

In joist floor systems joists and sheathing interact both by composite action of the joist and sheathing and by load sharing between joists resulting from the distribution of load by the sheathing. Current design practice does not directly include the benefits of composite action and load sharing, but rather is in part based upon a maximum deflection limit for a single joist. The joist is considered to have a modulus of elasticity corresponding to the mean modulus of elasticity of the lumber grade. However, in any given real floor, the modulus of elasticity of the joists will vary according to the characteristics of the lumber population which in turn is dependent upon the grading system used. If interaction with other components of the floor system is not considered, about one-half the joists would be expected to deflect in excess of the computed deflection, which often is at or close to the maximum deflection limit. The deflection characteristics of a population of floors with respect to design practices will depend on the magnitude of the counteracting effects of structural interaction and component variability.

A limited study of the effects of component variability, in particular that of MOE of the joists, was conducted by Dawson (19) as part of this project. Research on this aspect of the rational analysis of wood joist systems is continuing and only a brief review of the results is presented here.

A Monte Carlo simulation analysis was conducted using an assumed distribution of joist MOE with a mean MOE of 1.8×10^6 psi. The

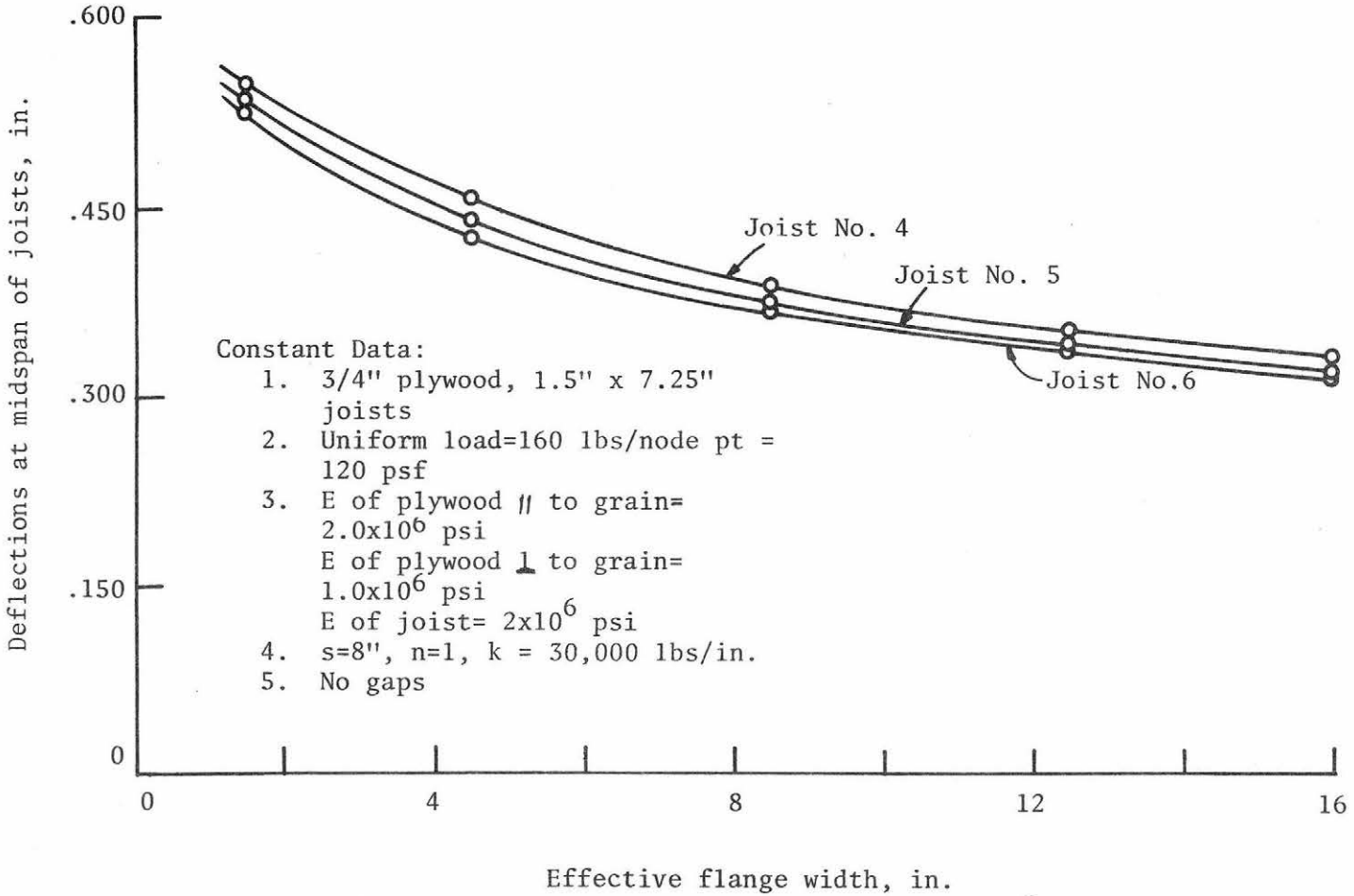

Fig. 6.6 Effective Flange Width vs Joist Deflections with Uniform Load

Monte Carlo method uses a technique including random number generation to simulate a set of joists with MOE values randomly chosen from a given population. Properties of this set of joists is then used as input to the mathematical model for floors and the behavior of the system is obtained. By repeating this procedure a large number of times (a set of 100 floors was analyzed in each case), a resulting distribution for floor behavior, in this case maximum deflection, can be obtained. Details of the Monte Carlo methods are described by Dawson (19).

Distributions of joist MOE values used in the analyses are shown in Fig. 6.7. Coefficients of variation for the three assumed distributions are .056 for the low, 0.215 for the medium, and 0.408 for the high variability populations.

As joist MOE was the variable in this study, other floor parameters, such as sheathing and connector properties and floor geometry, were held constant during a specific simulation. The constant floor parameters were selected such that the simulation floors would be generally typical of those currently being built for residential housing. Simulation of typical flooring systems using an accurate mathematical model provides deflection distributions from which conclusions of effects of variability on flooring systems can be drawn directly. This eliminates the need to predict the behavior of real floors by extrapolating the results obtained from use of a simplified floor system or deflection model.

In the above study a floor composed of eleven joists with 16" spacings was selected. The joist span of 160 inches was chosen based upon using 2 x 8" joists, a mean MOE of 1.8×10^6 psi, and a deflection limit of L/360, at a uniform load of 40 psf.

Results of the deflection simulations for the various floor configuration and joist MOE variability combinations are listed in Table 6.1. Simulation I was conducted using the floor model without gaps. The floors were assumed to have a sheathing thickness of 0.75 in. and a slip modulus of 30,000 lbs/in. A total of three hundred floors (one hundred for each degree of variability of the joist MOE distribution) were randomly generated and analyzed for deflections corresponding to a 40 psf uniform load.

Simulation II was also conducted using the mathematical floor model assuming no gaps. The floors had 0.5 inch sheathing and a slip

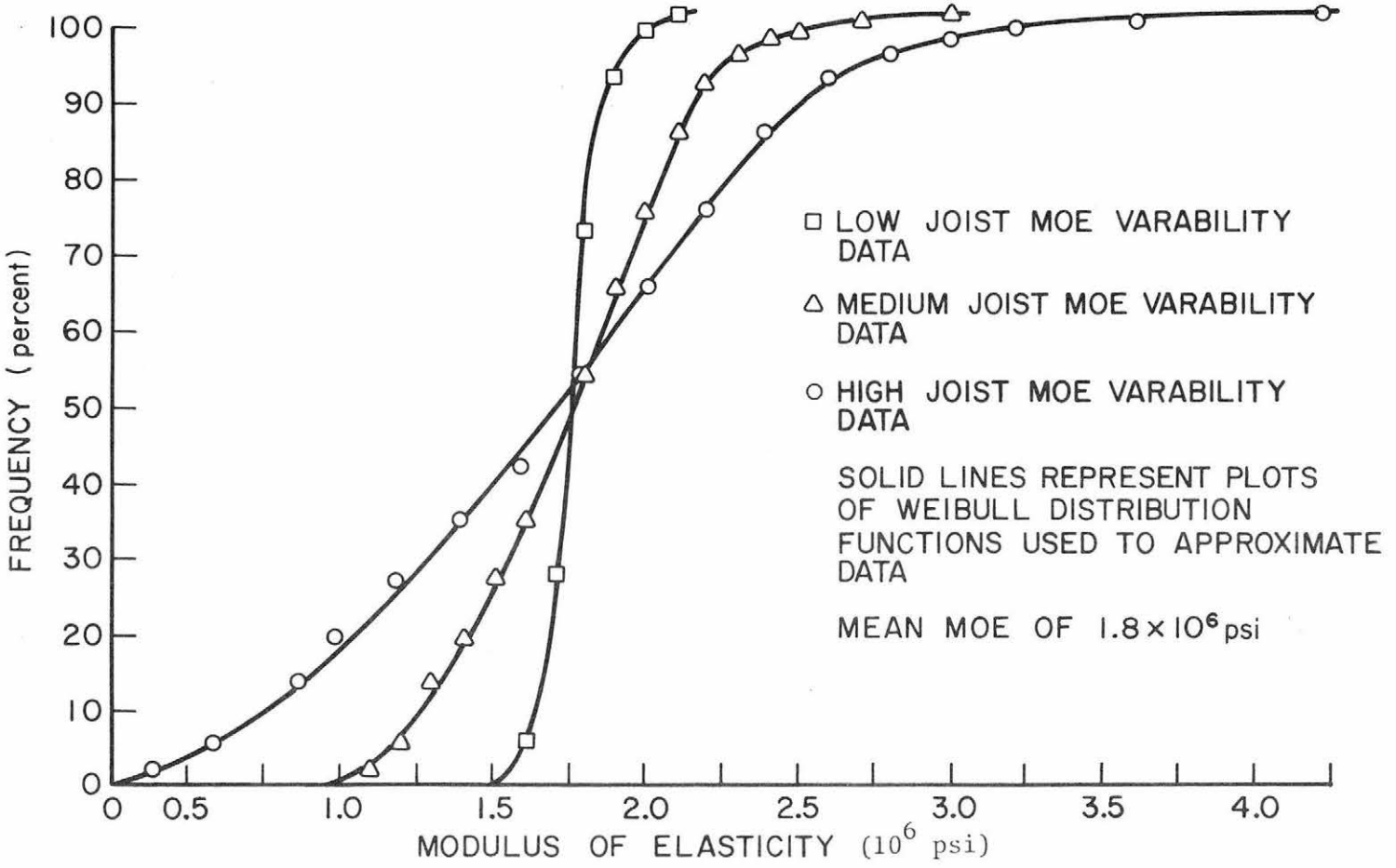

Fig. 6.7 Cumulative Distributions of Joist MOE Values

Table 6.2 Comparison of Average Floor Maximum Predicted Deflections

Simulation*	Floors with No MOE Variability	Floors with Low Joist MOE Variability	Floors with Medium Joist MOE Variability	Floors with High Joist MOE Variability
I	.266	.274	.296	.345
II	.304	.335	.374	.454
III	.386	.399	.436	.519
IV**	.444	.521	.919	1.327

*For assumptions made for each simulation, refer to text.
**Computed assuming no composite and no two-way action, i.e. joists only.
NOTE: To obtain the average floor maximum predicted deflections, the maximum deflections displayed by any of the eleven joists in the system have been averaged for each floor simulated.

modulus of 15,000 lbs/in. One hundred floors were generated from each of the three joist MOE distributions and analyzed for a uniform loading of 40 psf.

Simulation III utilized the finite element version of the floor model. The floors consisted of 0.75 in. sheathing with a slip modulus of 30,000 lbs/in. Open gaps in the sheathing strip were included.

The deflections of the floors corresponding to the configurations used in the three simulations were determined for joists of uniform 1.8×10^6 psi MOE. The purpose of this was to separate the effects of structural interaction and joist MOE variability on floor deflection. From Table 6.1 it can be observed that the presence of structural interaction markedly stiffens the floor in comparison to a joist only prediction. As greater amounts of joist MOE variability are introduced, the stiffness expected for the most highly deflected joist in the floor decreases. For the simulations conducted, only the mean maximum deflection of floor populations derived from the high variability joist MOE distribution exceeded L/360 deflection value computed for the joists only and neglecting joist variability. Thus, the beneficial influence of more restrictive grading, i.e., reducing the joist MOE variability, is clearly evident.

6.5 Evaluation of Stresses and Connector Forces in T-Beams

Limited study using the verified mathematical model has been made to evaluate the stresses and connector forces (or connector stresses in glued systems). Using the finite element model, these stresses have been obtained for a series of T-beams studied during the experimental phase of the project. A complete description of this work is given by Tremblay (73). Work on this aspect of the complete analysis for floors is continuing. A brief example illustrating the effects of composite action on the stresses in a T-beam is discussed below to demonstrate the capability of the developed mathematical model.

In Fig. 6.7, the stress distributions for a typical T-beam component of a floor system are shown as a function of slip modulus. In current design practice composite action is ignored and thus the flange of the T-beam cannot act to relieve stresses in the joist. For $k = 0$, the flange and joist act independently as two beams with equal deflection (friction neglected). For a k value of 60,000 lbs/in.,

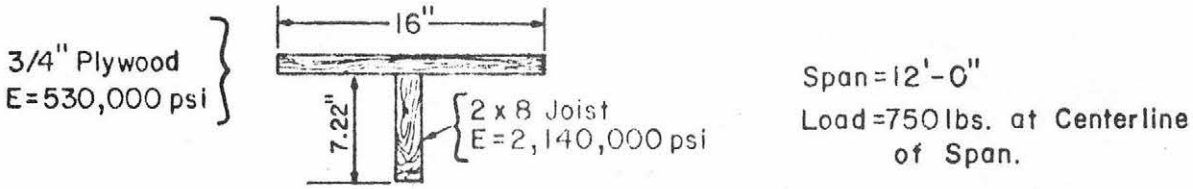

a) T-Beam Properties

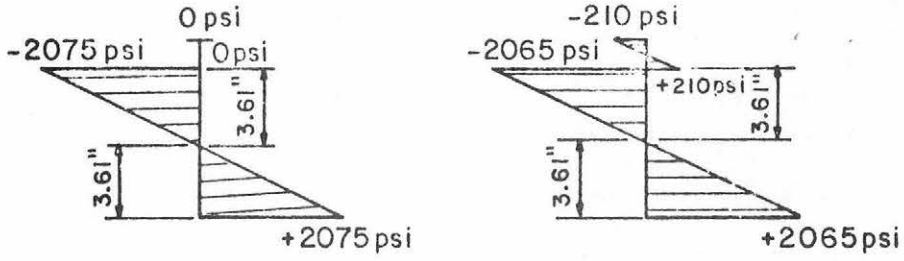

Current Design Assumption — Slip Modulus k = 0

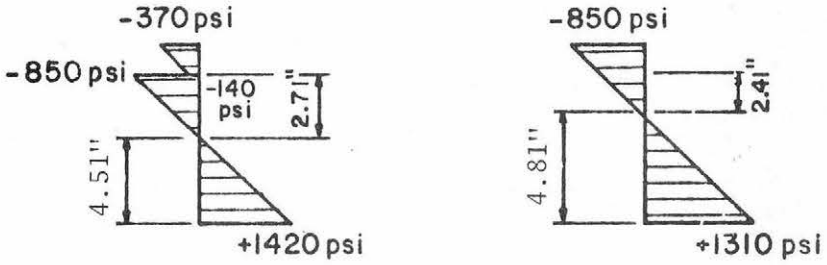

Slip Modulus k = 60,000 lbs/in. — Slip Modulus k = ∞

b) Stress Distributions for Various Values of Slip Modulus

Fig. 6.7 Effect of Composite Action on Bending Stress in a T-Beam

a reasonable value for some elastomerically glued or nailed beams, the maximum stress in the joist is seen to be greatly reduced. If full flange-joist continuity could be achieved (by rigid glues for example), k would equal infinity and the stresses in the joist would be further reduced. Thus, the effect of composite action is generally to reduce the maximum stresses in the joist.

The connector forces are also of considerable concern. Tremblay (73) has shown that connector forces in nailed systems tend to be somewhat greater than expected at working loads, particularly near gaps in sheathing. Details of connector force evaluations for the T-beam specimens tested can be found in his thesis.

6.6 Use of Verified Model to Develop Design Procedures

Design criteria for any structural system could be based on proper considerations of the system's behavior under both working and ultimate load levels. Present design of wood joist systems considers only deflection and working stress design with no recognition of structural interaction between the joist and sheathing elements. By using the developed mathematical model based on full recognition of structural interaction, along with its extension to enable prediction of the ultimate capacity of the system, a complete design method will be possible. Specific research tasks necessary to enable this final objective to be reached are described in the following sections. Work on developemnt of these design methods is now underway and will continue during the next three years.

6.6.1 Working Stress Design Procedures

Traditional practice evaluates the allowable design load for a wood joist system on the basis of working stresses or deflection performance as established by code agencies. While ultimate strength methods are fully recognized in using materials other than wood, only working stress methods are currently accepted with the later. To enable use of currently accepted evaluation procedures for wood structures a method of design based on accepted allowable unit stresses will be developed. This research involves extension of the mathematical model for floors to enable stress and connector force evaluation. In addition, simulation studies to determine predicted stress performance of a wide range of joist systems will be conducted. Thus, development of a working stress

design procedure will provide a readily acceptable method for utilizing the research results to achieve efficient use of wood under current design and material evaluation concepts.

6.6.2 Deflection Performance Design Procedures

For a wide range of wood joist systems, the primary limitation is the deflection performance currently calculated in design by neglecting interaction of the joist and sheathing components. Thus, a rational analysis procedure, such as the verified mathematical model of such systems, can provide the necessary evaluation method to demonstrate that the actual behavior of such systems is generally much better than that currently predicted. Limited simulation studies conducted as part of the previous research have demonstrated that design methods for deflection performance may be quantified using the developed mathematical model. The research proposed herein will complete this performance based design method.

6.6.3 Ultimate Strength Design Procedures

It has long been recognized that wood joist systems are conservatively designed from the standpoint of their ultimate capacity to carry static loads. Acceptance of design procedures recognizing this fact have not been possible, since no complete mathematical model existed which properly accounted for load-sharing and structural interaction of the complex system. The proper analysis of such systems must be capable of quantifying the nonlinear behavior present at overload due to the nonlinear action of connectors between joist and sheathing and other nonlinear material and system behaviors. Methods for extending the existing mathematical model to properly account for observed systems behavior will be developed. Necessary evaluation of connector behavior at overload levels and other nonlinear material properties will be accomplished using the facilities of the Wood Science Laboratory of Colorado State University. Simulation studies using available data on ultimate strength of wood joists will be conducted to fix probabilities of expected system capacity at ultimate load. At the completion of the study, a practical design method will be developed to enable this improved approach for assessing performance of wood joist systems.

6.6.4 Closure

The completion of the proposed research will provide the sound engineering base of quantified design methods to allow code agencies and industry to accept and utilize the radically improved design concepts. Thus, this investigation has the long-range goal of better utilization of a critical natural resource and assurance to the nation's consumers of reliable, safe and economical wood joist structural systems.

7. SUMMARY AND CONCLUSIONS

The goal of this research was to develop a mathematical model to predict the behavior of wood joist structural systems. As described in detail in this report, this desired mathematical model has been developed and its verification accomplished through an extensive series of full-scale tests on T-beams and floor systems, each with widely varying properties. New test methods for evaluating material properties of connections and components were also studied as an integral part of the overall research effort. The numerous papers, theses, and dissertations developed during the course of the study are listed in Section 1.4 and several more are in progress based on the extensive research accomplished by the principal investigators and graduate research assistants. The purpose of this report is to summarize this large amount of information and to provide a single-source reference to all those interested in reviewing and utilizing the results of the research.

Implications for some of the uses of the results of the research are discussed in Chapter 6. Using the verified model as the "testing machine" through computer analysis, a myriad of problems may now be investigated. In particular, future efforts will center on the development of design procedures and the evaluation of the effects of variability on the performance of wood joist structural systems. The role of component interaction in allowing for more efficient use of materials and for improved cost-benefit relationships, along with the effects of upgrading material properties can now be studied. Quantification of these important concepts is now possible. Methods of increasing the structural interaction between components in the systems can now be evaluated.

Thus, considerable progress has been made through this research toward the goals of better utilization of a critical natural resource and, at the same time, of the development of methods of analysis which will assure reliable and economical wood joist structural systems for the nation's consumers. Continued research aimed at the practical quantification of the results of this effort will allow the realization of these goals.

The authors extend an offer of cooperation to other researchers and to government and industry organizations in striving to achieve these common goals for the nation's benefit.

REFERENCES

1. Amana, E. J. and L. G. Booth, "Theoretical and Experimental Studies on Nailed and Glued Plywood Stressed-skin Components: Part 1. Theoretical Study," Journal of the Institute of Wood Science, Vol. 4 (1), 1967.

2. Amana, E. J. and L. G. Booth, "...Part 2. Experimental Study," Journal of the Institute of Wood Science, Vol. 4(2), 1967.

3. Amana, E. J. and L. G. Booth, "Theoretical and Experimental Studies on Nailed and Glued Plywood Stressed-skin Components: Part 1. Theoretical Study," Department of Civil Engineering, Imperial College, London.

4. Amana, E. J. and L. G. Booth, "Theoretical and Experimental Studies on Nailed and Glued Plywood Stressed-skin Components: Part 2. Experimental Study," Department of Civil Engineering, Imperial College, London.

5. American Plywood Association, "Plywood Design Specification, Supplement No. 3, Design of Plywood Stressed-skin Panels," Tacoma, Washington, 1970.

6. American Plywood Association, "APA Glued Floor System," October 1971.

7. American Plywood Association, Plywood Design Specification, November 1966.

8. American Softwood Lumber, Span Tables for Joists and Rafters, National Forest Products Association, September 1970.

9. Anderson, L. O., "Construction of Nu-Frame Research House," U. S. Forest Service Research Paper FPL 88, March 1968.

10. Anderson, L. O., Wood-Frame House Construction, Agriculture Handbook No. 73, U. S. Department of Agriculture, Forest Service, July 1970.

11. Anderson, L. O., "Low-Cost Wood Homes for Rural America -- Construction Manual," Agricultural Handbook No. 364, U. S. Dept. of Agriculture, Forest Service, May 1969.

12. Angleton, H. D., J. Colville, D. Snodgrass, "The Effect of Framing and Subfloor Attachment on the Stiffness of Residential Floors," NAHB, Residential Institute Laboratory Research Report LR-4, Rockville, Maryland, 1961.

13. Atherton, G. and S. E. Corder, "Strength of Floors with Douglas Fir Utility Grade Joists," Forest Research Laboratory, Oregon State University, Corvallis, Oregon, 1965.

14. Bodig, J. and J. R. Goodman, "Prediction of Elastic Parameters for Wood," Presented at the Annual Meeting of the Forest Products Research Society, Dallas, Texas, 1972, Wood Science 5(4): 249-264, April 1973.

15. Boyd, J. D., "Minimum Strength and Stiffness Necessary for Wooden Floors in Houses," Division of Forest Products Technical Paper No. 34, Commonwealth Scientific and Industrial Research Organization, Australia, Melbourne 1964.

16. Clark, L. G., "Deflection of Laminated Beams," Transactions, ASCE, Vol. 119, 721-736, 1954.

17. Countryman, D. R., "Composite Action in Light-Frame Construction with Adhesives," Proc. of the Symposium on Research to Improve Design of Light-Frame Structures, U. S. Forest Products Laboratory, Madison, Wisconsin, Vol. 25-26, February 1970.

18. Colville, J., Angleton, D. Snodgrass, et al., "Bridging in Residential Construction," NAHB, Residential Institute Laboratory Research Report LR-6, Rockville, Maryland, 1961.

19. Dawson, P. R., "Variability Simulations of Joist Floor Systems," M.S. Thesis, Colorado State University, Fort Collins, Colorado, September, 1974.

20. DeBonis, A. L., Combined Loading Effects on Nailed Wood Joints," M.S. Thesis, Colorado State University, Fort Collins, Colorado, June 1974.

21. Drawsky, Ronald H., "Stressed Skin Panel Tests," Laboratory Report No. 82, Douglas Fir Plywood Association, April 1960.

22. Fleischer, H. O., "Wood Housing: A World-Wide Look," Forest Products Journal, Vol. 21(12): 12-13, Dec. 1971.

23. Fleischer, H. O., "The Impact of Utilization Research on the Complete Use of the Forest," Wood Science and Technology, Vol. 5(4): 247-254, 1971.

24. Forest Products Laboratory, "Simply Supported Sandwich Beam," A Nonlinear Theory, No. 2157, September 1959.

25. Galligan, W. L. and Snodgrass, "Machine Stress Rated Lumber: Challenge to Design," Forest Products Journal, Vol. 20(9): 63-69, 1970.

26. Goodman, J. R. and E. P. Popov, "Layered Beam Systems with Interlayer Slip," Journal of the Structural Division, ASCE 94 (ST11): Proc. Paper 6214, 1968.

27. Goodman, J. R., "Layered Wood Systems with Interlayer Slip," Wood Science, Vol. 1(3): 148-158, 1969.

28. Goodman, J. R., "Layered Wood Systems with Interlayer Slip," Ph.D. Dissertation, University of California, Berkeley, California, 1967.

29. Goodman, J. R. and J. Bodig, "Orthotropic Strength of Wood in Compression," Wood Science, Vol. 4(2): 83-94, October 1971.

30. Goodman, J. R. and J. Bodig, "Orthotropic Elastic Properties in Wood in Compression," Journal of the Structural Division, ASCE 96(ST11): Proc. Paper 7682, 1970.

31. Goodman, J. R., M. E. Criswell, M. D. Vanderbilt and J. Bodig, "Implications of Rational Analysis of Wood Joist Housing Floor Systems," Third International Symposium of International Association for Housing Science, May 1974, Montreal, Canada.

32. Goodman, J. R., W. M. Henghold, and H. Y. Rassam, "Design Aspects of Mechanically Connected Composite Systems," accepted for presentation and publication, ASCE Specialty Conference on Selection, Design and Fabrication of Composite Materials for Civil Engineering, Carnegie-Mellon University, Pittsburgh, Pennsylvania, November 1972.

33. Goodman, J. R., M. D. Vanderbilt, M. E. Criswell and J. Bodig, "Composite and Two-Way Action in Wood Joist Floor Systems," Wood Science, Vol. 7, No. 2, 1974, 25-33.

34. Granholm, H., "Om Sammansatta Balkar Och Pelare Med Sarskild Hansyn Till Spikade Trakonstrucktioner (On Composite Beams and Columns with Particular Regard to Nailed Timber Structures)," Transactions, Chalmers Tekniska Hogskolas Handlingar, Gottenburg, Sweden, No. 88, 1949.

35. Henghold, W. M., "Layered Beam Vibrations Including Slip," Ph.D. Dissertation, Civil Engineering Department, Colorado State University, Fort Collins, June 1972.

36. Henghold, W. M. and J. R. Goodman, "Static and Dynamic Behavior of Layered Beams Including Slip," Presented and published, Sixth St. Louis Symposium on Composite Materials in Engineering Design, May 1972.

37. Hoyle, Robert J. Jr., Design Method for Structures Bonded with Elastomeric Adhesives. Part 1, Research Division, Washington State University, February 1970.

38. Hoyle, Robert J. Jr., "Behavior of Wood I-Beams Bonded with Elastomeric Adhesive," Bulletin 328, Washington State University, 1973.

39. Hoyle, Robert J. Jr., "Deflections of Twenty Experimental Wood Beams Using Method of Kuenzi and Wilkinson, FPL-152," Wood Technology Section, College of Engineering, Washington State University, September 1971.

40. Johnson, R. J. and H. D. Angleton, "Static and Dynamic Performance of a Minimum Wood Joist Floor Construction," Proc. of the Symposium on Research to Improve Design of Light-Frame Structures, U. S. Forest Products Laboratory, Madison, Wisconsin, February 25-26, 1970.

41. Kloot, N. H., and K. B. Schuster, "Load Distribution in Wooden Floors Subjected to Concentrated Loads," Division of Forest Products Technical Paper No. 29, Commonwealth Scientific and Industrial Research Organization, Australia, Melbourne, 1963.

42. Ko, M. R., "Layered Beam Systems with Interlayer Slip," M.S. Thesis, Civil Engineering Department, Colorado State University, Fort Collins, January 1973.

43. Kuenzi, E. W., "Theoretical Design of a Nailed or Bolted Joint under Lateral Load," U. S. Forest Products Laboratory Report No. D1951, 1955.

44. Kuenzi, E. W. and Thomas Lee Wilkinson, "Composite Beams — Effect of Adhesive or Fastener Rigidity," Forest Products Laboratory, U. S. Department of Agriculture, U.S.D.A. Forest Service Research Paper FPL 152, 1971.

45. Kuo, M. L., "Verification of a Mathematical Model for Layered T-Beams," M.S. Thesis, Colorado State University, Fort Collins, Colorado, March 1974.

46. Liu, J. S., "Verification of a Mathematical Model for Wood Joist Floor Systems," Ph.D. Dissertation, Colorado State University, Fort Collins, Colorado, August 1974.

47. McLain, T. E., "Nondestructive Evaluation of Full Size Wood Composite Panels," M.S. Thesis, Colorado State University, Fort Collins. Colorado, May 1973.

48. McLain, T. E. and J. Bodig, "Determination of Elastic Parameters of Full Size Wood Composite Boards," presented at Annual Meeting of Forest Products Research Society, June 1973.

49. National Association of Home Builders, "Performance of Glued Single-layer Plywood-to-wood joist Floor Systems," NAHB Research Foundation, Inc., "Static and Dynamic Performance of a Minimum Wood Joist Floor Construction," July 1970.

50. National Bureau of Standards, U. S. Department of Commerce, "Strength of Houses, Application of Engineering Principles to Structural Design," April 1948.

51. National Forest Products Association, "The Wood-Frame House as a Structural Unit," Technical Report No. 5, July/August 1965.

52. National Forest Products Association, "National Design Specification for Stress-Grade Lumber and its Fastenings," Washington, D. C., 1973.

53. National Forest Products Association, "Wood Structural Design Data," Washington, D.C., 1970.

54. National Research Council, "National Building Code of Canada, Part 4 - Design," Ottawa, Canada, 1965.

55. Newmark, N. M., C. P. Siess, and I. M. Viest, "Tests and Analysis of Composite Beams with Incomplete Interaction," Proceedings, Society for Experimental Stress Analysis, 9(1), 1951.

56. Noren, B., "Nailed Joints - Their Strength and Rigidity under Short-Term and Long-Term Loading," Swedish Forest Products Research Laboratory Report No. 22: 1968, Stockholm, 80 p.

57. Norris, C. B., W. S. Ericksen, and W. J. Kommers, "Flexural Rigidity of a Rectangular Strip of Sandwich Construction — Comparison Between Mathematical Analysis and Results of Tests," Forest Products Laboratory Report 1505A, 1952.

58. O'Halloran, M. R., J. Bodig, and D. C. Bowen, "Nondestructive Parameters of Lodgepole Pine Dimension Lumber in Bending," Forest Products Journal, 22(2): 43-41, 1972.

59. Onysko, D. M., "Performance of Wood-Joist Floor Systems -- A Literature Review," Information Report OP-X-24, Forest Products Laboratory, Ottawa, Ontario, January 1970.

60. Patterson, D. W., "Nailed Wood Joints under Lateral Loads," M.S. Thesis, Colorado State University, 82 p., 1973.

61. Penner, B., "Experimental Behavior of Wood Flooring Systems," M.S. Thesis, Civil Engineering Department, Colorado State University, Fort Collins, January 1973.

62. Pleshkov, P. F., Teoriia Rascheta Depviannykh Sostavnnykh Sterzhnei (Theoretical Studies of Composite Wood Structure), Moscow, 192 p., 1952.

63. Polensek, Anton, George H. Atherton, Stanley E. Corder, Jack L. Jenkins, "Response of Nailed Wood-Joist Floors to Static Loads," Forest Products Journal, September 1972.

64. Polensek, Anton, "Frequency Analysis of Timber-Joist Floors," M.S. Thesis, Oregon State University, 833.18:812.71--015.5:(043)P765, June 1969.

65. Polensek, A. and G. H. Atherton, "Performance of Wood Joist Floor Systems Under Static and Dynamic Loads," Proc. of the Symposium on Research to Improve Design of Light-Frame Structures, U.S. Forest Products Laboratory, Madison, Wisconsin, Vol. 25-26, February 1970.

66. Rose, John D., "American Plywood Association Laboratory Report 118," American Plywood Association.

67. Russell, W. A., "Deflection Characteristics of Residential Wood-Joist Floor Systems," Housing Research Paper No. 30, Housing and Home Finance Agency, Washington, D.C., 1954.

68. Seiss, C. P., I. M. Viest and N. M. Newmark, "Small Scale Tests of Shear Connectors of Composite T-beams," Bulletin 396, University of Illinois Experiment Station, Vol. 49, No. 45, 1952.

69. Sliker, Alan, "Joist Deflections Simulated by a Computer Program," Forest Products Journal, Vol. 22, No. 9, 1972.

70. Sliker, Alan and Stanley Woell, "Computer Simulation of Joist Deflections in the Floor of a Factory-Manufactured House," Michigan State University Agricultural Experiment Station.

71. Talbott, John W., Low-Profile Wood Floor Systems, Washington State University Institute of Technology, Bulletin 277, December 1963.

72. Thompson, E. T., J. R. Goodman and M. D. Vanderbilt, "Finite Element Analysis of Layered Systems with Interlayer Slip," Publication Pending.

73. Tremblay, G. A., "Nonlinear Analysis of Layered T-Beams with Interlayer Slip," M.S. Thesis, Colorado State University, Fort Collins, Colorado, September, 1974.

74. U. S. Forest Products Laboratory, American Plywood Association, National Forest Products Association, Southern Forest Products Association, Western Wood Products Association, (Sponsors) Proceedings of Symposium on Research to Improve Design of Light-Frame Structures, February 1970.

75. U. S. Forest Service, "Outlook for Meeting Future Timber Demand," U. S. Department of Agriculture Report CI No. 8, 1972.

76. Vanderbilt, M. D., Matrix Structural Analysis, Quantum Publishers, Inc., New York, 1974.

77. Vanderbilt, M. D., J. R. Goodman, M. E. Criswell and J. Bodig, Service and Overload Behavior of Wood Joist Floor Systems," Presented at the ASCE Structural Engineering Meeting, San Francisco, California, April 1973. Also Journal of the Structural Division, ASCE 100(ST1): 1974.

78. Wilkinson, T. L., "Theoretical Lateral Resistance of Nailed Joist," Journal of the Structural Division, ASCE 91(ST5): 1971.

79. Wilkinson, T. L., "Analysis of Nailed Joints with Dissimilar Members," Journal of the Structural Division, ASCE 98(ST9): 1972.

APPENDIX A

RESULTS OF EXPERIMENTAL TESTS ON FLOORS

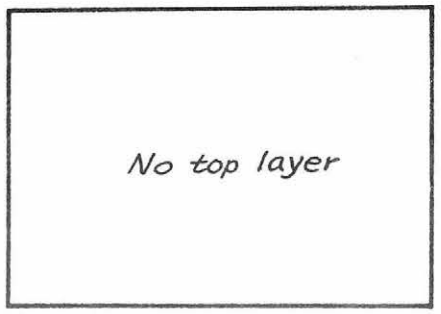

Plan of Top Sheathing Layer

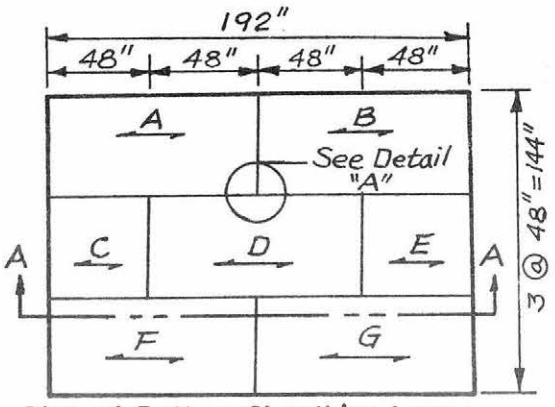

Plan of Bottom Sheathing Layer

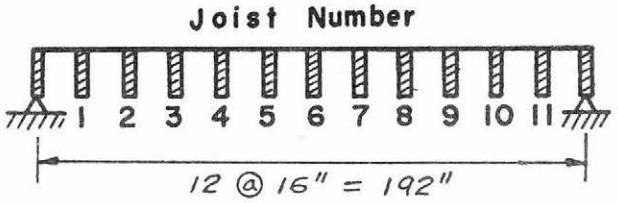

Section A-A

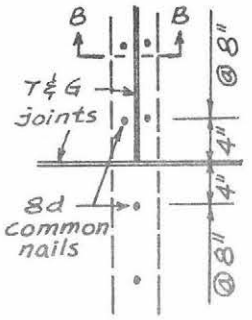

Detail "A"

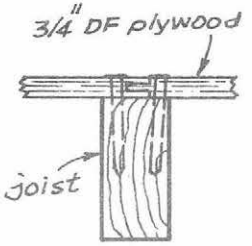

Section B-B

Material	Property	Joist Number										
		1	2	3	4	5	6	7	8	9	10	11
2×8 DF joist	Actual Size, in (width x depth)	1.49 × 7.24	1.48 × 7.14	1.47 × 7.21	1.49 × 7.22	1.48 × 7.17	1.48 × 7.20	1.44 × 7.05	1.47 × 7.24	1.46 × 7.17	1.48 × 7.21	1.51 × 7.26
	Average MOE ∥ Grain, 10^6 psi	2.41	2.56	2.42	2.54	2.46	1.70	1.38	1.76	1.63	1.85	1.87

Joist Data

Layer	Material	Thickness in.	Gap	Connector	Average MOE, 10^6 psi															
					A		B		C		D		E		F		G		H	
					∥	⊥	∥	⊥	∥	⊥	∥	⊥	∥	⊥	∥	⊥	∥	⊥	∥	⊥
Bottom	3/4 DF plywood	3/4	T&G	8d nails @ 8"	1.38	0.51	1.46	0.56	1.40	0.53	1.31	0.42	1.40	0.53	1.40	0.55	1.42	0.59	—	—
Top	—	—	—	—	—	—	—	—	—	—	—	—	—	—	—	—	—	—	—	—

Sheathing Data

Fig. A1 Layout and Data of Specimen F3-8D16-1

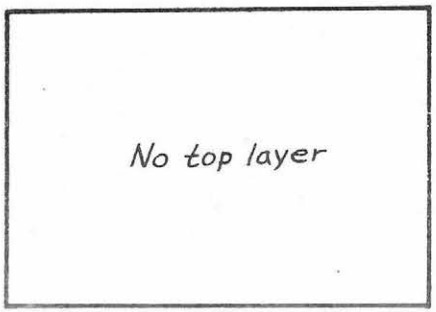

Plan of Top Sheathing Layer

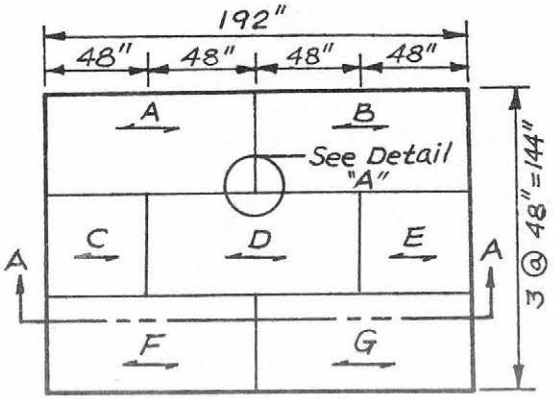

Plan of Bottom Sheathing Layer

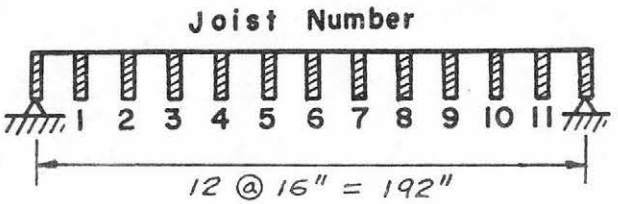

Section A-A

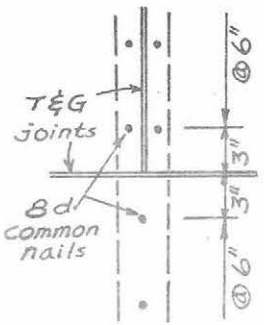

Detail "A"

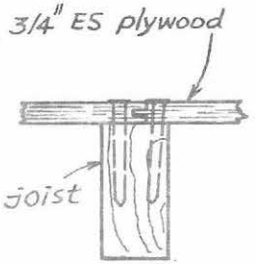

Section B-B

Material	Property	Joist Number										
		1	2	3	4	5	6	7	8	9	10	11
2×12 ES joist	Actual Size, in (width x depth)	1.52 × 11.21	1.52 × 11.20	1.52 × 11.13	1.51 × 11.51	1.50 × 11.23	1.52 × 11.14	1.50 × 11.18	1.51 × 11.20	1.50 × 11.08	1.50 × 11.27	1.53 × 11.18
	Average MOE ∥ Grain, 10^6 psi	1.31	0.92	0.87	1.35	1.28	1.39	1.15	0.97	1.09	0.98	1.06

Joist Data

Layer	Material	Thickness in.	Gap	Connector	Average MOE, 10^6 psi															
					A		B		C		D		E		F		G		H	
					∥	⊥	∥	⊥	∥	⊥	∥	⊥	∥	⊥	∥	⊥	∥	⊥	∥	⊥
Bottom	3/4 ES plywood	5/8	T&G	8d nails @ 6"	1.29	0.42	1.39	0.40	1.37	0.39	1.49	0.40	1.37	0.39	1.48	0.46	1.29	0.44	—	—
Top	—	—	—	—	—	—	—	—	—	—	—	—	—	—	—	—	—	—	—	—

Sheathing Data

Fig. A2 Layout and Data of Specimen F4-12E16-1

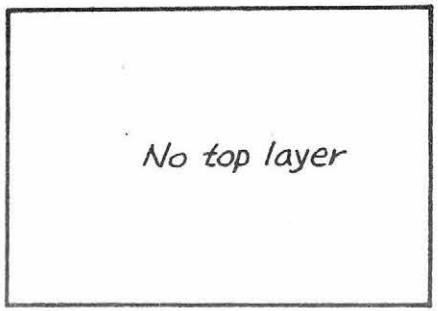

Plan of Top Sheathing Layer

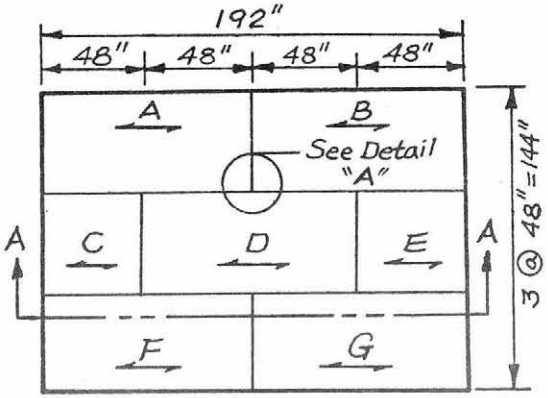

Plan of Bottom Sheathing Layer

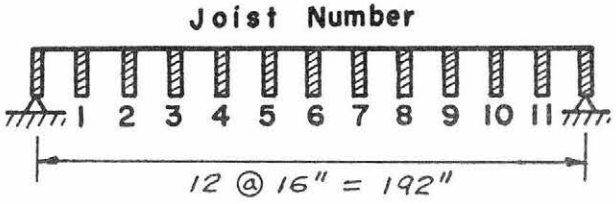

Section A-A

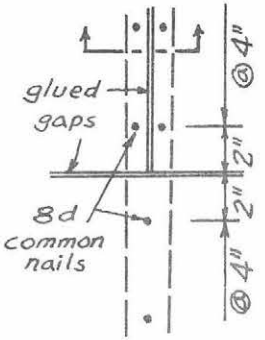

Detail "A"

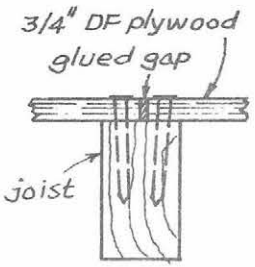

Section B-B

Material	Property	Joist Number										
		1	2	3	4	5	6	7	8	9	10	11
2×8 DF joist	Actual Size, in (width x depth)	1.47 × 7.21	1.47 × 7.21	1.50 × 7.29	1.49 × 7.22	1.45 × 7.06	1.51 × 7.29	1.49 × 7.23	1.50 × 7.27	1.51 × 7.28	1.48 × 7.04	1.48 × 7.26
	Average MOE ∥ Grain, 10^6 psi	1.29	1.24	1.22	1.45	1.56	1.21	1.44	1.08	1.53	1.42	1.01

Joist Data

Layer	Material	Thickness in.	Gap	Connector	Average MOE, 10^6 psi															
					A		B		C		D		E		F		G		H	
					∥	⊥	∥	⊥	∥	⊥	∥	⊥	∥	⊥	∥	⊥	∥	⊥	∥	⊥
Bottom	3/4 DF plywood	3/4	glued	8d nails @ 4"	1.31	0.52	1.29	0.56	1.25	0.53	1.56	0.55	1.25	0.53	1.33	0.58	1.21	0.61	—	—
Top	—	—	—	—	—	—	—	—	—	—	—	—	—	—	—	—	—	—	—	—

Sheathing Data

Fig. A3 Layout and Data of Specimen F5-8D16-1

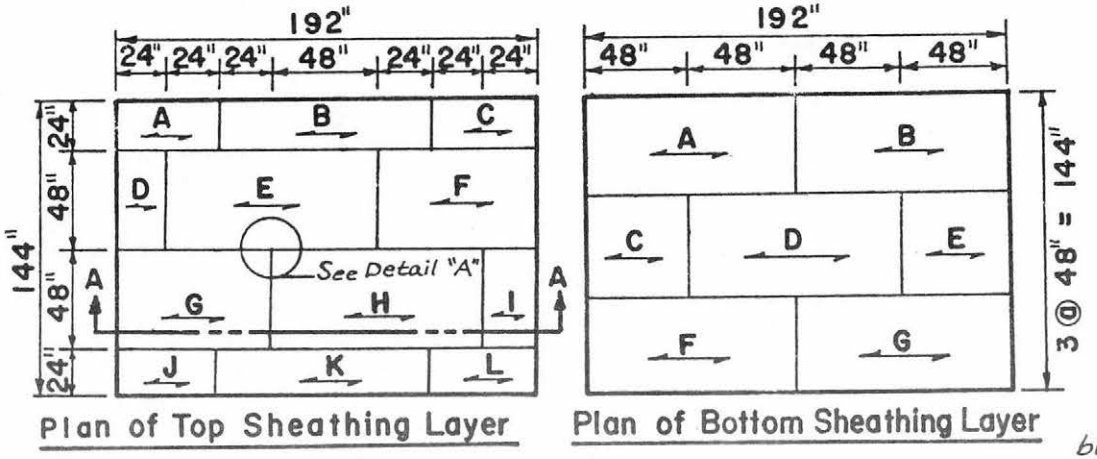

Plan of Top Sheathing Layer

Plan of Bottom Sheathing Layer

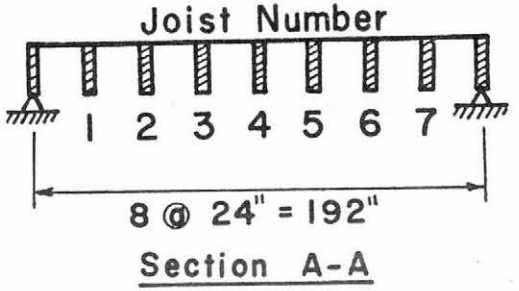

Section A-A

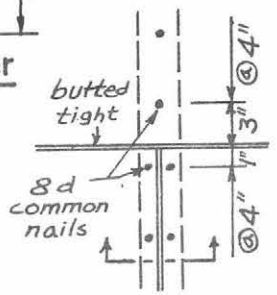

Detail "A"

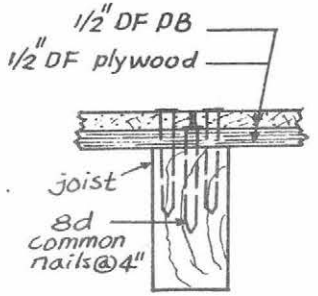

Section B-B

Material	Property	Joist Number						
		1	2	3	4	5	6	7
2×12 DF joist	Actual Size, in. (width x depth)	1.50 × 11.10	1.49 × 11.07	1.49 × 11.01	1.48 × 11.12	1.51 × 11.12	1.51 × 11.16	1.51 × 11.25
	Average MOE ‖ Grain, 10^6 psi	1.47	1.58	2.39	1.39	1.68	1.37	1.31

Joist Data

Layer	Material	Thickness in.	Gap	Connector	Average MOE, 10^6 psi																					
					A		B		C		D		E		F		G		H		I		J		K		L	
					‖	⊥	‖	⊥	‖	⊥	‖	⊥	‖	⊥	‖	⊥	‖	⊥	‖	⊥	‖	⊥	‖	⊥	‖	⊥	‖	⊥
Bottom	1/2 DF plywood	1/2	butted 1/16" gap	8d nails @ 4"	1.83	0.23	1.62	0.24	1.64	0.25	1.79	0.22	1.64	0.25	1.61	0.24	1.66	0.24	—	—	—	—	—	—	—	—	—	—
Top	1/2 DF PB	1/2	butted no gap	6d nails @ 4"	0.60	0.48	0.60	0.48	0.60	0.48	0.45	0.34	0.46	0.35	0.62	0.51	0.45	0.34	0.45	0.35	0.62	0.51	0.45	0.35	0.45	0.35	0.45	0.35

Sheathing Data

Fig. A4 Layout and Data of Specimens F7-12D24-1 and F7-12D24-2

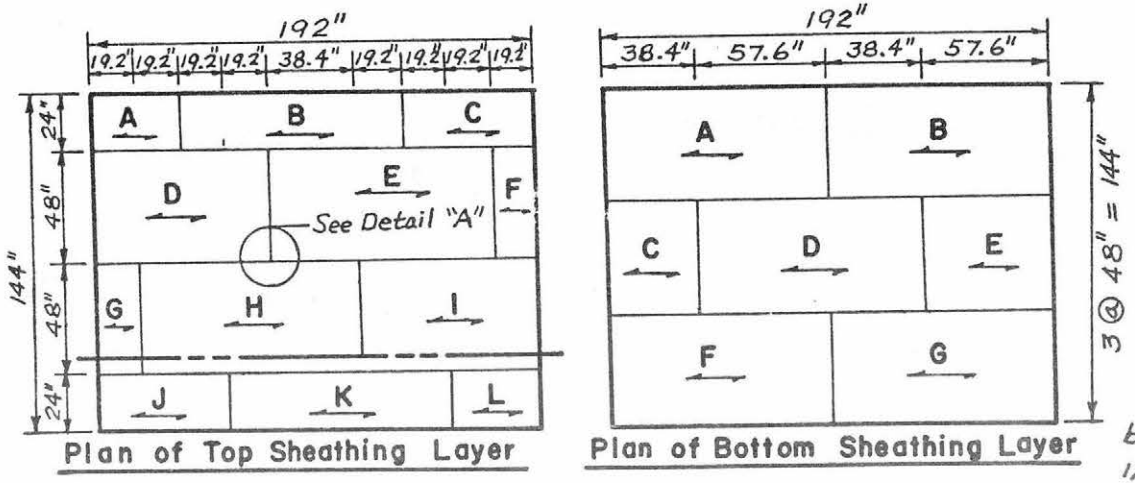

Plan of Top Sheathing Layer

Plan of Bottom Sheathing Layer

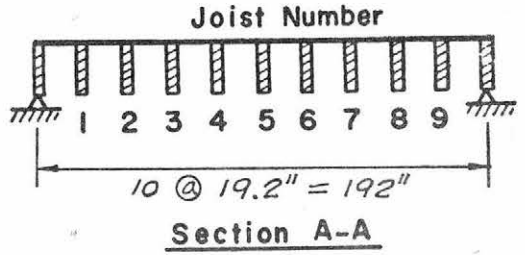

Section A-A

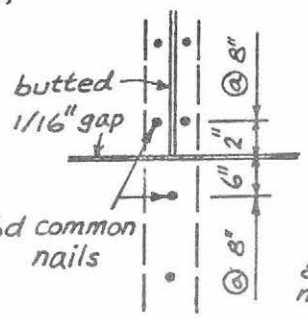

Detail "A"

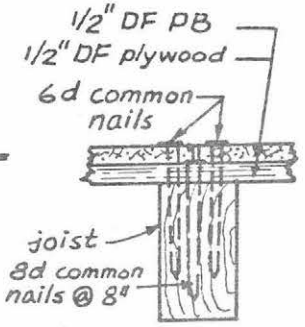

Section B-B

Material	Property	Joist Number 1	2	3	4	5	6	7	8	9
2x8 DF joist	Actual Size, in. (width x depth)	1.58 x 7.21	1.50 x 7.20	1.50 x 7.14	1.49 x 7.25	1.48 x 7.30	1.48 x 7.19	1.48 x 7.29	1.51 x 7.24	1.50 x 7.30
	Average MOE Grain, 10^6 psi	1.83	2.41	2.31	2.15	2.07	2.58	2.08	2.27	1.94

Joist Data

Layer	Material	Thickness in.	Gap	Connector	Average MOE, 10^6 psi A ∥	A ⊥	B ∥	B ⊥	C ∥	C ⊥	D ∥	D ⊥	E ∥	E ⊥	F ∥	F ⊥	G ∥	G ⊥	H ∥	H ⊥	I ∥	I ⊥	J ∥	J ⊥	K ∥	K ⊥	L ∥	L ⊥
Bottom	1/2 DF plywood	1/2	butted 1/16" gap	8d nails @ 8"	1.58	0.25	1.47	0.26	1.25	0.27	1.90	0.24	1.25	0.27	1.66	0.24	1.50	0.21	—	—	—	—	—	—	—	—	—	—
Top	1/2 DF PB	1/2	butted tight	6d nails @ 8"	0.62	0.50	0.62	0.50	0.62	0.50	0.65	0.51	0.58	0.47	0.65	0.51	0.62	0.51	0.47	0.35	0.62	0.51	0.62	0.50	0.62	0.50	0.62	0.50

Sheathing Data

Fig. A5 Layout and Data of Specimens F8-8D19.2-1 and F8-8D19.2-2

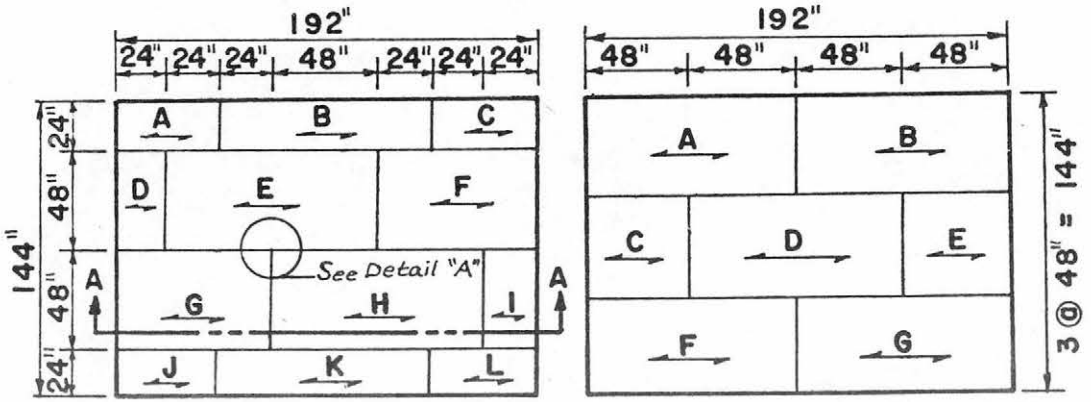

Plan of Top Sheathing Layer

Plan of Bottom Sheathing Layer

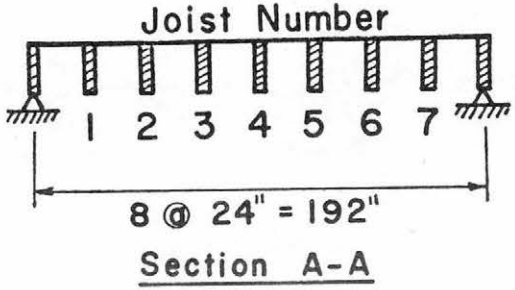

Section A-A

Material	Property	Joist Number						
		1	2	3	4	5	6	7
2×8 ES joist	Actual Size, in. (width x depth)	1.48 × 7.13	1.51 × 7.16	1.51 × 7.19	1.48 × 7.17	1.51 × 7.21	1.50 × 7.24	1.50 × 7.18
	Average MOE ∥ Grain, 10^6 psi	1.16	1.48	1.41	1.25	1.69	1.44	1.64

Joist Data

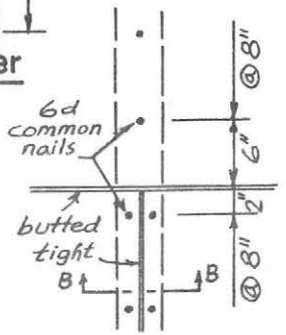

Detail "A"

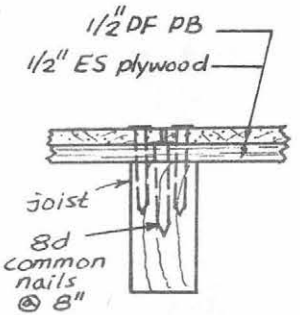

Section B-B

Layer	Material	Thickness in.	Gap	Connector	Average MOE, 10^6 psi																					
					A		B		C		D		E		F		G		H		I		J		K		L	
					∥	⊥	∥	⊥	∥	⊥	∥	⊥	∥	⊥	∥	⊥	∥	⊥	∥	⊥	∥	⊥	∥	⊥	∥	⊥	∥	⊥
Bottom	1/2 ES plywood	3/8	butted 1/16" gap	8d nails @ 8"	1.45	0.21	1.56	0.23	1.47	0.21	1.53	0.23	1.47	0.21	1.42	0.22	1.59	0.22	—	—	—	—	—	—	—	—	—	—
Top	1/2 DF PB	1/2	butted tight	6-d nails @ 8"	0.42	0.32	0.57	0.47	0.42	0.32	0.44	0.34	0.58	0.47	0.44	0.32	0.44	0.34	0.45	0.34	0.44	0.32	0.42	0.32	0.57	0.47	0.42	0.32

Sheathing Data

Fig. A6 Layout and Data of Specimens F9-8E24-1 and F9-8E24-2

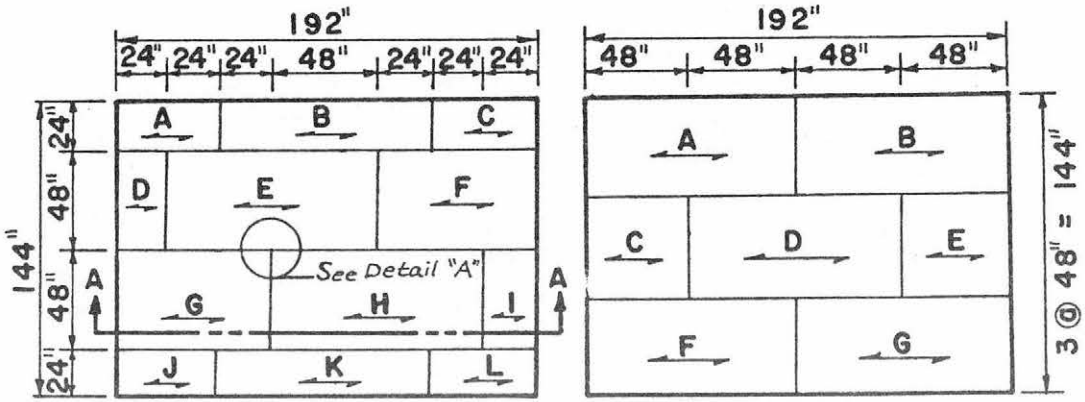

Plan of Top Sheathing Layer

Plan of Bottom Sheathing Layer

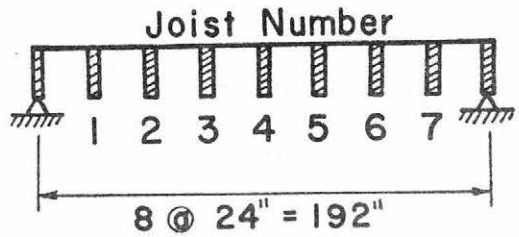

Section A-A

Material	Property	Joist Number						
		1	2	3	4	5	6	7
2×8 ES joist	Actual Size, in. (width x depth)	1.50 × 7.15	1.51 × 7.24	1.52 × 7.22	1.52 × 7.22	1.52 × 7.25	1.52 × 7.24	1.50 × 7.20
	Average MOE ∥ Grain, 10^6 psi	1.66	1.62	1.20	1.49	1.39	1.25	1.49

Joist Data

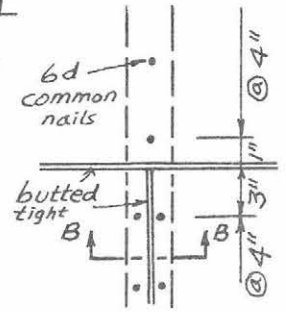

Detail "A"

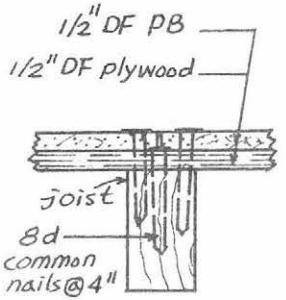

Section B-B

Layer	Material	Thickness in.	Gap	Connector	Average MOE, 10^6 psi																							
					A		B		C		D		E		F		G		H		I		J		K		L	
					∥	⊥	∥	⊥	∥	⊥	∥	⊥	∥	⊥	∥	⊥	∥	⊥	∥	⊥	∥	⊥	∥	⊥	∥	⊥	∥	⊥
Bottom	1/2 DF plywood	1/2	butted 1/16" gap	8d nails @ 4"	1.54	0.26	1.39	0.26	1.83	0.23	1.61	0.23	1.83	0.23	1.76	0.25	1.50	0.25	—	—	—	—	—	—	—	—	—	—
Top	1/2 DF PB	1/2	butted tight	6d nails @ 4"	0.42	0.32	0.57	0.47	0.58	0.47	0.58	0.47	0.61	0.51	0.44	0.32	0.44	0.34	0.63	0.51	0.44	0.34	0.42	0.32	0.57	0.47	0.42	0.32

Sheathing Data

Fig. A7 Layout and Data of Specimens F10-8E24-1 and F10-8E24-2

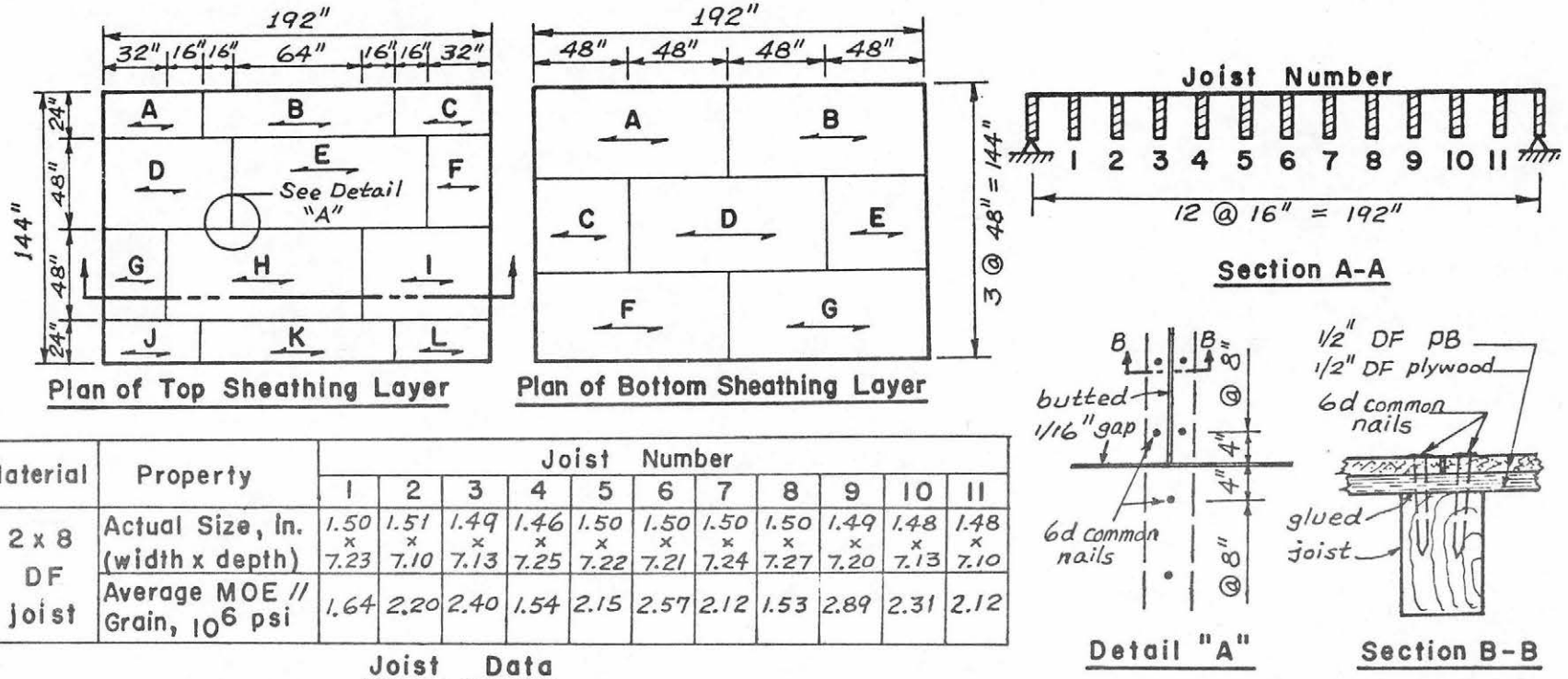

Material	Property	Joist Number 1	2	3	4	5	6	7	8	9	10	11
2 x 8 DF joist	Actual Size, in. (width x depth)	1.50 x 7.23	1.51 x 7.10	1.49 x 7.13	1.46 x 7.25	1.50 x 7.22	1.50 x 7.21	1.50 x 7.24	1.50 x 7.27	1.49 x 7.20	1.48 x 7.13	1.48 x 7.10
	Average MOE // Grain, 10^6 psi	1.64	2.20	2.40	1.54	2.15	2.57	2.12	1.53	2.89	2.31	2.12

Joist Data

Layer	Material	Thickness in.	Gap	Connector	Average MOE, 10^6 psi A		B		C		D		E		F		G		H		I		J		K		L	
					//	⊥	//	⊥	//	⊥	//	⊥	//	⊥	//	⊥	//	⊥	//	⊥	//	⊥	//	⊥	//	⊥	//	⊥	//	⊥
Bottom	1/2 DF plywood	1/2	glued	glue	1.26	0.22	1.63	0.26	1.48	0.26	1.67	0.24	1.48	0.26	1.49	0.24	1.50	0.26	—	—	—	—	—	—	—	—	—	—
Top	1/2 DF PB	1/2	butted 1/16 gap	6d nails @ 8"	0.58	0.47	0.62	0.50	0.44	0.34	0.47	0.35	0.46	0.34	0.58	0.47	0.58	0.47	0.42	0.35	0.45	0.34	0.62	0.50	0.62	0.50	0.62	0.50

Sheathing Data

Fig. A8 Layout and Data of Specimens F11-8D16-1 and F11-8D16-2

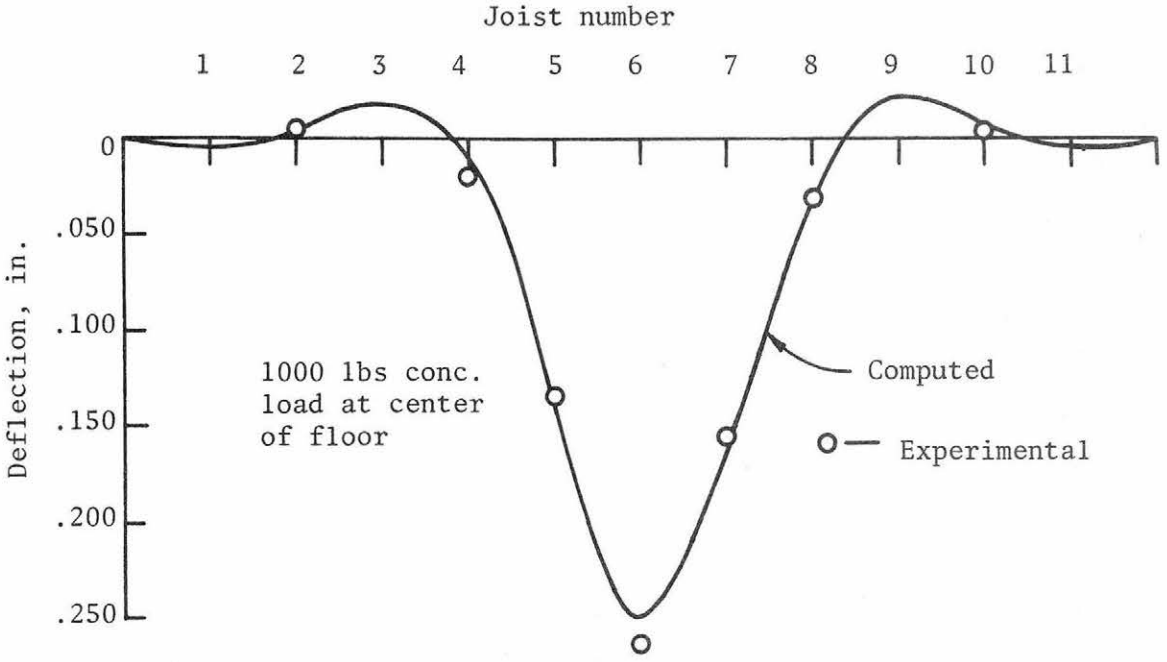

(a) Deflection profile at centerline of joists

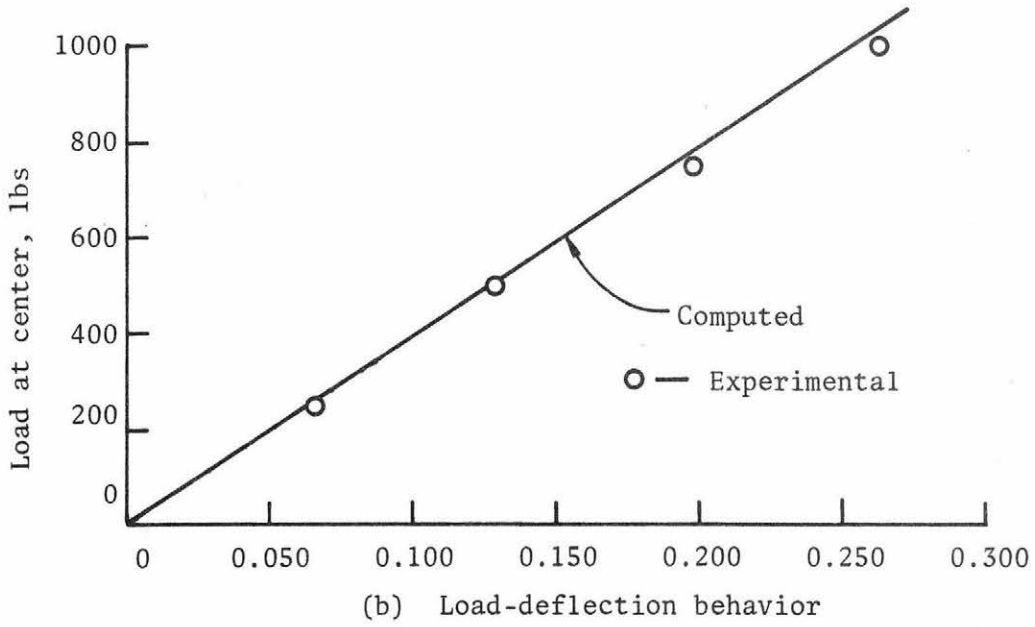

(b) Load-deflection behavior

Fig. A9 Computed vs Measured Results of Floor Specimen F3-8D16-1

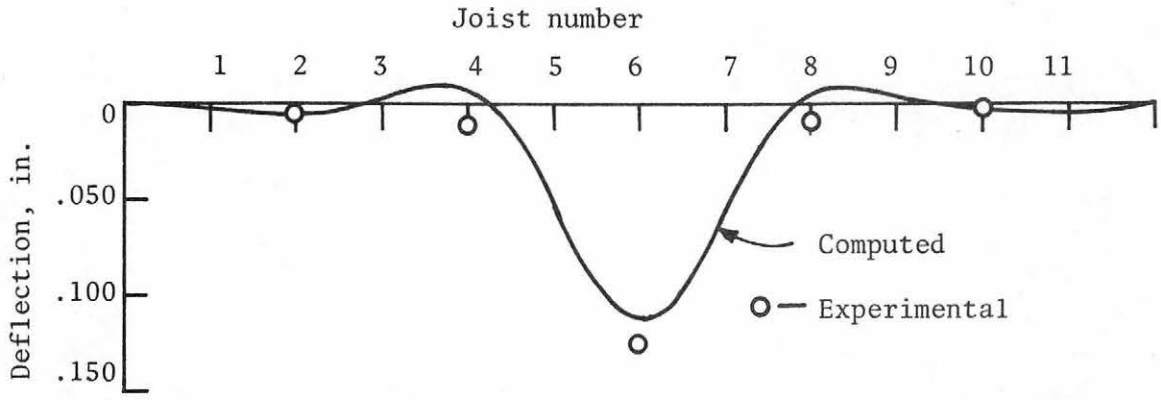

(a) Deflection profile at centerline of joists

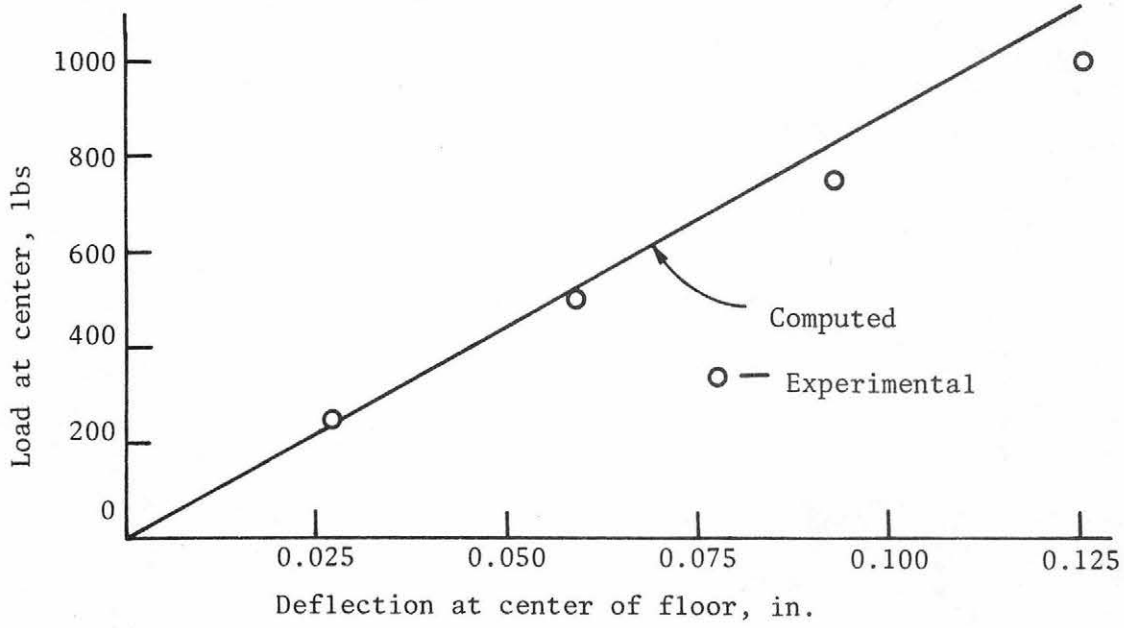

(b) Load-deflection behavior

Fig. A10 Computed vs Measured Results of Floor Specimen F4-8E16-1

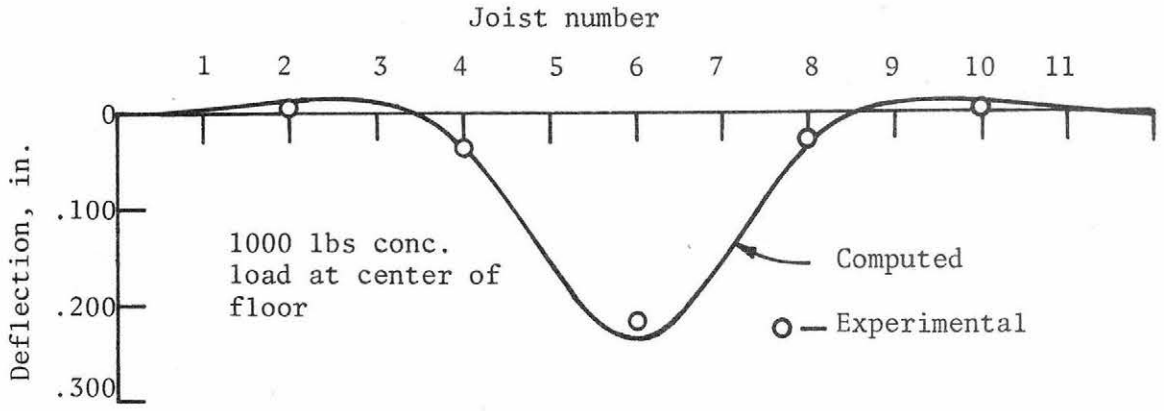

(a) Deflection profile at centerline of joists

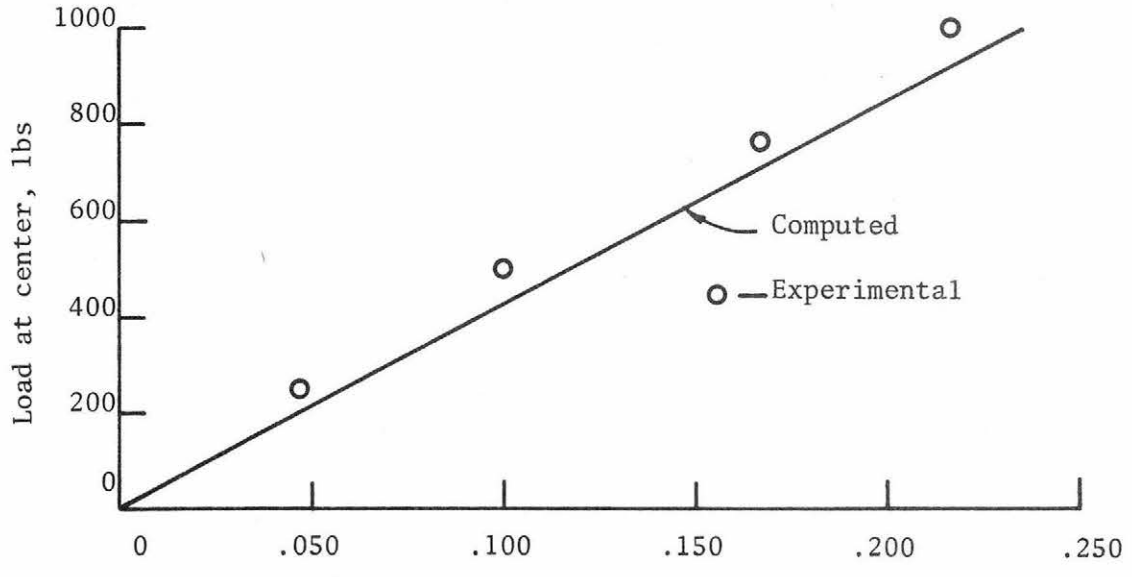

(b) Load-deflection behavior

Fig. A11 Computed and Measured Results of Floor Specimen F5-8D16-1

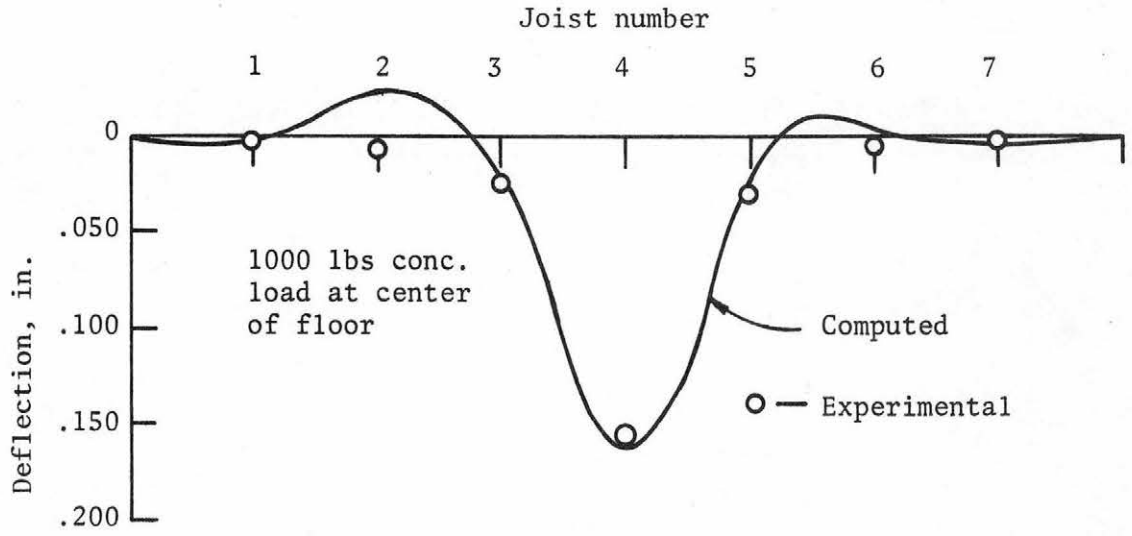

(a) Deflection profile at centerline of joists

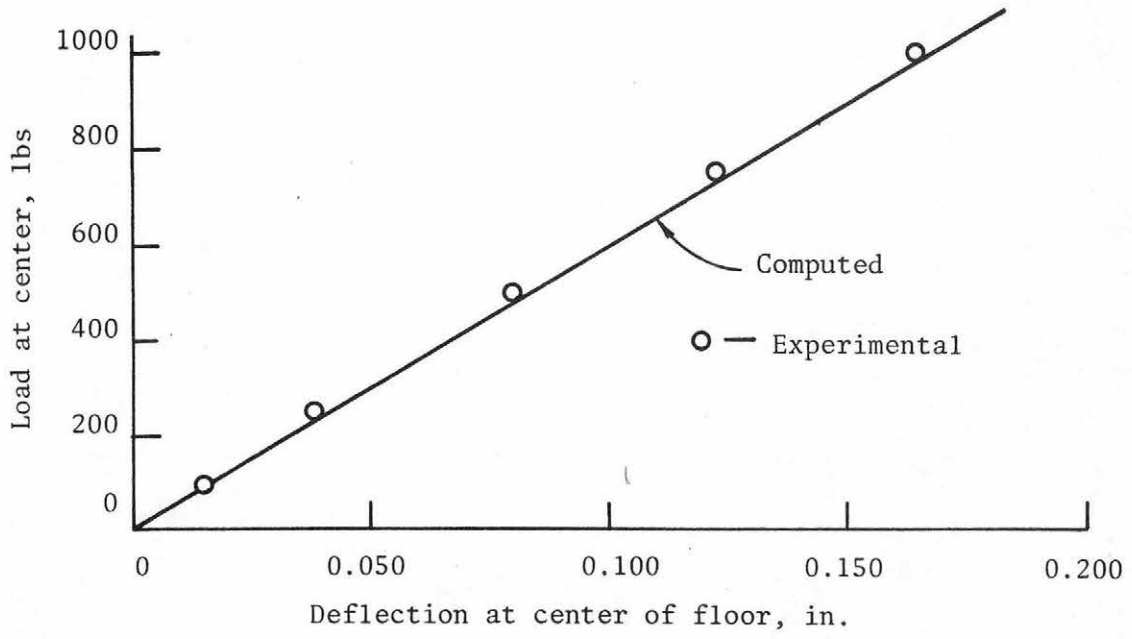

(b) Load-deflection behavior

Fig. A12 Computed vs Measured Results of Floor Specimen F7-12D24-1

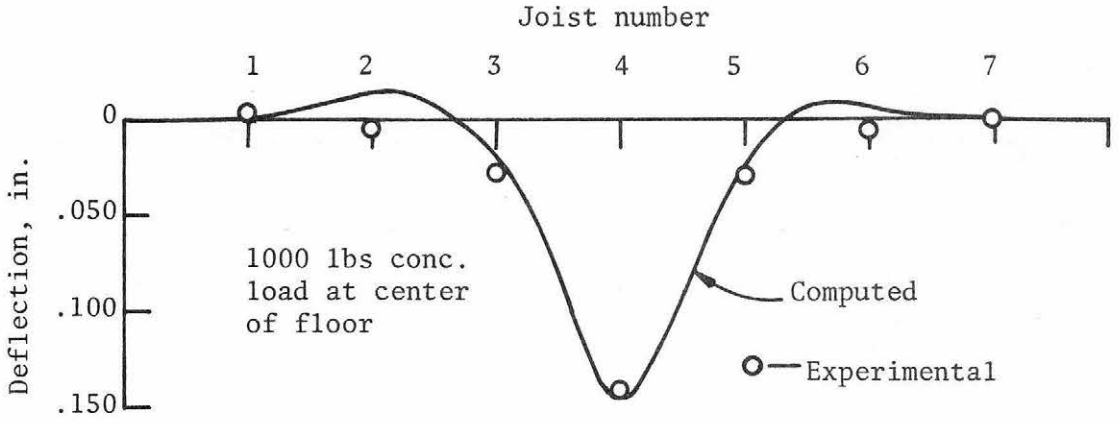

(a) Deflection profile at centerline of joists

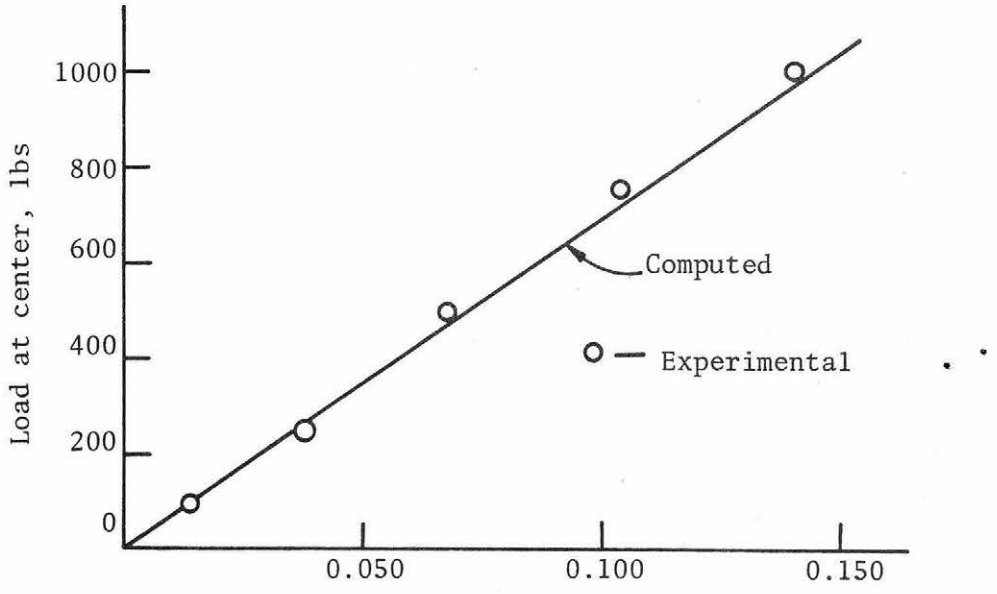

(b) Load-deflection behavior

Fig. A13 Computed vs Measured Results of Floor Specimen F7-12D24-2 (Nails of Top Layer Not Driven into Joists)

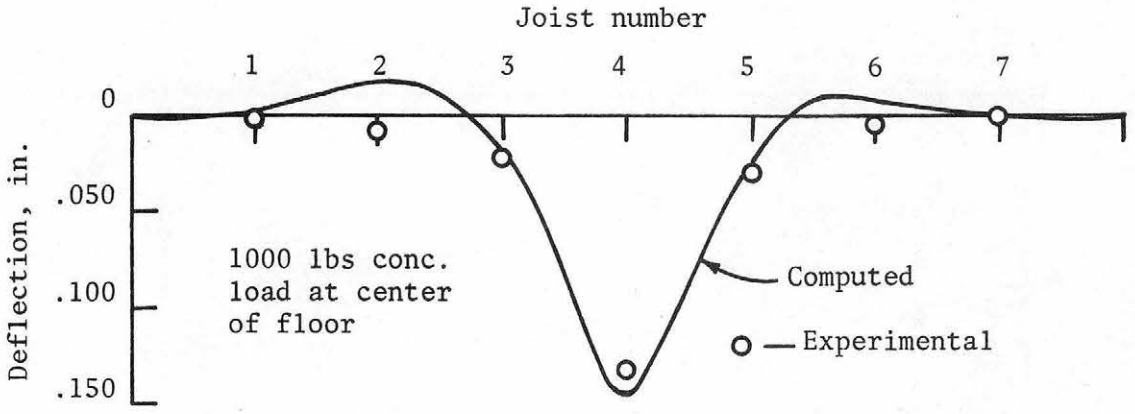

(a) Deflection profile at centerline of joists

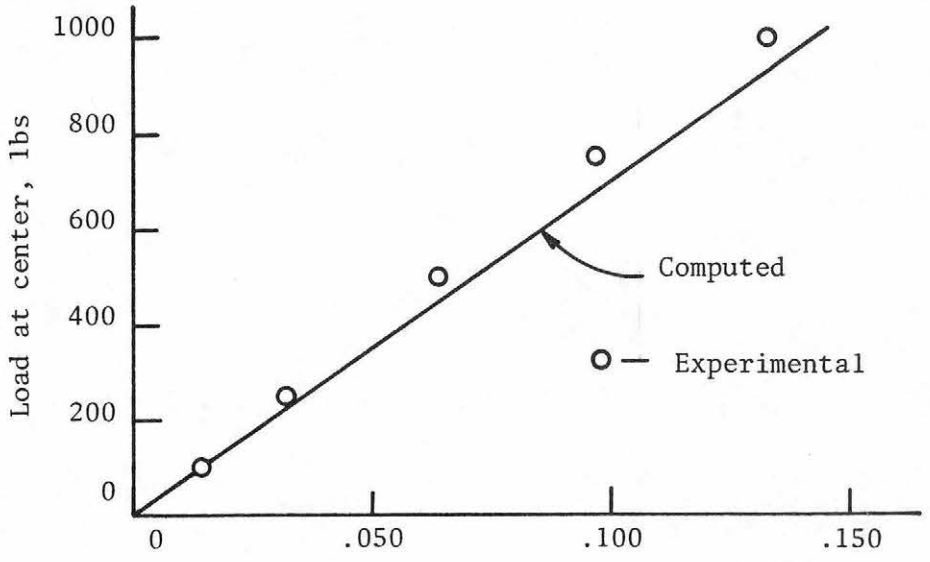

(b) Load-deflection behavior

Fig. A14 Computed vs Measured Results of Floor Specimen F7-12D24-2 (Nails of Top Layer Driven into Joists)

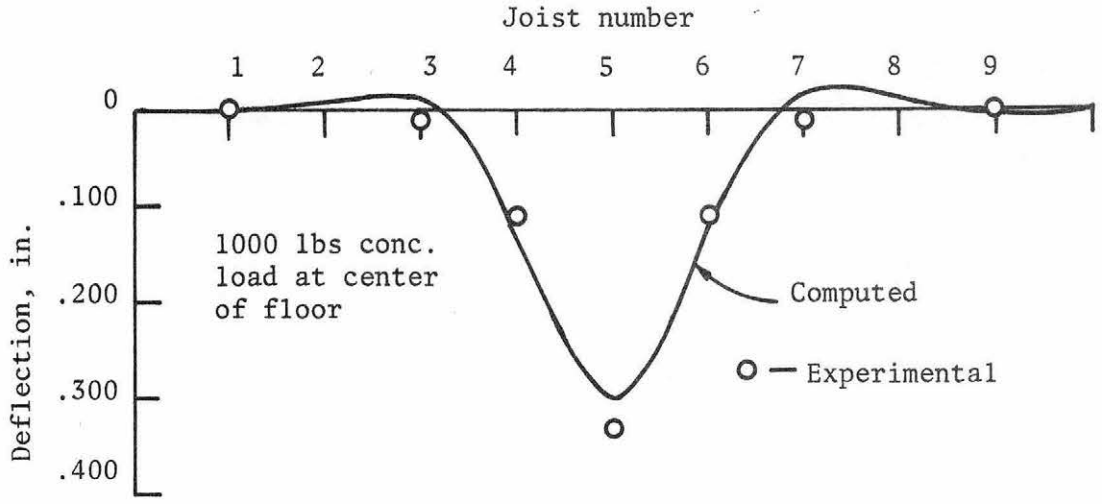

(a) Deflection profile at centerline of joists

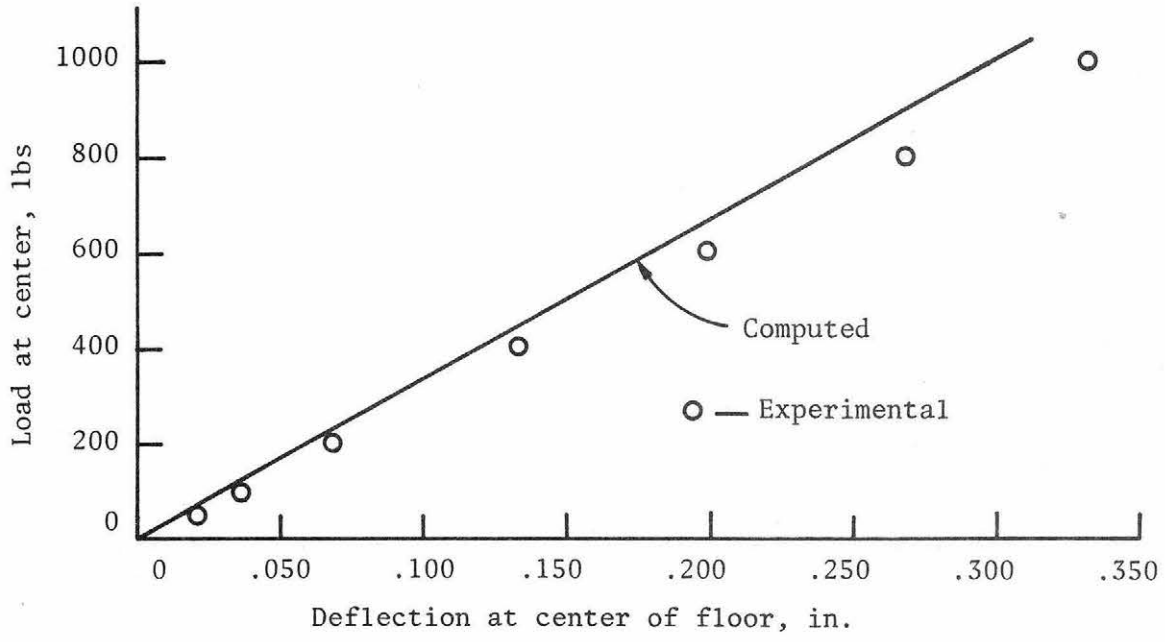

(b) Load-deflection behavior

Fig. A15 Computed vs Measured Results of Floor Specimen F8-8D19.2-1

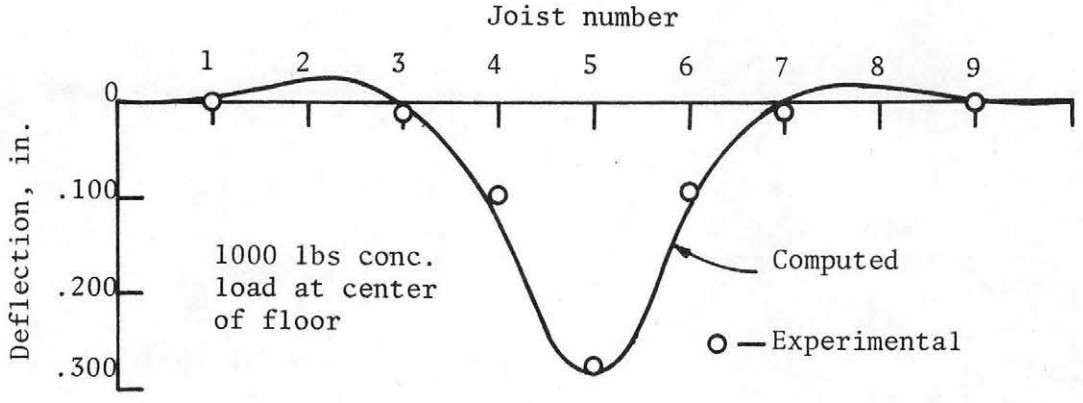

(a) Deflection profile at centerline of joists

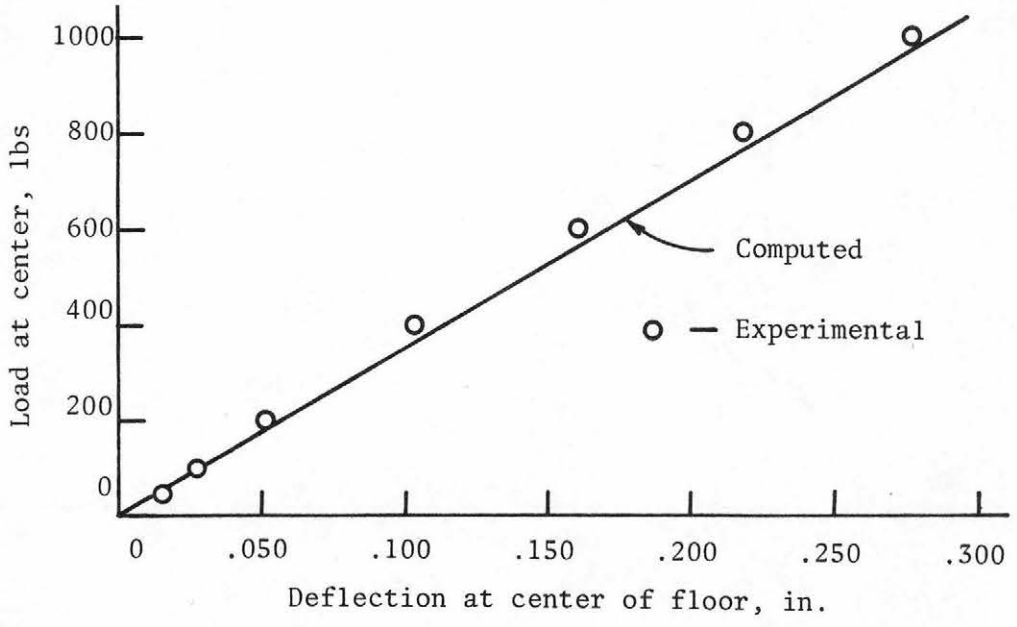

(b) Load-deflection behavior

Fig. A16 Computed vs Measured Results of Floor Specimen F8-8D19.2-2 (Nails of Top Layer Not Driven into Joists)

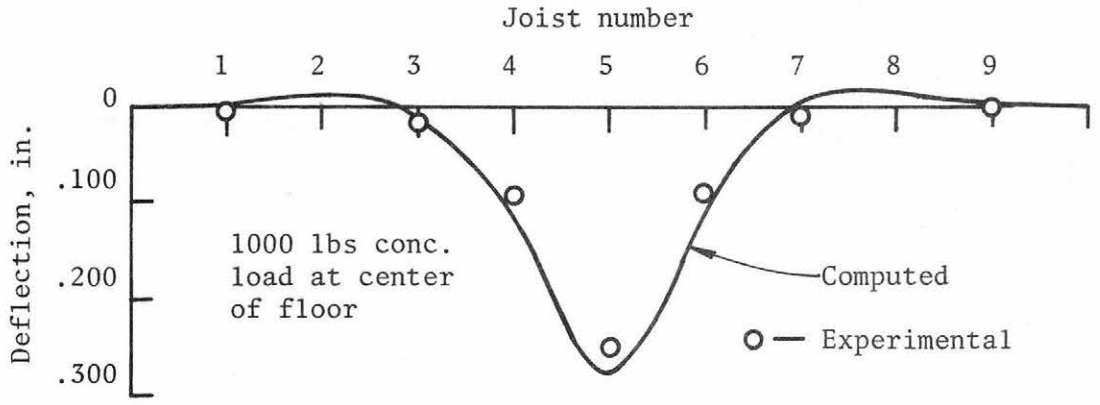

(a) Deflection profile at centerline of joists

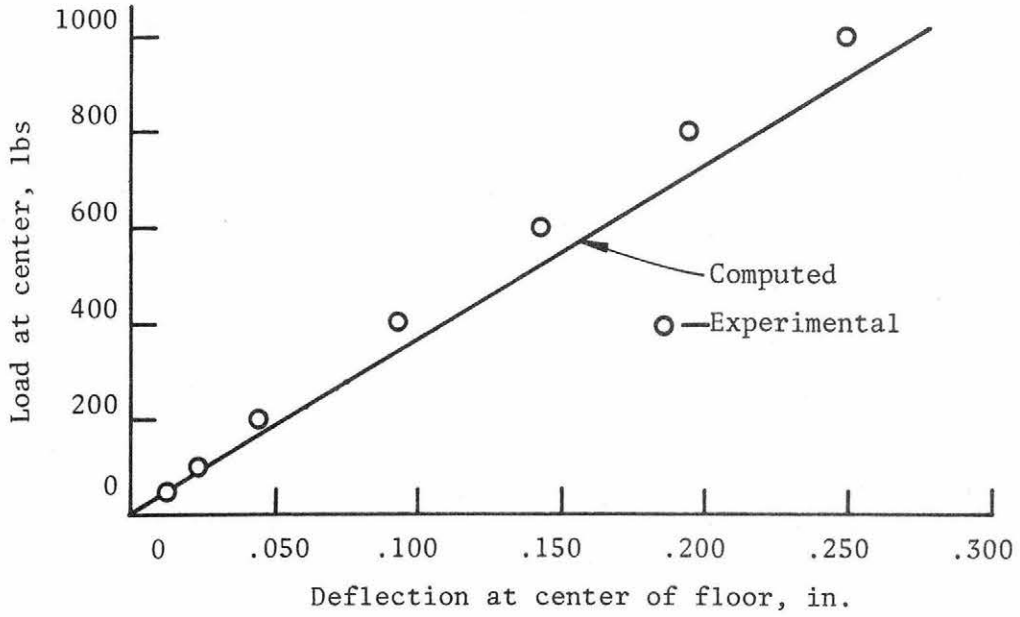

(b) Load-deflection behavior

Fig. A17 Computed vs Measured Results of Floor Specimen F8-8D19.2-2 (Nails of Top Layer Driven into Joists)

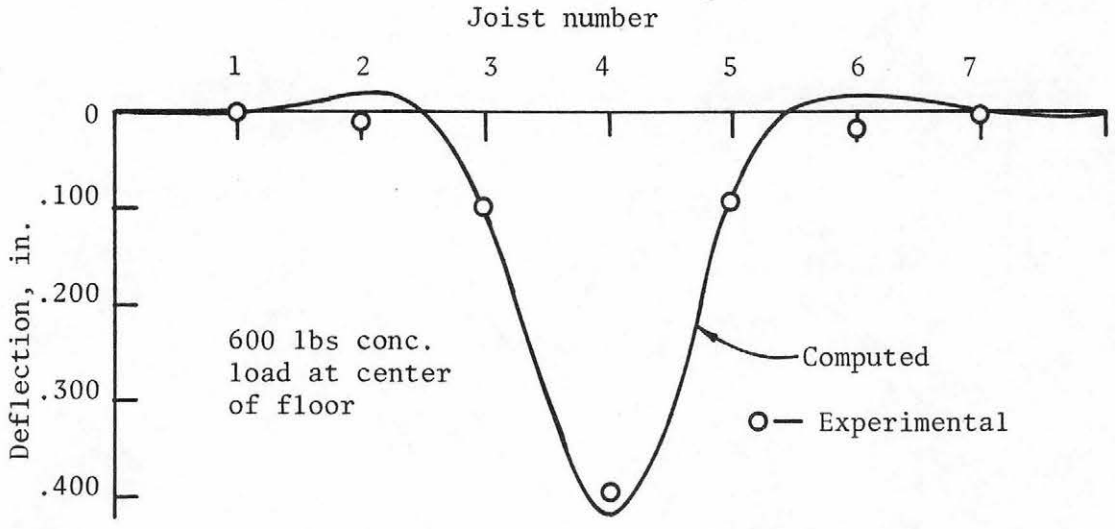

(a) Deflection profile at centerline of joists

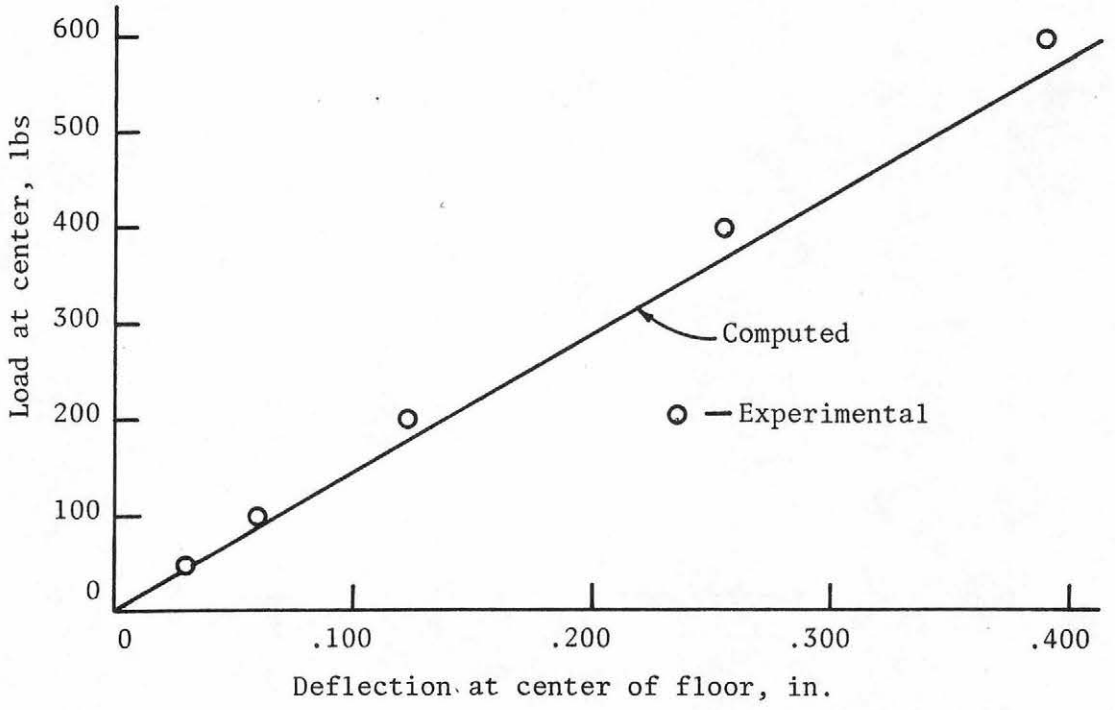

(b) Load-deflection behavior

Fig. A18 Computed vs Measured Results of Floor Specimen F9-8E24-1

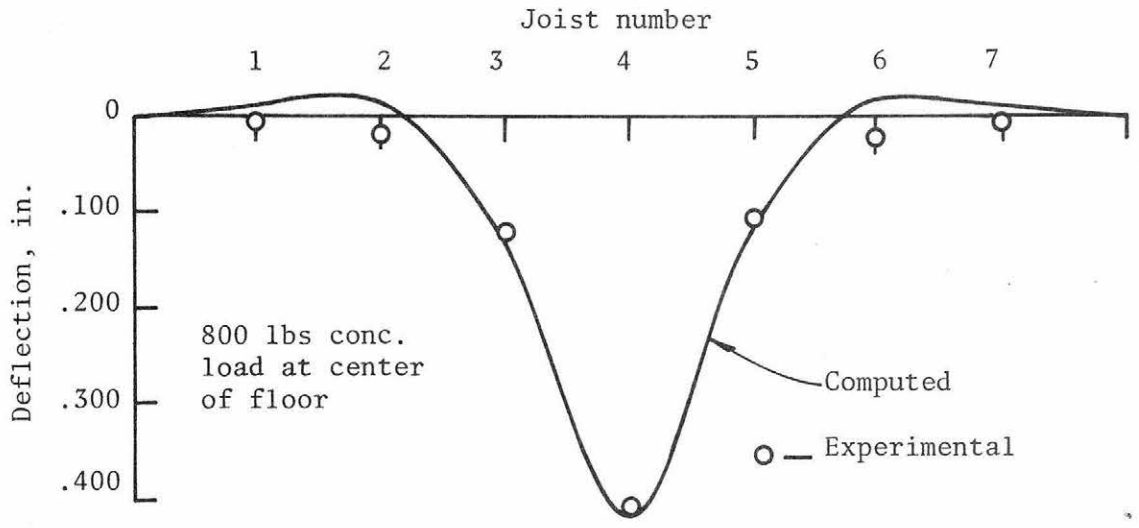

(a) Deflection profile of centerline of joists

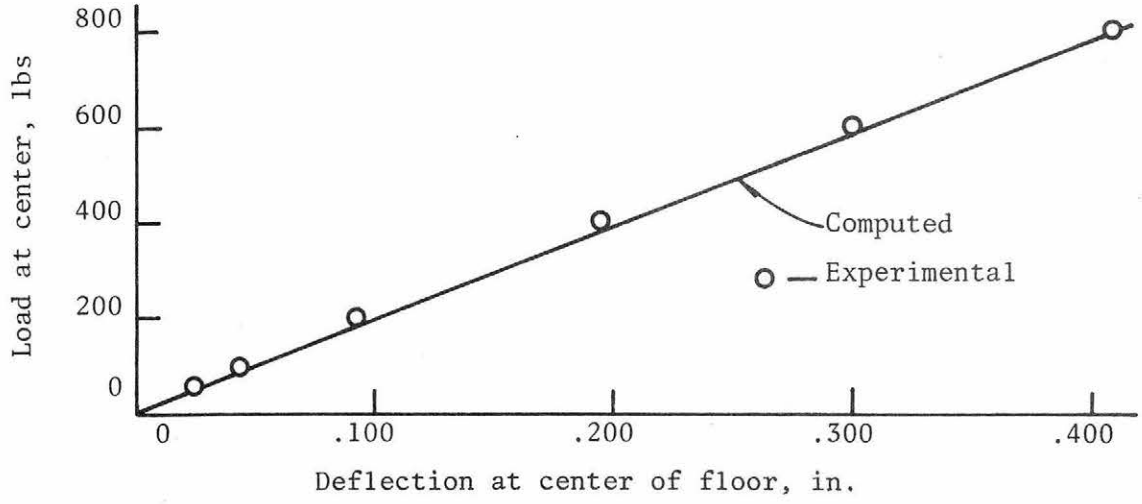

(b) Load-deflection behavior

Fig. A19 Computed vs Measured Results of Floor Specimen F9-8E24-2 (Nails of Top Layer Not Driven into Joists)

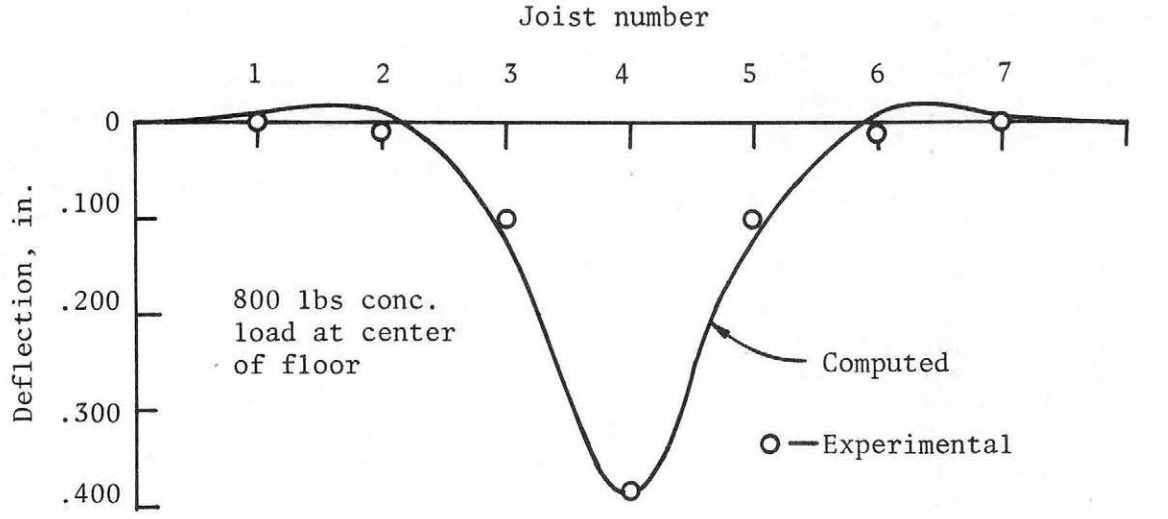

(a) Deflection profile at centerline of joists

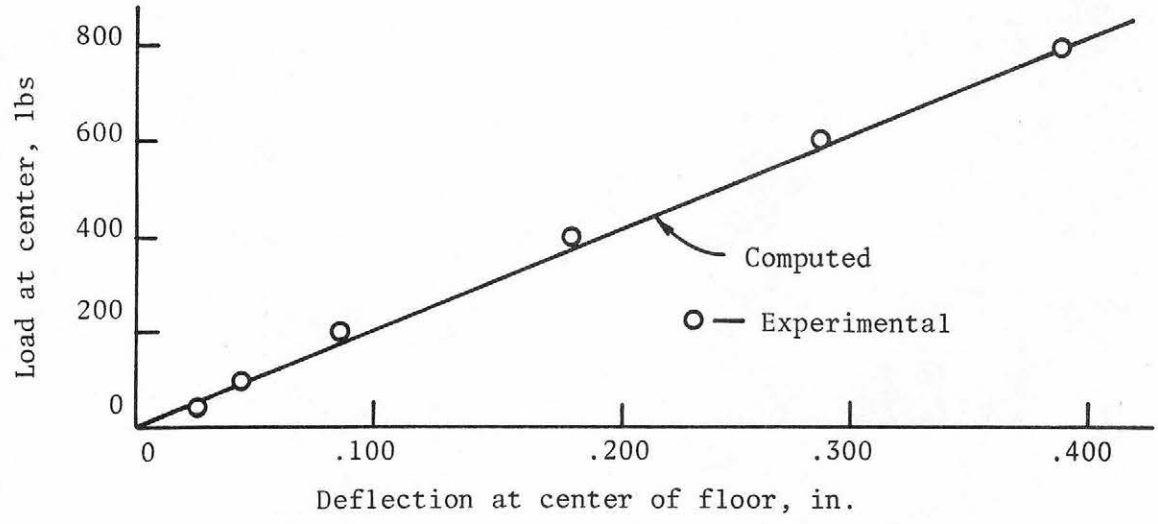

(b) Load-deflection behavior

Fig. A20 Computed vs Measured Results of Floor Specimen F9-8E24-2 (Nails of Top Layer Driven into Joists)

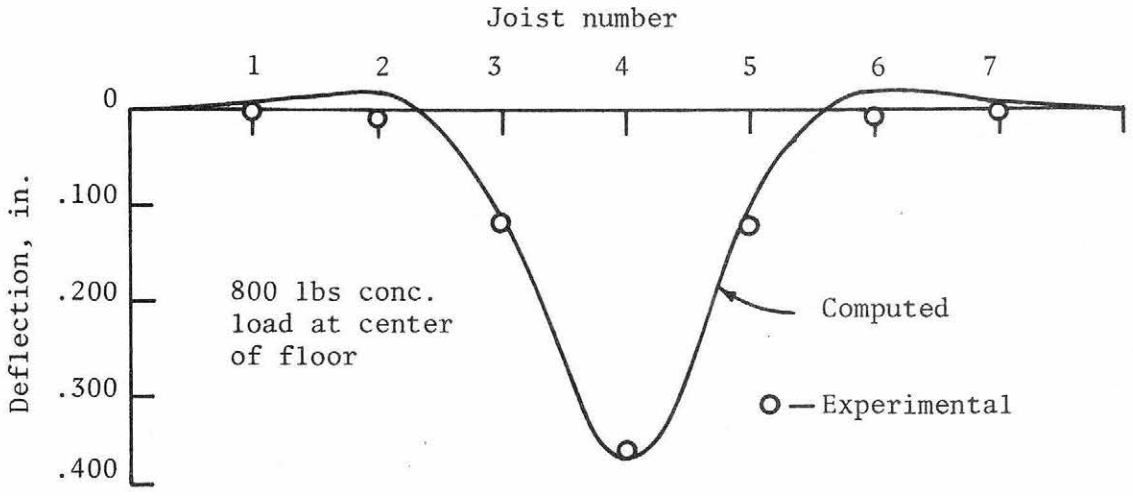

(a) Deflection profile at centerline of joists

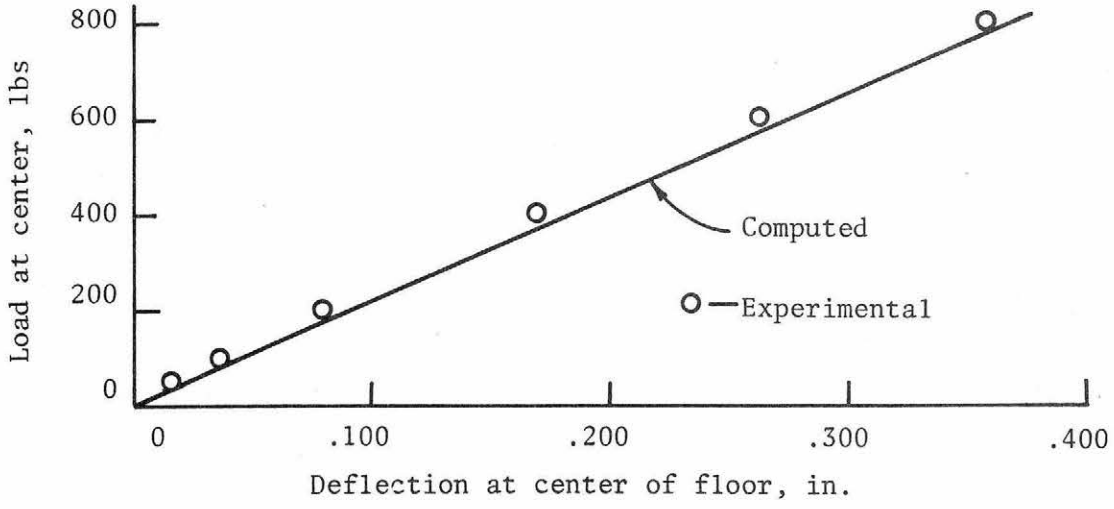

(b) Load-deflection behavior

Fig. A21 Computed vs Measured Results of Floor Specimen F10-8E24-1

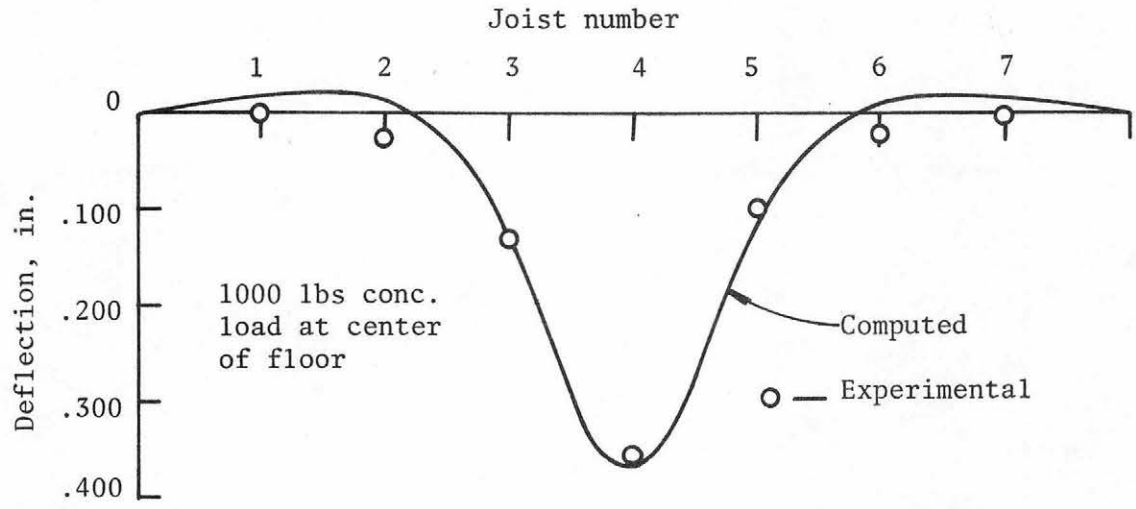

(a) Deflection profile at centerline of joists

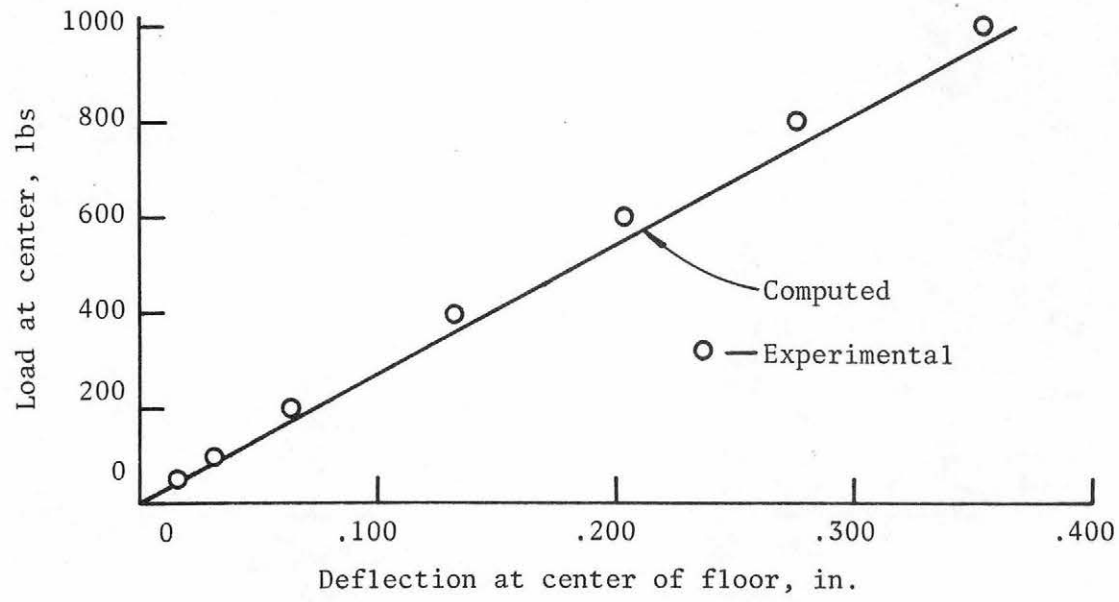

(b) Load-deflection behavior

Fig. A22 Computed vs Measured Results of Floor Specimen F10-8E24-2 (Nails of Top Layer Not Driven into Joists)

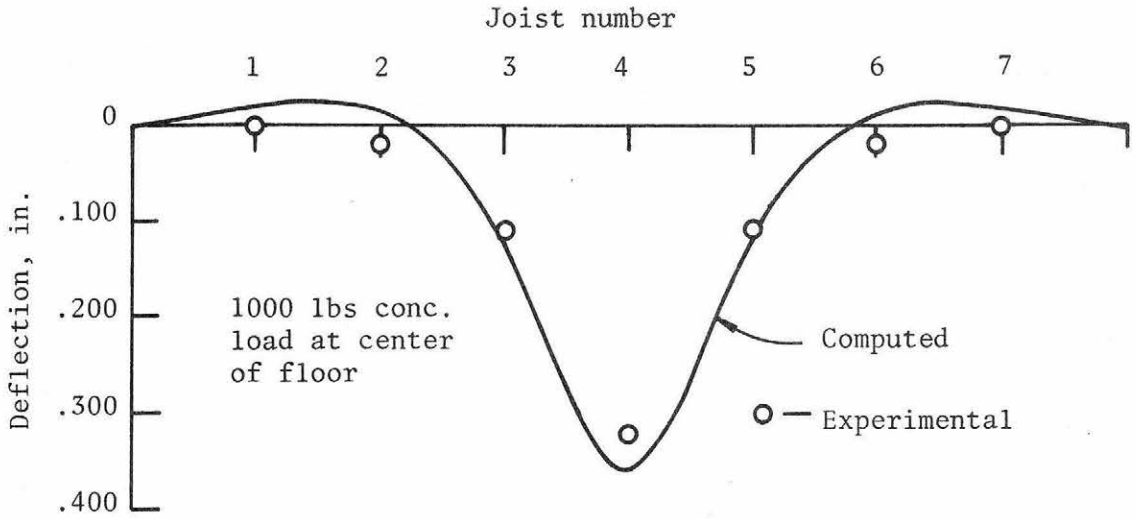

(a) Deflection profile at centerline of joists

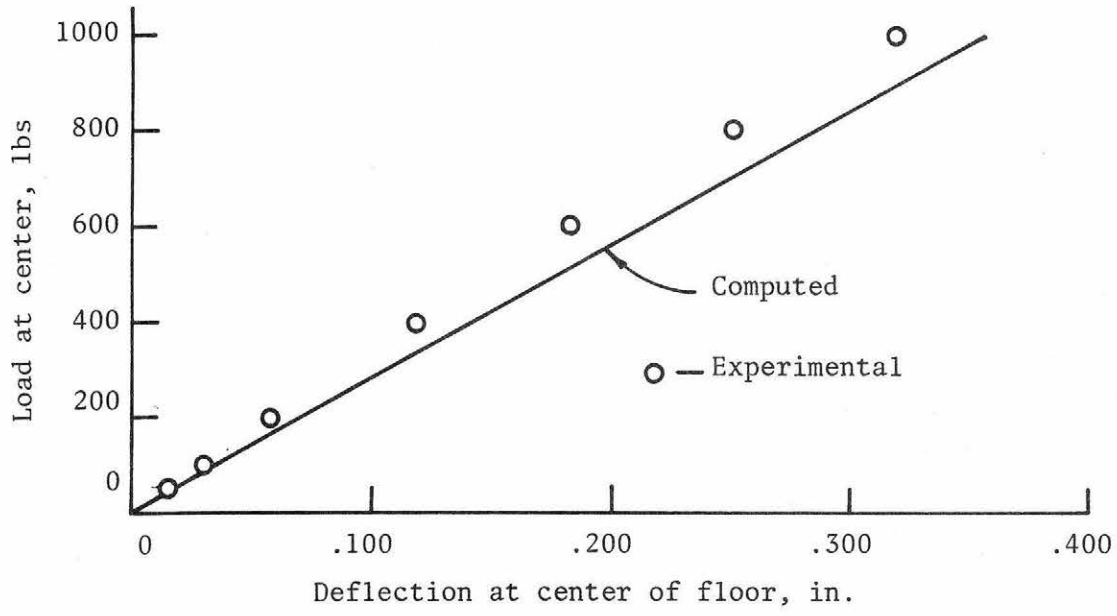

(b) Load-deflection behavior

Fig. A23 Computed vs Measured Results of Floor Specimen F10-8E24-2 (Nails of Top Layer Driven into Joists)

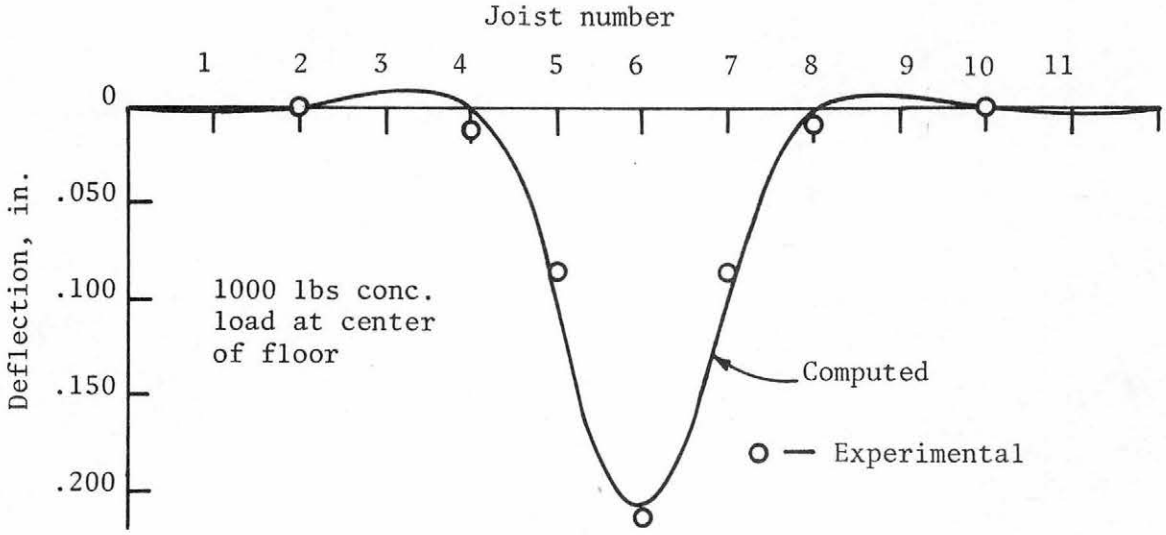

(a) Deflection profile at centerline of joists

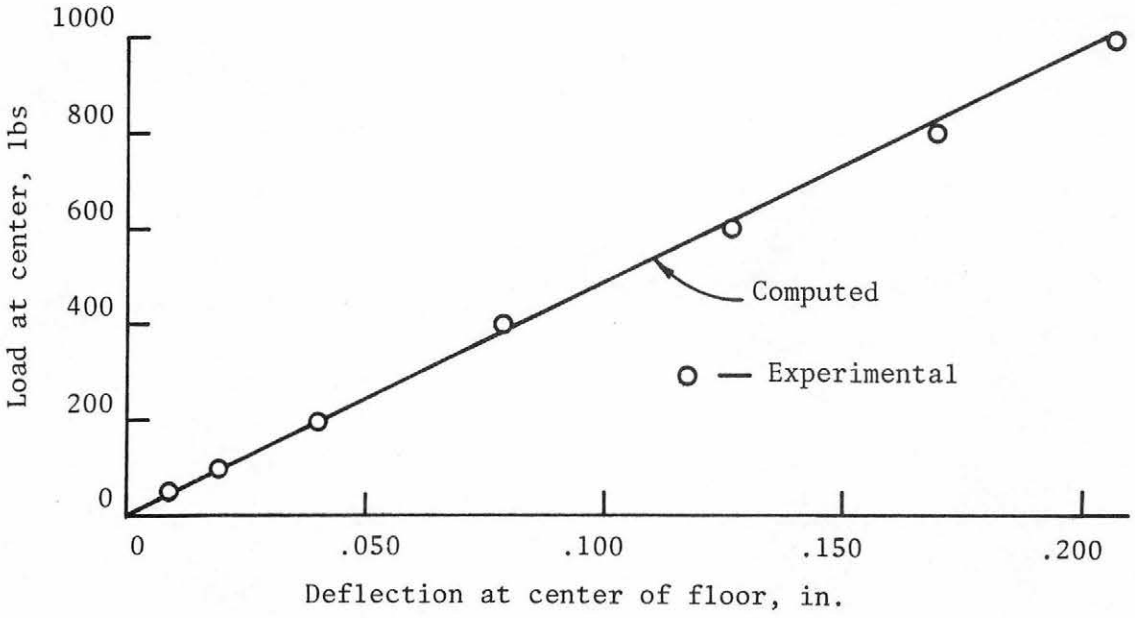

(b) Load-deflection behavior

Fig. A24 Computed vs Measured Results of Floor Specimen F11-8D16-1

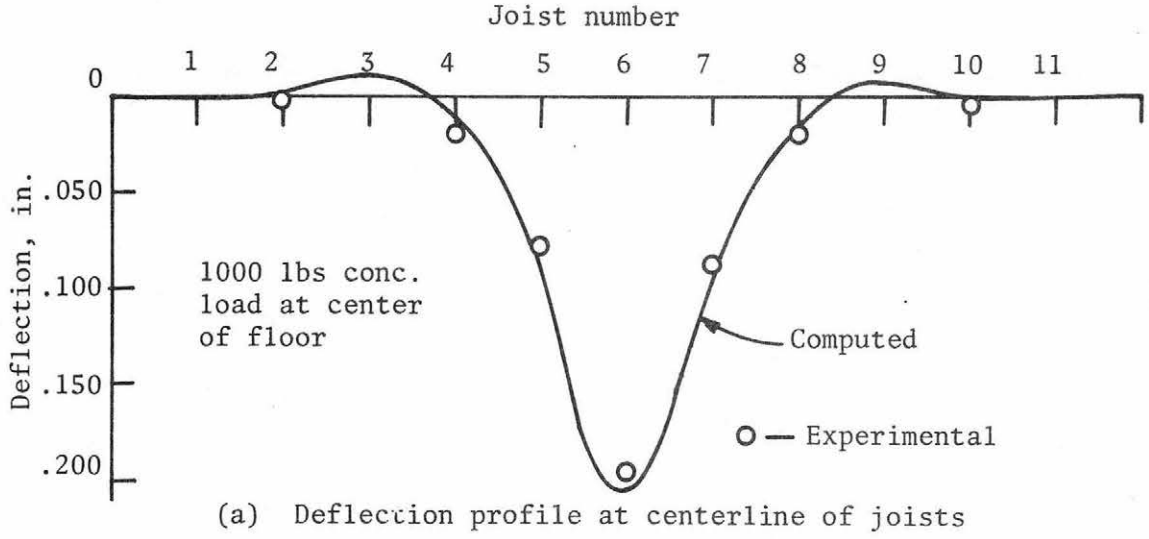

(a) Deflection profile at centerline of joists

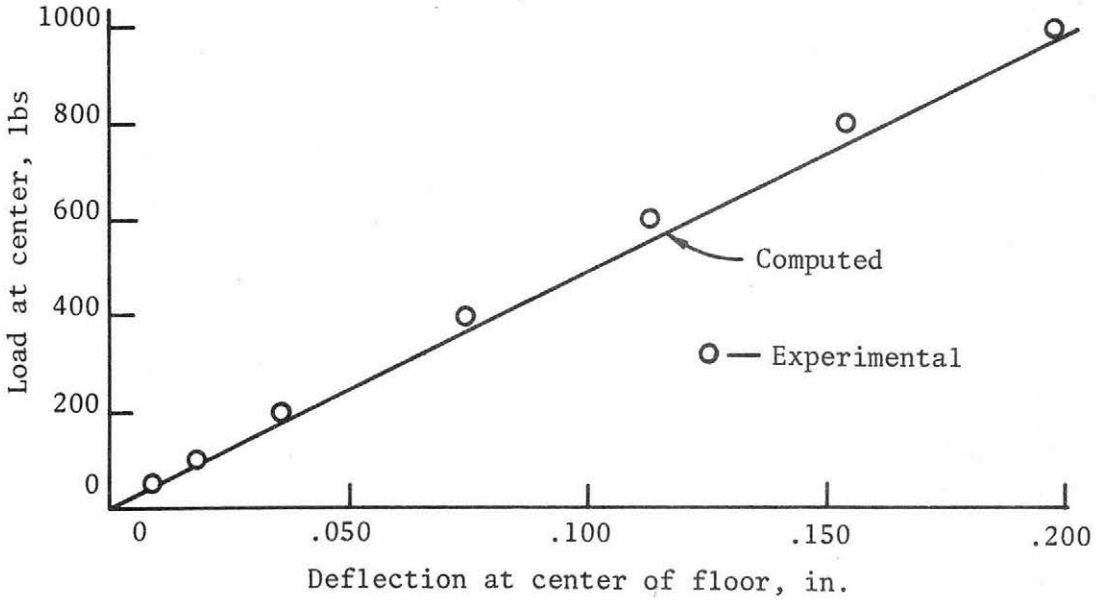

(b) Load-deflection behavior

Fig. A25 Computed vs Measured Results of Floor Specimen F11-8D16-2 (Nails of Top Layer Not Driven into Joists)

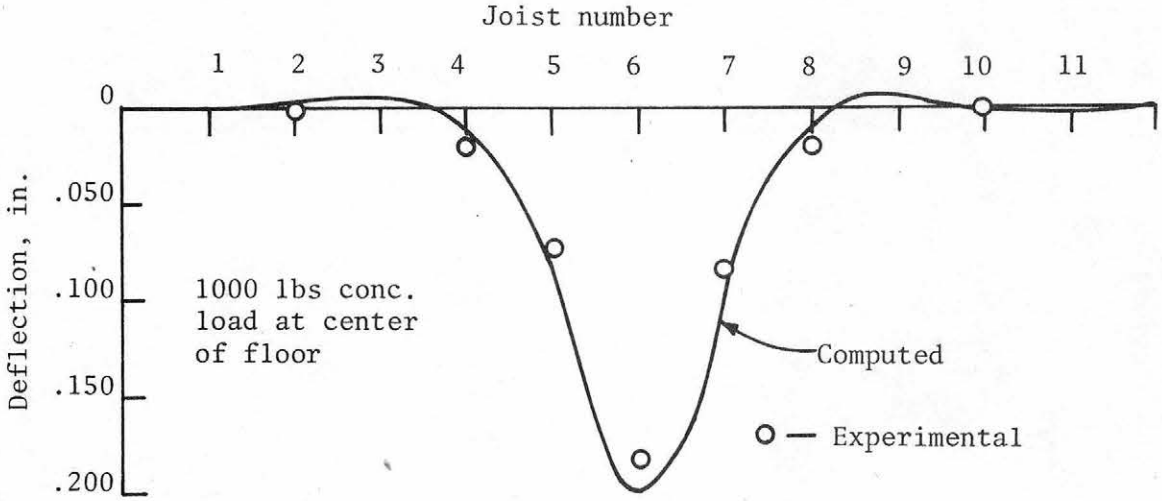

(a) Deflection profile at centerline of joists

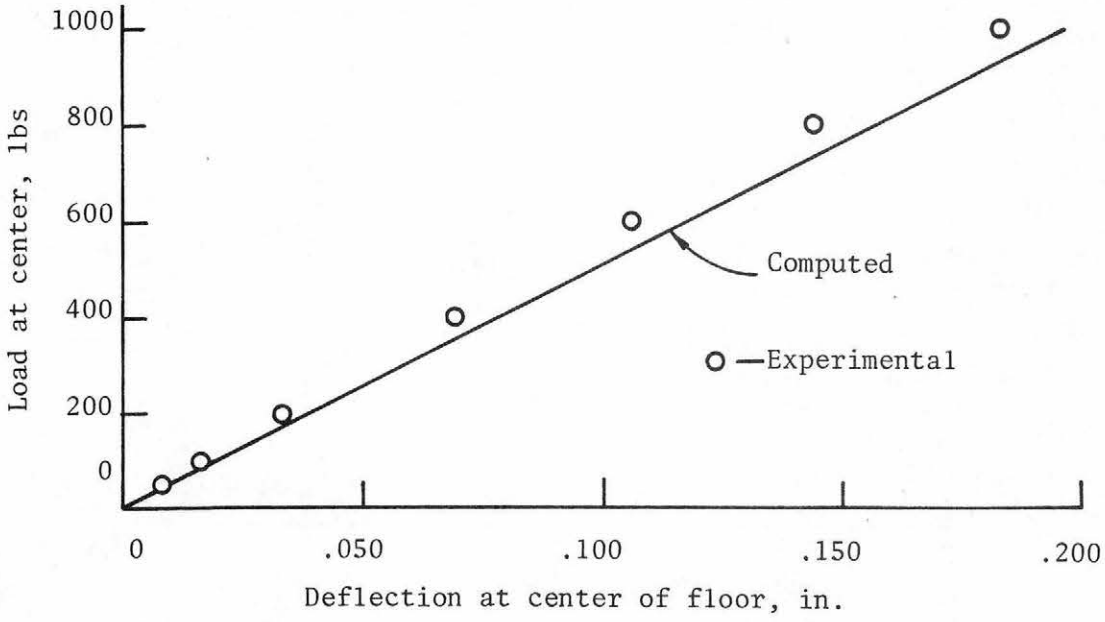

(b) Load-deflection behavior

Fig. A26 Computed vs Measured Results of Floor Specimen F11-8D16-2 (Nails of Top Layer Driven into Joists)